EFFECT OF DOSE AND DURATION OF DPTA NONOate TREATMENT ON HUMAN LUNG CANCER STEM CELL PHENOTYPE INDUCTION

Miss Nuttida Yongsanguanchai

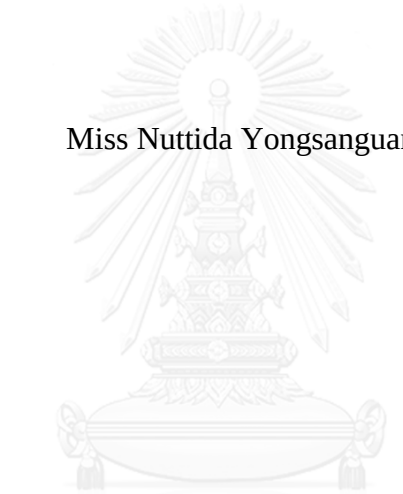

A Dissertation Submitted in Partial Fulfillment of the Requirements
for the Degree of Doctor of Philosophy Program in Pharmaceutical Technology
Department of Pharmaceutics and Industrial Pharmacy
Faculty of Pharmaceutical Sciences
Chulalongkorn University
Academic Year 2014

ผลของขนาดและระยะเวลาในการให้ DPTA NONOate ต่อการเหนี่ยวนำให้เกิดฟีโนไทป์ของเซลล์ต้นกำเนิดมะเร็งปอดของมนุษย์

นางสาวณัฐธิดา ยงค์สงวนชัย

วิทยานิพนธ์นี้เป็นส่วนหนึ่งของการศึกษาตามหลักสูตรปริญญาวิทยาศาสตรดุษฎีบัณฑิต
สาขาวิชาเทคโนโลยีเภสัชกรรม ภาควิชาวิทยาการเภสัชกรรมและเภสัชอุตสาหกรรม
คณะเภสัชศาสตร์ จุฬาลงกรณ์มหาวิทยาลัย
ปีการศึกษา 2557

Thesis Title	EFFECT OF DOSE AND DURATION OF DPTA NONOate TREATMENT ON HUMAN LUNG CANCER STEM CELL PHENOTYPE INDUCTION
By	Miss Nuttida Yongsanguanchai
Field of Study	Pharmaceutical Technology
Thesis Advisor	Associate Professor Pithi Chanvorachote, Ph.D.
Thesis Co-Advisor	Professor Apiwat Mutirangura, M.D. Ph.D

Accepted by the Faculty of Pharmaceutical Sciences, Chulalongkorn University in Partial Fulfillment of the Requirements for the Doctoral Degree

.....Dean of the Faculty of Pharmaceutical Sciences
(Assistant Professor Rungpetch Sakulbumrungsil, Ph.D.)

THESIS COMMITTEE

.....Chairman
(Assistant Professor Nontima Vardhanabhuti, Ph.D.)
.....Thesis Advisor
(Associate Professor Pithi Chanvorachote, Ph.D.)
.....Thesis Co-Advisor
(Professor Apiwat Mutirangura, M.D. Ph.D)
.....Examiner
(Assistant Professor Angkana Tantituvanont, Ph.D.)
.....Examiner
(Supannikar Tawinwung, Ph.D.)
.....External Examiner
(Professor Pimchai Chaiyen, Ph.D.)

ณัฐธิดา ยงค์สงวนชัย : ผลของขนาดและระยะเวลาในการให้ DPTA NONOate ต่อการเหนี่ยวนำให้เกิดฟีโนไทป์ของเซลล์ต้นกำเนิดมะเร็งปอดของมนุษย์ (EFFECT OF DOSE AND DURATION OF DPTA NONOate TREATMENT ON HUMAN LUNG CANCER STEM CELL PHENOTYPE INDUCTION) อ.ที่ปรึกษาวิทยานิพนธ์หลัก: รศ. ภก. ดร. ปิติ จันทร์วรโชติ, อ.ที่ปรึกษาวิทยานิพนธ์ร่วม: ศ. นพ. ดร. อภิวัฒน์ มุทิรางกูร, 122 หน้า.

แม้การรักษาโรคมะเร็งได้มีความก้าวหน้าและพัฒนาเป็นอย่างมากในช่วงทศวรรษที่ผ่านมา อัตราความสำเร็จในการรักษาหมู่ผู้ป่วยโรคมะเร็งยังคงไม่เป็นที่น่าพอใจเนื่องจากปัญหาที่พบในเคมี บำบัดและการกำเริบของโรคมะเร็ง งานวิจัยที่เกิดขึ้นใหม่ได้ชี้ให้เห็นว่าเซลล์ต้นกำเนิดมะเร็ง (Cancer Stem Cell) อยู่เบื้องหลังปัญหาการดื้อยาและการกลับมาของโรค แต่ความเข้าใจในการควบคุม และ พฤติกรรมของเซลล์ต้นกำเนิดมะเร็งในปัจจุบันยังคงจำกัด การเปลี่ยนแปลงของสารทางชีวภาพที่พบในสภาวะแวดล้อมของก้อนมะเร็งอาจส่งผลกระทบเซลล์ต้นกำเนิดมะเร็งหรือเซลล์มะเร็งให้มี stemness เพิ่มขึ้นหรือลดลงได้ งานวิจัยนี้ได้แสดงให้เห็นว่าไนตริกออกไซด์ (NO) สารชีวภาพที่มีความสำคัญต่อการส่งสัญญาณระหว่างเซลล์นั้นมีระดับเพิ่มขึ้นในก้อนมะเร็ง จึงสามารถส่งผลกระทบต่อการเหนี่ยวนำให้เกิดฟีโนไทป์ของเซลล์ต้นกำเนิดมะเร็งในเซลล์มะเร็งปอดของมนุษย์ เซลล์H292 และ เซลล์H460 ผลของการสัมผัสสารไนตริกออกไซด์ในระยะเวลายาวส่งผลให้ลักษณะรูปร่างของเซลล์มะเร็งค่อย ๆ เปลี่ยนแปลงไปคล้ายกับเซลล์ต้นกำเนิดมะเร็งมากขึ้น การสัมผัสสารไนตริก ออกไซด์ในระยะเวลายาวเหนี่ยวนำให้เกิดฟีโนไทป์ของเซลล์ต้นกำเนิดมะเร็ง โดยการแสดงออกที่เพิ่มขึ้นของโปรตีน marker CD133 และ ALDH1A1 ในเซลล์ที่สัมผัสไนตริกออกไซด์ ผลกระทบเหล่านี้สามารถย้อนกลับได้เมื่อหยุดให้สารไนตริกออกไซด์เป็นระยะเวลา 7 วัน นอกจากนี้ผลกระทบดังกล่าวสามารถทำซ้ำได้อีกโดยใช้สารให้ไนตริกออกไซด์อีกชนิดหนึ่งคือ SNAP และที่สำคัญผลทั้งหมดสามารถถูกยับยั้งเมื่อให้สาร PTIO ที่จะไปจับกับไนตริกออกไซด์ในอาหารเลี้ยงเซลล์ สุดท้ายการวิจัยครั้งนี้เปิดตัวกลไกของไนตริกออกไซด์ในการกระตุ้นการทำงานของโปรตีน caveolin -1 (Cav -1) ให้เพิ่มขึ้น และ อยู่เบื้องหลังพฤติกรรมก้าวร้าวของเซลล์มะเร็ง รวมถึงความต้านทานการตายแบบ อะนอยคิส การเจริญเติบโตอาณานิคม พฤติกรรมการเคลื่อนที่ของเซลล์มะเร็งและการรุกราน การค้นพบนี้แสดงให้เห็นบทบาทใหม่ของไนตริกออกไซด์ในการเหนี่ยวนำให้เกิดฟีโนไทป์ของเซลล์ต้นกำเนิดมะเร็งและความสำคัญของสารต่อพฤติกรรมก้าวร้าว ของเซลล์มะเร็งผ่านการ กระตุ้นโปรตีน Cav -1

ภาควิชา	วิทยาการเภสัชกรรมและเภสัชอุตสาหกรรม	ลายมือชื่อนิสิต .....
สาขาวิชา	เทคโนโลยีเภสัชกรรม	ลายมือชื่อ อ.ที่ปรึกษาหลัก .....
ปีการศึกษา	2557	ลายมือชื่อ อ.ที่ปรึกษาร่วม .....

5377101133 : MAJOR PHARMACEUTICAL TECHNOLOGY
KEYWORDS: CANCER STEM CELL / NITRIC OXIDE / CAVEOLIN-1 / CD133 / ALDH1A1 / NON SMALL CELL LUNG CANCER

NUTTIDA YONGSANGUANCHAI: EFFECT OF DOSE AND DURATION OF DPTA NONOate TREATMENT ON HUMAN LUNG CANCER STEM CELL PHENOTYPE INDUCTION. ADVISOR: ASSOC. PROF. PITHI CHANVORACHOTE, Ph.D., CO-ADVISOR: PROF. APIWAT MUTIRANGURA, M.D. Ph.D, 122 pp.

Tremendous advances have been made in the treatment of cancers during the past decades, but success rate among cancer patients is still dismal, largely due to problems associated with chemo/radio-resistance and relapse. Emerging evidence has indicated that cancer stem cells (CSCs) are behind the resistance and recurrence problems, but our understanding of their regulation is limited. Rapid reversible changes of CSC-like cells within tumors may result from the effect of biological mediators found in tumor microenvironment. This research showed how nitric oxide (NO), a key cellular modulator whose level is elevated in many tumors, affect CSC-like phenotypes of human non-small-cell lung carcinoma (NSCLC) H292 and H460 cells. Exposure of NO gradually altered the cell morphology towards mesenchymal stem-like shape. NO exposure promoted CSC-like phenotype indicated by increased expression of known CSC markers, CD133 and ALDH1A1, in the exposed cells. These effects of NO on stemness were reversible after cessation of the NO treatment for 7 days. Furthermore, such effect was reproducible using another NO-donor, SNAP. Importantly, inhibition of NO by the known NO scavenger PTIO strongly inhibited cellular CSC-like phenotype. Lastly, this research unveiled the underlying mechanism of NO action through the activation of caveolin-1 (Cav-1), which is up regulated by NO and is responsible for the aggressive behavior of the cells. These findings indicate a novel role of NO in CSC regulation and its importance in aggressive cancer behaviors through Cav-1 up regulation.

Department:	Pharmaceutics and Industrial Pharmacy	Student's Signature	.....
		Advisor's Signature	.....
Field of Study:	Pharmaceutical Technology	Co-Advisor's Signature	.....
Academic Year:	2014		

ACKNOWLEDGEMENTS

This accomplishment could not been achieved without the great guidance and encouragement from my advisors, committee members, academic staffs, colleagues, friends and family.

I would like to express my special appreciation and thanks to my advisor, Associate Professor Dr. Pithi Chanvorachote who kindly gave me the priceless opportunity to study and develop my skill of knowledge and ways of thinking. My deep gratitude is expressed to Professor Dr. Apiwat Mutirangura, M.D., my thesis co-advisor, for his generosity in expanding my laboratory intellectual and skills. I am sincerely grateful to the committee members for their help in improving and constructing my dissertation.

My appreciation is stated to my lovely colleagues especially in Dr. Pithi's and Dr. Apiwat's laboratories. I would like to thank them for always being there for me, their friendly advice and aspiring guidance. Also, I would like to thank them for their beautiful friendship and precious memories.

Furthermore, I would like to express special thanks to my friends and family for supporting me throughout the course and would like to dedicate this dissertation to my parents.

Finally, my gratefulness is expressed to THE 90TH ANNIVERSARY OF CHULALONGKORN UNIVERSITY FUND (Ratchadaphiseksomphot Endowment Fund) for their grant support.

CONTENTS

Page

Page

LIST OF TABLES

Table **Page**

LIST OF FIGURES

Figure **Page**

LIST OF ABBREVIATIONS

Akt, protein kinase B

Cav-1, caveolin-1

CSCs, cancer stem cells

DPTA, dipropylenetriamine

eNOS, endothelial nitric oxide synthases

EMC, extracellular matrix

FBS, fetal bovine serum

HRP, horseradish peroxidase

iNOS, inducible nitric oxide synthases

MTT, 3-(4,5-dimethylthiazol-2-yl)-2,5-diphenyltetrazolium bromide

NADPH, nicotinamide adenine dinucleotide phosphate

nNOS, neuronal nitric oxide synthases

NO, nitric oxide

NOS, nitric oxide synthases

NSCLC, non-small-cell lung carcinoma

PBS, phosphate buffer saline

PI, propidium iodide

PTIO, 2-(4-carboxy-phenyl)-4,4,5,5 tetramethylimidazoline-1-oxy-3-oxide

RPMI, Roswell Park Memorial Institute

SNAP, *S*-nitroso-*N*-acetylpenicillamine

CHAPTER I
INTRODUCTION

According to the 2014 American Cancer Society's annual cancer statistics, lung cancer remains as one of the most common malignancies and is the leading cause of cancer-related deaths worldwide (Siegel, 2014). Increasing evidence has indicated the role of cancer stem cells (CSCs) in cancer aggressiveness, chemoresistance and relapse; they are being considered as the underlying cause of the high mortality rate of cancer (Marie-Egyptienne, 2012, Hermann, 2007, Merlos-Suárez, 2011, Perona, 2011). The concept of tumor as having heterogeneous cancer cell population with a sub-population of cells possessing a high tumorigenic potential and stem-like property was first described in 1997 (Bonnet, 1997). This sub-population is commonly known as tumor-initiating cells, tumor-propagating cells or CSCs, and has been identified in many types of cancer (Collins, 2005, Eramo, 2008, Li, 2007, Ma, 2007, Ponti, 2005, Ricci-Vitiani, 2007, Singh, 2003). CSCs have been suggested as the rationale behind chemo/radio-resistance and cancer relapse (Bao, 2006, Bertolini, 2009, Creighton, 2009, Levina, 2008, Zhang, 2012) and have been a target of new cancer therapeutic strategies. Recent studies have revealed the possibility of cancer cells being induced by their surrounding microenvironment and gain cancer stem cells properties (Yang, 2009).

Nitric oxide (NO), a free radical gaseous molecule, renowned for its involvement in assorted biological, physiological and pathological processes (Moncada, 1991). Even though, NO is an extremely unstable gas with *in vivo* half-life of no more than 6 seconds, its high lipid solubility and small molecular size facilitates

cell membrane permeation. NO was initially identified as a transcellular messenger molecule synthesized by a family of enzymes called nitric oxide synthases (NOS), comprising of inducible NOS (iNOS), endothelial NOS (eNOS) and neuronal NOS (nNOS), through the conversion of L-arginine in the presence of oxygen and nicotinamide adenine dinucleotide phosphate (NADPH) (Marletta, 1993, Moncada, 1989). A number of studies pointed out that all three isoforms of NOS are involved in the process of cancer development and progression (Thomsen, 1995, Thomsen, 1994, Fujimoto, 1997, Ambs, 1998). Not only does the NOS expression is highly detectable in various cancers, but also the NO level is frequently up-regulated in tumor areas (Fukumura, 2006, Lala, 1998). Previous studies indicated that NO could render cells resistant to death induced by various stimuli (Chanvorachote, 2006, Chanvorachote, 2009, Wongvaranon, 2013). NO also regulates cancer cell migration and invasion (Sanuphan, 2013), and increased NOS expression and activity have been reported in metastatic lung cancer cells (Puhakka, 2003). Clinical data further support the role of NO in lung cancer and metastasis. A high level of NO was observed in the lung of lung cancer patients (Masri, 2005, Liu, 1998) and a positive correlation between NO, its stable end-products ‘nitrite and nitrate’ and its generator NOS with advanced cancer staging and poor survival in lung cancer patients has been reported (Arias-Díaz, 1994, Colakogullari, 2006, Esme, 2008). Animal studies further showed that genetic ablation of NOS suppressed lung tumor formation in mice (Kisley, 2002). Together these studies strongly support the role of NO in tumorigenesis and metastasis, although the underlying mechanisms remain obscure.

This research hypothesize that NO may mediate its pro-carcinogenic effects through CSCs due to their importance in cancer aggressiveness described above.

Further hypothesizes is that NO may mediate its effects through Caveolin-1 (Cav-1) since its expression has been linked to cancer aggressiveness (Chunhacha, 2012a, Grande-Garcia, 2007, Halim, 2012, Ho, 2002, Lin, 2005, Luanpitpong, 2010, Rungtabnapa, 2011) and since NO has been shown to be a key regulator of Cav-1 in human lung cancer cells (Chanvorachote, 2009). Cav-1 is a scaffolding protein found in the cellular structure caveolae, which has been shown by our group and others to regulate the aggressiveness of cancer cells by increasing their motility and resistance to anoikis (Chunhacha, 2012a, Grande-Garcia, 2007, Halim, 2012, Ho, 2002, Lin, 2005, Luanpitpong, 2010, Rungtabnapa, 2011). It has also been shown to increase cell survival under non-adherent conditions via Mcl-1 stabilization (Chunhacha, 2012b) and up-regulation of activated protein kinase B (Akt) (Chanvorachote, 2013). In this study, molecular and pharmacological approaches were used to investigate the role of NO in Cav-1 and CSC regulation and their impact on the cellular aggressive properties of human lung cancer cells. This research demonstrated for the first time that NO play an important role in the CSC-like transformation of lung cancer cells. Although Cav-1 is up-regulated during the transformation and is responsible for the anoikis resistance and invasive properties of the cells, it is not required for the stem-like phenotype.

CHAPTER II
LITERATURE REVIEW

Lung cancer

Cancer has always been a major health problem in many parts of the world including the United States (U.S.) itself. Not only being a commonly diagnosed disease, cancer is also the dominant cause of death worldwide. Siegel and co-worker have a figure that shows the total number of cancer deaths in men (year 1991-2010) and in women (year 1992-2010), where the actual numbers of deaths due to cancer are represented by the blue lines and the red lines exhibits the expected number of deaths if the rates of cancer death had continued at its peak (Siegel, 2014). This has proven that within the past few years, actions have been made in order to prevent cancer related death. However, both graphs signified that the number of cancer deaths still increases terrifyingly throughout the decades.

Every year, the American Cancer Society would compiles cancer-associated data collected by the help of numerous institutes in the U.S. and analyze the data to estimate cancer statistics for the next coming year. Siegel et al., had another figure which show the estimated new cancer cases and deaths for ten leading cancer types in male and female population of the U.S. for the year 2014. Up to 116,000 male patients are estimated to be diagnose with lung & bronchus related cancer, which concludes to be 14% of the new cancer cases in U.S. males and 106,210 (13%) in U.S. females. Estimated total deaths due to cancer in the year 2014 are 310,010 males and 275,710

females, where the top causes of death are lung & bronchus cancer.

Lung cancer has always been in the top three most diagnosed cancer type and is continuously the main cause of death in both genders. Table 1A and B listed the statistics of the top three leading cancer type within the past 20 years in U.S. male and female respectively. The three leading cancer types in male are colorectum, lung & bronchus and prostate cancer, while in female are colorectum, lung & bronchus and breast cancer. Even though lung & bronchus cancer are not the highest diagnosed cancer type in both gender, but it has always caused the highest number of cancer death. This garnered scientist attention to focus more on improving lung cancer statistics.

Table 1A and B Statistics of the top three leading cancer type within the past 20 years in U.S. male and female.

A

	MALE					
	Estimated New Cases			**Estimated Deaths**		
Year \ Cancer Type	**Colorectum**	**Lung & bronchus**	**Prostate**	**Colorectum**	**Lung & bronchus**	**Prostate**
1994 (Boring, 1994)	12%	16%	32%	10%	33%	13%
1999 (Landis, 1999)	10%	15%	29%	10%	31%	13%
2004 (Jemal, 2004)	11%	13%	33%	10%	32%	10%
2009 (Jemal, 2009)	10%	15%	25%	9%	30%	9%
2014 (Siegel, 2014)	8%	14%	27%	8%	28%	10%

B

	FEMALE					
	Estimated New Cases			Estimated Deaths		
Year \ Cancer Type	Colorectum	Lung & bronchus	Breast	Colorectum	Lung & bronchus	Breast
1994 (Boring, 1994)	13%	13%	32%	11%	23%	18%
1999 (Landis, 1999)	11%	13%	29%	11%	25%	16%
2004 (Jemal, 2004)	11%	12%	32%	10%	25%	15%
2009 (Jemal, 2009)	10%	14%	27%	9%	26%	15%
2014 (Siegel, 2014)	8%	13%	29%	9%	26%	15%

Lung cancer can be divided into two key groups, small cell lung cancer (SCLC) and non-small cell lung cancer (NSCLC). NSCLC is the most common type of lung cancer, which is found approximately up to 80% in lung cancer patients. The reason behind the low survival rate in patients diagnosed with lung cancer is because by the time lung cancer patients got diagnosed are mostly when the cancer is already at the advanced stage, meaning the cancer has already spread to other sites throughout the patient's body. Furthermore, lung cancer patients have higher relapse statistics; in which the cause of these intractable have recently been pointed out that cancer stem cells (CSCs) are to blame (Marie-Egyptienne, 2012, Hermann, 2007, Merlos-Suárez, 2011, Perona, 2011). In the past decades, remarkable progresses have been made in the treatment of cancer. However, success rate among lung cancer patients is still grim mainly due to difficulties related to chemo/radio-resistance and relapses.

Cancer stem cells (CSCs)

Cancer stem cells or originally called tumor-initiating cells are a small population of cancer cells within a tumor, which have tumor propagating property. The idea of cancer stem cells was first introduced in the year 1997 by Bonnet & Dick and soon was confirmed by multiple research groups (Bonnet, 1997, Collins, 2005, Eramo, 2008, Li, 2007, Ma, 2007, Ponti, 2005, Ricci-Vitiani, 2007, Singh, 2003). Traditional stochastic model stated that any somatic cell could become cancerous after acquiring series of sequential mutation during a long period of time (Fig. 1). However, mature somatic cells generally consist of a short life span therefore, the probability of successful mutation within one cell life span would be very low (Fulda, 2010). An alternative model, the cancer stem cell model, has overcome the stochastic model. According to the CSCs model, the mutation only affects the long-lived stem cells, which eventually mutate to CSCs (Rossi, 2008). These CSCs exhibits deregulated self-renewal, have the ability to form tumors and can proliferate indefinitely (Bonnet, 1997, Lobo, 2007). Cancer stem cells and normal stem cells are somewhat alike as they are both capable of self-renewal and can produce differentiated progeny (Singh, 2003, Ricci-Vitiani, 2007, Goodell, 1996, Spangrude, 1988, O'Brien, 2007, Al-Hajj, 2003). However, dissimilar to the high regulated differentiation and self-renewal process of normal stem cells, CSCs endure abnormal differentiation and uncontrolled self-renewal that in turn leads to the third hallmark of CSCs, tumor formation (Singh, 2003, Ricci-Vitiani, 2007, Goodell, 1996, Spangrude, 1988, O'Brien, 2007, Al-Hajj, 2003, Vermeulen, 2008). Moreover, similar to somatic stem cells CSCs can metastasize to distant tissues and organs, and are resistance to apoptosis stimulants (Domen, 2000,

Domen, 1998).

Multiple researches have verified CSCs as the reason behind cancer relapse and that existing treatments can induce stemness in cancer cells (Bao, 2006, Bertolini, 2009, Creighton, 2009, Levina, 2008, Zhang, 2012). These indicate that CSCs can be induced or selected by their surrounding microenvironment.

Types of aggressive cancer cells

Currently, there are only two aggressive cancer cell types that have been well distinguished; CSCs and epithelial-mesenchymal transition (EMT). Aggressive cancer cells have the ability to survive through metastasis and form tumor at the secondary site. The initial step of metastasis is migration, the cancer cells would migrate to the nearest vascular site; these cells typically emits EMT or CSCs property. Then the cells would invade through the vessel's wall in order to get into the blood stream. When in the blood stream, the cells would have to survive in a non-detach state, in other words, they would have to be anoikis resistant. Lastly, aggressive cancer cells have tumor initiating property and can form new tumor at the secondary site.

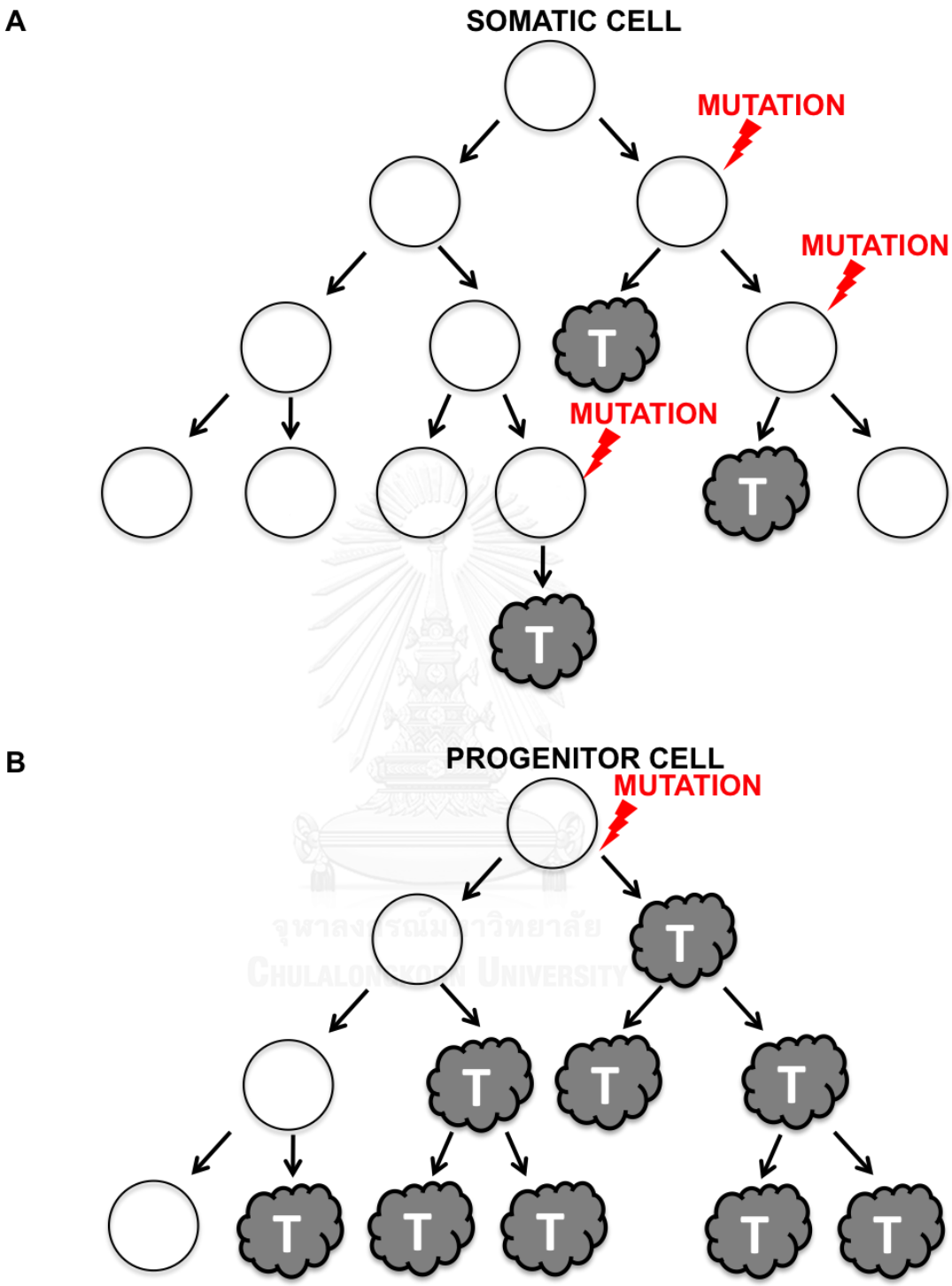

Figure 1 (**A**) The Stochastic (traditional) model of cancer development (**B**) The (alternative) cancer stem cell model.

EMT is believe to be another type of cell that exhibit aggressive behavior. EMT cells are epithelial-like cell that had transformed into mesenchymal-like cell. The epithelial cells would lose their cell polarity and cell-cell adhesion, and would gain migratory and invasive properties. EMT cells are very similar to CSC and is believe to be the cancer cell first step in transforming into CSC. EMT and CSC cells are somewhat similar. Since, both type of cells are the reason behind aggressive cancer, both type of cells have the ability to survive through the metastasis process. These cells migrate and invade faster than normal cancer cell and would not under go anoikis when detached. EMT and CSC morphology are mechenchymal-like, spindal fibroblast-like shape. The different between these two cells type are that, EMT cells tend to have high proliferation rate, while CSC proliferate very slowly. Furthermore, CSC can form tumor, is self-renewal, have high pluripotency and are more chemoresistance. Moreover, different makers are used to distinguish cancer cells between these two cell types.

CSCs markers for lung cancer

Numerous CSCs markers have been established and confirmed. Some markers could be used to identify both somatic stem cells and CSCs, and some could be used to identify CSCs in various types of cancer. Table 2 displays CSC markers found in some NSCLC cell lines.

Table 2 Expression of putative CSC markers in NSCLC cell lines.

Cell line	CD44+	CD24+	CD133+	ALDH+	CD34+
A549	+++	+++	++	++	-
EKVX	+++	+++	+	+++	ND
HOP-62	+++	±	+	++	ND
HOP-92	+++	±	±	±	ND
NCI-H226	+++	+	±	+++	ND
NCI-H23	++	±	±	±	±
NCI-H460	++	++	±	+	++

CD133 or prominin-1 is a pentaspan membrane protein, it was the first member of the prominin family indentified. Uptodate, its precise functions still remain unclear. This 5-transmembrane protein have a molecular weight of 120kDa single chain-polypeptide made up of 865 amino acids (Miraglia, 1997). ALDH1A1 or aldehyde dehydrogenase 1 family, member A1 belongs to aldehyde dehydrogenases family of proteins that catalyze aldehydes to acid conversion. ALDH1A1 is involved in drug resistance and have been establish as CSCs marker by many research groups.

CD133 and ALDH1A1 are the two most widely used CSCs markers not only in lung cancer but also in all type of cancers. Numerous group of researchers had identify CSCs both in the laboratories and clinically using these two CSCs markers (Akunuru, 2012, Collins, 2005, Eramo, 2008, Ma, 2007, Ricci-Vitiani, 2007, Singh, 2003, Pirozzi, 2011, Levina, 2008, Mihatsch, 2011, Bertolini, 2009, Croker, 2009, Hermann, 2007, Kim, 2011, Silva, 2011, Alamgeer, 2013). Previous research used CD133 and

ALDH1A1 as CSCs marker in lung cancer cell lines. Lung tumor cell lines were treated with doxorubicin, cisplatin, or etoposide resulted in drug-selected cells that have high CSCs markers such as CD133 suggesting that chemotherapy may lead to the propagation of CSCs (Levina, 2008). Furthermore, Mihatsch and colleague investigated radioresistant tumor cells in NSCLC A549 cells and breast cancer cell line SK-BR-3 in *in vitro.* Results obtained in both cell line were a positive correlation between $ALDH1^+$ cells and significantly high radio resistant property, while other markers such as Sox2, Oct4 and CD133 displayed no general pattern (Mihatsch, 2011). On the other hand, clinical wise, Bertolini and his team found that in 60 primary tissue samples, NSCLCs with $CD133^+$ are highly tumorigenic, displays stem-like features and does not die in cisplatin treatment (Bertolini, 2009). Also, Alamgeer and his group examined CD133 and ALDH1A1 expression in 205 patients diagnosed with early stage NSCLC patholodic stage I. This study was a 5-year ongoing project and at the end resulting in 62 relapses and 58 cancer-related deaths. The CSCs markers CD133 and ALDH1A1 expression both correlates directly to the recurrence (self-renewal capacity) of the cancer. Overexpression of ALDH1A1 alone significantly predicted poor recurrence-free survival, while coexpression of ALDH1A1/CD133 establish an even stronger significated correlation to poor survival in early-stage NSCLC patients (Alamgeer, 2013).

In-vitro identification of CSCs

CSCs, is currently being investigated and have been shedding new knowledge every day. To confirm that a cancer cell have CSC property, a combination of unique

experiments should be performed to help strengthen the obtained results, as different assay have its own limitation on interpretation. A widely used method of exploring CSCs is by *in vitro* studying previously establish cell lines (Mather, 2012).

Flow cytometry is one of the first assay used to indentify CSCs. Either by FACscan (hoesct) or CSCs marker, flow cytometry helps quantify the number of CSCs in the injected population. Another widely used assay is western blot. Collected protein lysate of interested population can be probe with CSCs marker antibodies. The band developed from western blot assay can be quantified by densitometry software representing the level of CSCs marker proteins.

CSCs exhibits similar morphology as normal stem cell. CSCs morphology are usually describe as fibroblast-like shape, mesenchymal-like shape or cells with high polarity forming a neuronal-like drendrites. In addition, migration, invation and anoikis assays are normally used for *in vitro* analysation to represent *in vivo* metastasis process. These assays are usually performed to analyze for cells with EMT or CSCs propeties. Moreover, the *in vitro* assays that examine CSCs hallmark are angchorage-independent colony formation assay and primary and secondary spheroid formation assay (Kitamura, 2009). Lastly, genes and proteins can be scan through microarray or protein-array. These process help scan thousands of genes/proteins that have been up-regulated or down-regulated between the treatment samples and the control samples. Interested genes can be compared to data on NCBI webpage and analyzed using various program.

Nitric oxide (NO)

In the year 1992 NO was named 'Molecule of the Year'. NO was discovered by three US scientists whom had received Nobel prize in the year 1998– Robert F. Furchgott, PhD, Louis J. Ignarro, PhD, and Ferid Murad, MD, PhD (SoRelle, 1998). NO is a multifunctional free radical gaseous molecule. It is renowned for its involvement in assorted biological, physiological and pathological processes (Moncada, 1991). NO was initially identified as a transcellular messenger molecule synthesized by a family of enzymes called nitric oxide synthases (NOS) through the conversion of L-arginine amino acid, in the presence of oxygen and NADPH (nicotinamide adenine dinucleotide phosphate with extra hydrogen) (Fig. 2) (Marletta, 1993, Moncada, 1989).

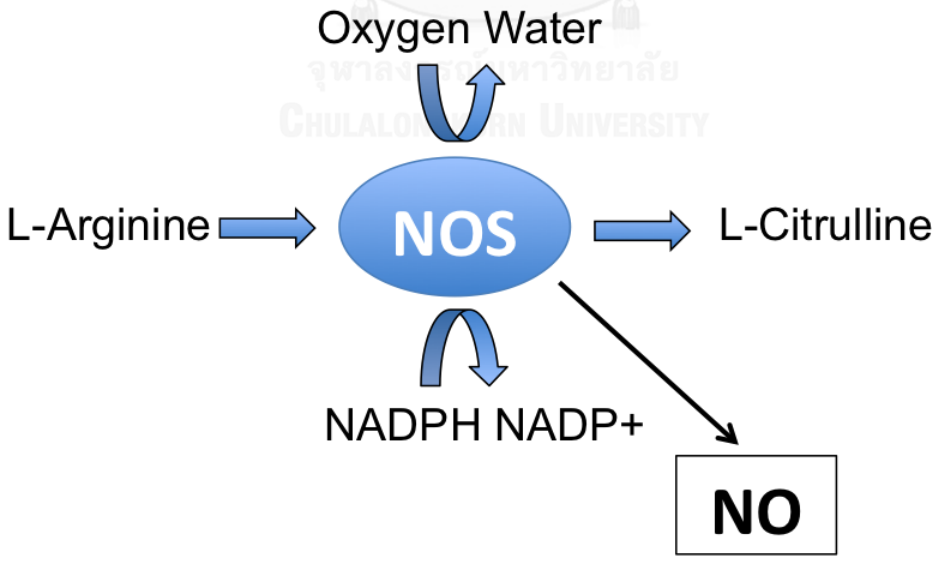

Figure 2 NO production process.

NO is an extremely unstable gas having an *in vivo* half-life of lesser than 6 seconds. However, its small molecular size and its lipid soluble property allow it to be highly membrane permeable (Moncada, 1991). Nitric oxide has been proven to play a critical role in is the regulation of inflammatory-immune process, which leads to chronic inflammation and cancerous tumor progression (Clancy, 1995, Clancy, 1998, Weiming, 2002, Wink, 1998). Tumours are made up of multiple cell types interacting and secreting signaling factors into the complex microenvironment. Nitric oxide is the key molecule being produced from crosstalk between cells and inflammation within the tumor microenvironment (Cook, 2004, Decker, 2008, Esme, 2008). Interestingly, multiple researchers have reported controversies on nitric oxide effect in tumor progression as it can either inhibit or amplify tumor growth depending on the level of nitric oxide in the environment (Fig. 3) (Dhar, 2003, Jenkins, 1995, Lala, 1998, Muntané, 2010, Thomsen, 1998).

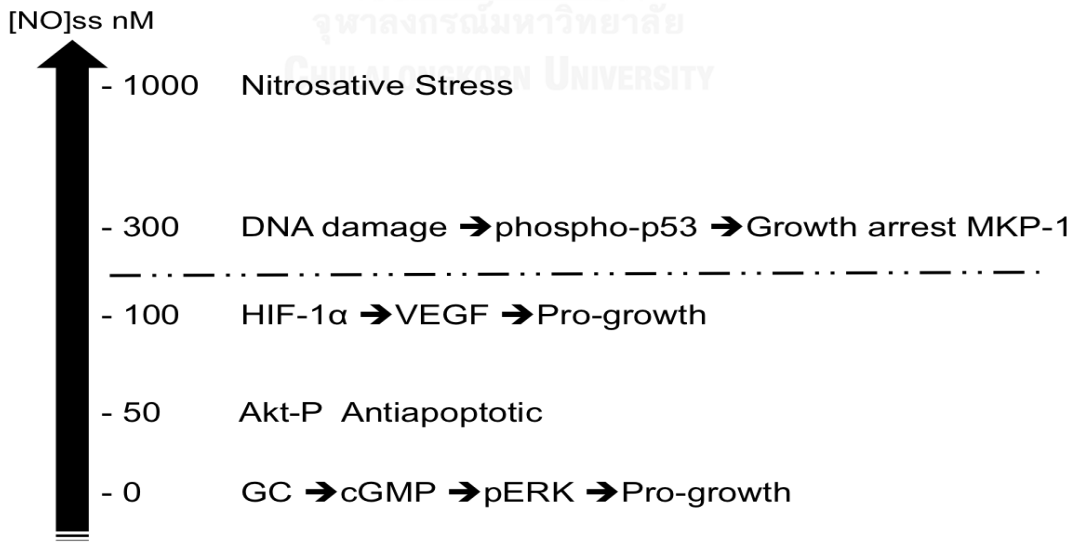

Figure 3 Correlation between NO concentration and cell's molecular mechanisms.

Currently, an only known receptor for NO is soluble guanylyl cyclase (sGC). The word soluble means that it can be completely intracellular. sGC have a molecular weight of 72 kDa. It structure consist of an alpha-beta heterodimer in which a heme binds to the beta domain. NO bind to the heme and in turn increases the sGC activity to at least 200 folds. However, under oxidative stress condition, Fe(II)sGC oxidization can lead to it loosing its heme and therefore are unable to response to NO induction (Poulos 2006).

Nitric oxide and cancer

The NO production enzyme family, NOS, consist of three types of NOS: inducible NOS (iNOS or NOS2), endothelial NOS (eNOS or NOS3) and neuronal NOS (nNOS or NOS1). Several studies had pointed out that all three isoforms of NOS are involved in the process of cancer development and progression (Thomsen, 1995, Thomsen, 1994, Fujimoto, 1997, Ambs, 1998). Not only does the NOS expression is highly detectable in various cancers, but also the NO level is frequently up-regulated in tumor areas (Fukumura, 2006, Lala, 1998). Previous studies indicated that NO could render cells resistant to death induced by various stimuli (Chanvorachote, 2006, Chanvorachote, 2009, Wongvaranon, 2013). NO also regulates cancer cell migration and invasion (Sanuphan, 2013), and increased NOS expression and activity have been reported in metastatic lung cancer cells (Puhakka, 2003). Clinical data further support the role of NO in lung cancer and metastasis. A high level of NO was observed in the lung of lung cancer patients (Masri, 2005, Liu, 1998) and a positive correlation between NO, its stable end-products ‘nitrite and nitrate’ and its generator NOS with advanced

cancer staging and poor survival in lung cancer patients has been reported (Arias-Díaz, 1994, Colakogullari, 2006, Esme, 2008). Animal studies further showed that genetic ablation of NOS suppressed lung tumor formation in mice (Kisley, 2002). Together these studies strongly support the role of NO in tumorigenesis and metastasis, although the underlying mechanisms remain obscure.

A protein that have been linked to both NO and cancer aggressiveness is Caveolin-1 (Cav-1) protein. Cav-1 is a scaffolding protein found in the cellular structure caveolae with a molecular weight of approximately 22kDa. NO had been proven to be the key regulator of Cav-1 in human lung cancer cells (Chanvorachote, 2009). By inhibiting the ubiquitination of Cav-1 and in turn increases the accumulation level of the Cav-1 protein. Also, Cav-1 have been revealed as a cancer aggressiveness regulator. Cav-1 have been shown to incresase cells' motility and resistance to anoikis (Chunhacha, 2012a, Grande-Garcia, 2007, Halim, 2012, Ho, 2002, Lin, 2005, Luanpitpong, 2010, Rungtabnapa, 2011). On the other hand, Cav-1 has also been established as having tumor suppressor role in some cancer type (Hino, 2003, Han, 2009, Wiechen, 2001).

Nitric oxide donors and scavenger

Dipropylenetriamine NONOate or (3,3′-(Hydroxynitrosohydrazino)bis-1-propanamine) is a nitric oxide donor with a molecular weight of 191.23. One mole of DPTA gives out two moles of NO. It is a slowly releasing NO donor and has a half-life of 5 hours at 22-25°C. DPTA is highly water-soluble. DPTA is one of the most

commonly used NO donor in *in-vitro* experiments, mainly because its control release property.

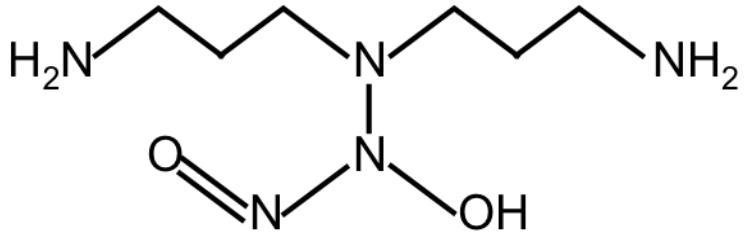

Figure 4 Dipropylenetriamine NONOate (DPTA)

S-Nitroso-N-acetyl-DL-penicillamine; SNAP; N-(acetyloxy)-3-nitrosothiovaline or SNAP is a spontaneous NO donor with a moleculare weight of 220.25. SNAP has a half-life of approximately 4.6 hours. One mole of SNAP gives out one mole of NO. However, SNAP is light sensitive and therefore needed to be protected from light. SNAP is also one of the widely used NO-donor, due to its long half-life.

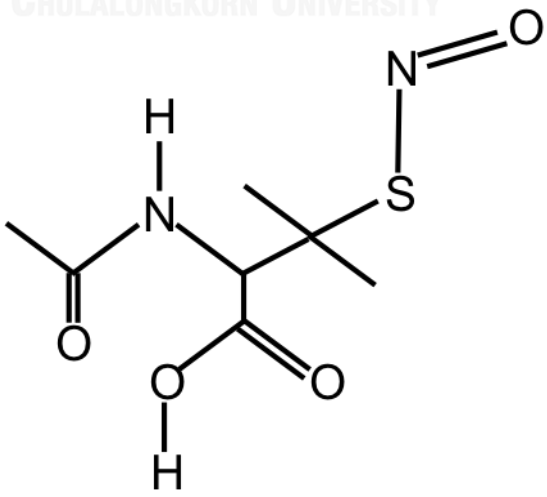

Figure 5 S-Nitroso-N-acetyl-DL-penicillamine (SNAP)

2-(4-carboxy-phenyl)-4,4,5,5 tetramethylimidazoline-1-oxy-3-oxide or PTIO is a well known NO scavenger. PTIO has a molecular weight of 233.29. This compound is a stable NO scavenger that functions by scavenging and trapping NO radicals. PTIO affects only NO free radical molecules without affecting NOS. The reaction between PTIO and NO produces NO_2 and 2-phenyl-4,4,5,5-tetramethylimidazoline-1-oxyl. PTIO is a commonly used NO scavenger.

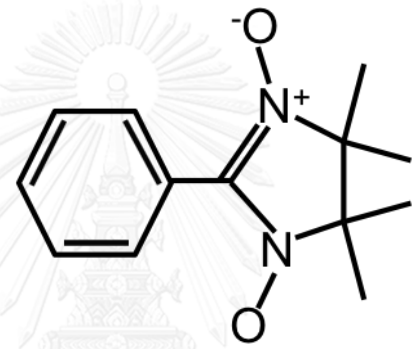

Figure 6 2-(4-carboxy-phenyl)-4,4,5,5 tetramethylimidazoline-1-oxy-3-oxide (PTIO)

CHAPTER III
MATERIALS AND METHODS

Materials

NCI-H292 cells, NCI-H460 cells and pEX_Cav-1-YFP plasmid were obtained from the American Type Culture Collection ATCC® (Manassas, VA). Roswell Park Memorial Institute (RPMI) 1640 medium, fetal bovine serum (FBS), L-glutamine, penicillin/streptomycin, phosphate buffer saline (PBS) and trypsin-EDTA were obtained from GIBCO (Grand Island, NY, USA). Dipropylenetriamine (DPTA) NONOate, 3-(4,5-dimethylthiazol-2-yl)-2,5-diphenyltetrazolium bromide (MTT), Hoechst 33342, propidium iodide (PI), dimethyl sulfoxide (DMSO), actinomycin D andagarose and ethylenediaminetetraacetic acid (EDTA) were obtained from Sigma Chemical, Inc. (St. Louis, MO, USA). Matrigel was obtained from BD Biosciences (San Jose, CA, USA). Complete Mini cocktail protease inhibitor was obtained from Roche Molecular Biochemicals (Indianapolis, IN, USA). Quick Start™ Bradford protein assay, sodium dodecyl sulfate-polyacrylamide gel electrophoresis (SDS-PAGE) and nitrocellulose membranes were obtained from Bio-Rad Laboratories (Hercules, CA, USA). ALDH1A1, β-actin, anti-goat IgG-HRP, 2-(4-carboxy-phenyl)-4,4,5,5 tetramethylimidazoline-1-oxy-3-oxide (PTIO) and shRNA-Cav-1 plasmid were obtained from Santa Cruz Biotechnology (Santa Cruz, CA, USA). Thermo Scientific SuperSignal® West Pico chemiluminescent substrate were obtained from Pierce Biotechnology, Inc. (Rockford, IL, USA). TRIzol® reagent were obtained from the

Ambion Inc. (Austin, TX, USA). *S*-nitroso-*N*-acetylpenicillamine (SNAP), PrestoBlue®, lipofectamine 2000 reagent and alexa Fluor 488-conjugated goat anti-rabbit IgG (H+L) secondary antibody was obtained from Invitrogen (Carlsbad, CA, USA). CD133 primary antibody was obtained from Cell Applications (San Diego, CA, USA) and Cav-1, anti-rabbit IgG-HRP, anti-mouse IgG-HRP primary antibody was obtained from Cell Signaling Technology (Beverly, MA, USA).

Methods

Cell culture

Human non-small cell lung cancer NCI-H292 and NCI-H460 cells were cultured and maintained in the Roswell Park Memorial Institute (RPMI) 1640 medium, supplemented with 10% fetal bovine serum (FBS), 2 mM L-glutamine and 1% penicillin/streptomycin at 37°C in a 5% CO_2 humidified incubator. For experiments, cells were seeded into six-well plates at an initial plating density of 2×10^5 cells/well. Cells were allowed to adhere to the surface of the plates for 4 hours after which they were treated with the indicated concentrations of freshly prepared NO donor, PTIO or not treated in the case of the control cells. The treated cells were sub-cultured and exposed to fresh NO every three days. The cells were subsequently collected at day 7 and day 14 post-treatment for further analysis.

Treatment preparation

DPTA NONOate, SNAP and PTIO were all dissolved with PBS to make a stock solution concentration of 10,000 μM. Small amount of all treatments were aliquots into

eppendrops in order to reduce any unnecessary freeze-thaw cycles. Stock solutions were kept in -20°C.

Cytotoxicity assay

Cells were seeded into 96-well plates at the density of $1x10^4$ cells/well and were allowed to settle overnight. Cells were then treated with various concentrations of DPTA NONOate and analyzed for cell viability using 3-(4,5-dimethylthiazol-2-yl)-2,5-diphenyltetrazolium bromide (MTT) assay according to the manufacturer's protocol. Briefly, after 24 hours of treatment, the medium was replaced with 100 µl of 0.5 mg/ml MTT solution and was incubated in 37°C in a 5% CO_2 humidified incubator, with the absent of light for 4 hours. MTT solution was then replaced with 100µl of DMSO in order to dissolve the formed formazan crystals. Absorbance was detected at a wavelength of 570nm by Anthros microplate reader (Durham, NC, USA). The cell viability was calculated by dividing the optical density (OD) of the treated cells by that of the control cells.

$$\% \text{ Cell viability} = \frac{OD_{570} \text{ treatment}}{OD_{570} \text{ control}} \times 100$$

Apoptosis and necrosis evaluation assay

Similar to the cell viability assay, NCI-H292 or NCI-H460 cells were previously seeded into 96-well plates at the concentration of $1x10^4$ cells/well and were allowed to settle overnight. The cells were then treated with varied dose of DPTA NONOate. After 24 hours, cells were then incubated with 10 µg/ml of Hoechst 33342 and 5 µg/ml of

propidium iodide (PI) for 30 minutes at 37°C. Hoechst stained the apoptotic cells with fragmented nuclei and/or condensed chromatin while PI positively stained dead necrotic cells. The fluorescence images were visualized and captured under a fluorescence microscope (Olympus IX51 with DP70).

Cell proliferation assay

NCI-H292 and NCI-H460 untreated cells and the treated day 7 and day 14 cells were previously seeded onto 96-well plates at the density of $5x10^3$ cells/well and were left to settle overnight. Cells were then treated with varied dose of DPTA NONOate. Cell proliferation was determined at 24, 48 and 72 hours by PrestoBlue® assay according to the manufacturer's protocol (Invitrogen).

Plasmid transient and stable transfection

Transient transfection of over express Cav-1 and its knockdown shRNA plasmids was performed on sub confluent (70%) monolayers of NCI-H292 and NCI-H460 cells by transfecting with pEX_Cav-1-YFP (ATTC) or shRNA-Cav-1 (Santa Cruz) plasmid in serum-free RPMI 1640 medium using Lipofectamine 2000 reagent, according to the manufacturer's protocol (Invitrogen). After 2 hours (NCI-H292) or 12 hours (NCI-H460), the medium was replaced with RPMI 1460 containing 10% FBS. To obtain stable transfectants, cells were then cultured and selected with appropriate antibiotic for 30 days. Expression of the Cav-1 was verified by Western blot assay. The cells were cultured in antibiotic-free RPMI 1640 medium for at least two passages before further experiments.

Cell morphology characterization assay

NCI-H292 and NCI-H460 treated cells at day 7 and day 14 and untreated cells were wash thoroughly with PBS and 1 ml of complete RPMI 1640 medium was added per well. Phase contrast images were visualized and captured under a phase contrast microscope (Olympus IX51 with DP70).

Cell migration assay

Wound-healing assay was used to determine cell migration. NCI-H292 and NCI-H460 treated day 7 and day 14 cells and untreated cells were seeded into 96-well plates at the concentration of $2x10^4$ cells/well and were allowed to settle overnight. The overnight medium was removed and each well were scratched equally using a 20-200 µl pipette tip. Two lines were drawn perpendicularly to the scratched line on the bottom of each well using thin tip marker pen. The lines were used as reference to pin point the exact position of four fields for image capturing during each time point. 100 µl of fresh RPMI 1640 medium was added into each well before imaging. The phase contrast images were visualized and captured under a phase contrast microscope (Olympus IX51 with DP70).

Cell invasion assay

The cell invasion assay was performed in modified Boyden chambers with 8 µm pore filter inserts in 24-well plates (Corning Life Sciences). The upper chambers of the inserts were coated with 50 µL of 0.5% Matrigel from BD Biosciences (San Jose, CA,

USA) before the addition of NCI-H292 or NCI-H460 3×10^4 cells in serum-free medium. The lower chamber was filled with RPMI 1640 medium containing 10% FBS as a chemo attractant. Cells were allowed to invade for 24 hours before the non-invading cells in the upper chamber were removed with a cotton swab and the invading cells in the lower chamber were fixed with ice-cold methanol for 10 minutes and stained with 10 μg/mL of Hoechst 33342 for 30 minutes. The stained cells were then visualized and scored under a fluorescence microscope (Olympus IX51 with DP70).

Anoikis assay

NCI-H292 or NCI-H460 cells treated for 7 and 14 days and untreated cells were trypsinized into single cell suspension before seeding onto separated Costar® 6-well ultralow attachment plates (Corning Life Sciences) at a density of 5×10^5 cells/well in complete RPMI 1640 medium. Suspended cells were incubated at 37°C in a 5% CO_2 humidified incubator. At various time points, cells from each treatment wells were titulated and 4 lots of 100 μl of the cell suspension was harvested and seeded onto 4 independent wells in a 96 well-plate. Cell viability was assessed by MTT assay.

Anchorage-independent growth assay

Anchorage-independent cell growth was determined by soft agar colony formation assay. Soft agar was prepared by using a 1:1 mixture of RPMI 1640 medium containing 10% FBS : 1% agarose. 500 μl/well of the mixture was added onto 24-well plates and was allowed to solidify in 4°C refrigerator for 5 minutes in order to form a bottom layer. Then an upper cellular layer consisting of $3x10^3$ cells/mL in 2:1 agarose gel mixture of

RPMI 1640 medium containing 10% FBS : 1% agarose was added on top of the bottom layer. The upper layer was left to solidified at 37°C in a 5% CO_2 humidified incubator for two hours before 500 μl of RPMI 1640 medium containing 10% FBS was added to the system. Colonies were allowed to form at 37°C in a 5% CO_2 humidified incubator for 2 weeks. Colony formation was determined and captured using a Canon PowerShot G12 camera and a phase contrast microscope (Olympus IX51 with DP70).

Spheroids formation assay

Primary and secondary spheroids were grown using adjusted method from Kantara et al (Kantara, 2014). NCI-H292 or NCI-H460 cells were washed with PBS and made into cell suspension using 1mM EDTA before seeding approximately 5×10^3 cells/well onto 12-wells ultralow attachment plate using RPMI 1640 serum free medium and allowed to form spheroids in a 37°C, 5% CO_2 humidified incubator. Treated cells were treated every three days identical to normal treatment cycle. Phase contrast image of formed primary spheroids were taken at day 7 of treatment using a phase contrast microscope (Olympus IX51 with DP70). Primary spheroids were then resuspended into single cells by using 1mM EDTA and again 5×10^3 cells were seeded onto 12-wells ultralow attachment plate in 1ml of RPMI 1640 serum free medium per well. Again, treated cells were treated every three days. Secondary spheroids were allowed to form in a 37°C, 5% CO_2 humidified incubator for 30 days. Phase contrast image of secondary spheroids were taken at day 30 of treatment using a phase contrast microscope (Olympus IX51 with DP70).

Western blot analysis

NCI-H460 and NCI-H292 treated day 7 and day 14 cells and untreated cells were washed with ice-cold PBS to remove unwanted fragments. Cell extraction were performed by incubating the cells with lysis buffer containing 1% Triton X-100, 150 mM NaCL, 50 mM Tris-HCl (pH 7.5), 20 mM EDTA, 50 mM NaF, 100 mM phenylmethylsulfonyl fluoride (PMSF) and complete Mini cocktail protease inhibitor for 45 minutes on ice. Insoluble debris were pelleted using centrifugation at 14,000g for 5 minutes at 4°C, cell lysates supernatant were collected and determined for protein content using Quick Start™ Bradford protein assay. Whole cells extracts were mixed with Laemmli loading buffer (225 mM Tris-HCL (pH 6.8), 6% SDS, 30% glycerol, 9% 2-mercaptoethanol and 0.009% bromphenol blue) and boiled at 95°C for 5 minutes. Identical amount of proteins (40 µg) were resolved on 7.5% or 10% SDS–polyacrylamide gel electrophoresis (SDS–PAGE) and transferred onto nitrocellulose membranes using standard procedures. The membranes were blocked with 5% non-fat dry milk in TBST (25 mM Tris–HCl, pH 7.4, 125 mM NaCl, 0.1% Tween 20) for 30 minutes, followed by incubation with appropriate primary antibodies at 4°C overnight. Membranes were then washed three times with TBST for 10 minutes, followed by incubation with horseradish peroxidase-coupled isotype-specific secondary antibodies for 2 hours at room temperature. The immune complexes were detected by chemiluminescence and quantified by imaging densitometry using analyst/PC densitometry software (Bio-Rad Laboratories, Hercules, CA).

Immunofluorescence assay

Glass cover slips (20 mm x 20 mm) were soaked in ethanol, washed with PBS and placed onto each well in a 6-well plate before being left in a lamina hood UV for 30 minutes. NCI-H460 and NCI-H292 cells treated for 14 days and untreated cells were washed with ice-cold PBS and trypsinized into cell suspension. Cells were seeded onto the previously prepared 6-well plates at the density of $5x10^5$ cells/well and allowed to adhere for 24 hours. The cells were fixed at room temperature for 10 minutes with 3.7% formaldehyde, permeabilized and then blocked for 30 minutes in a PBS solution containing 0.5% saponin and 1% FBS. Cells were then incubated with CD133 (Cell Applications) primary antibody for 2 hours before being washed and incubated with Alexa Fluor 488-conjugated goat anti-rabbit IgG (H+L) secondary antibody (Invitrogen) for 1 hour. The glass cover slips were lifted off the 6-well plates and soaked in Tween 20. Excess amount of Tween 20 was allowed to drip off before placing the cove slip faced down onto microscope slide. The clover slip was mounded onto the slide with clear nail polish. Immunofluorescence images were acquired by fluorescence microscope (Olympus IX51 with DP70).

Flow cytometry analysis

NCI-H460 and NCI-H292 treated day 14 cells and untreated cells were washed with PBS and collected using 1 mM EDTA solution. Briefly, cells were fixed and blocked then incubated on ice with CD133 primary antibody for 1 hour. Followed by 30 minutes incubation with Alexa Fluor 488-conjugated goat anti-rabbit IgG (H+L) secondary antibody, on ice and omitted from light. Fluorescence intensity was scored by flow

cytometry using a 488-nm excitation beam and a 519-nm band-pass filter (FACSort, Becton Dickinson, Rutherford, NJ). The mean fluorescence intensity was quantified by CellQuest software (Becton Dickinson).

Microarray analysis

Total RNA of NCI-H460 untreated cells and the treated day 14 cells were isolated using TRIzol® reagent according to the manufacturer's protocol. The total RNA concentration and purity were measured using Thermo Scientific NanoDrop 2000 spectrophotometer (Rockford, IL, USA). The RNA integrity number (RIN) was measured using Agilent's 2100 Bioanalyzer (Santa Clara, CA, USA) before shipping the total RNA sample to Origen Laboratories Ltd. (Singapore) for microarray analysis. CU-DREAM program was used to analyzed the raw data and gene probes with significant differences ($p<0.01$) were chosen for further evaluation using the Bioconductor R statistic program (Aporntewan, 2011).

Statistical analysis

All data were expressed as mean ± S.D. The reproducibility of the results was confirmed in at least three independent sets of experiments. Data shown in figures were from a representative set of experiments after normalized to the results of the non-treated controls. Statistical differences were determined using two-way ANOVA for repeated measures and a post hoc test for group comparison. $P < 0.05$ were considered as statistically significant.

Experimental design

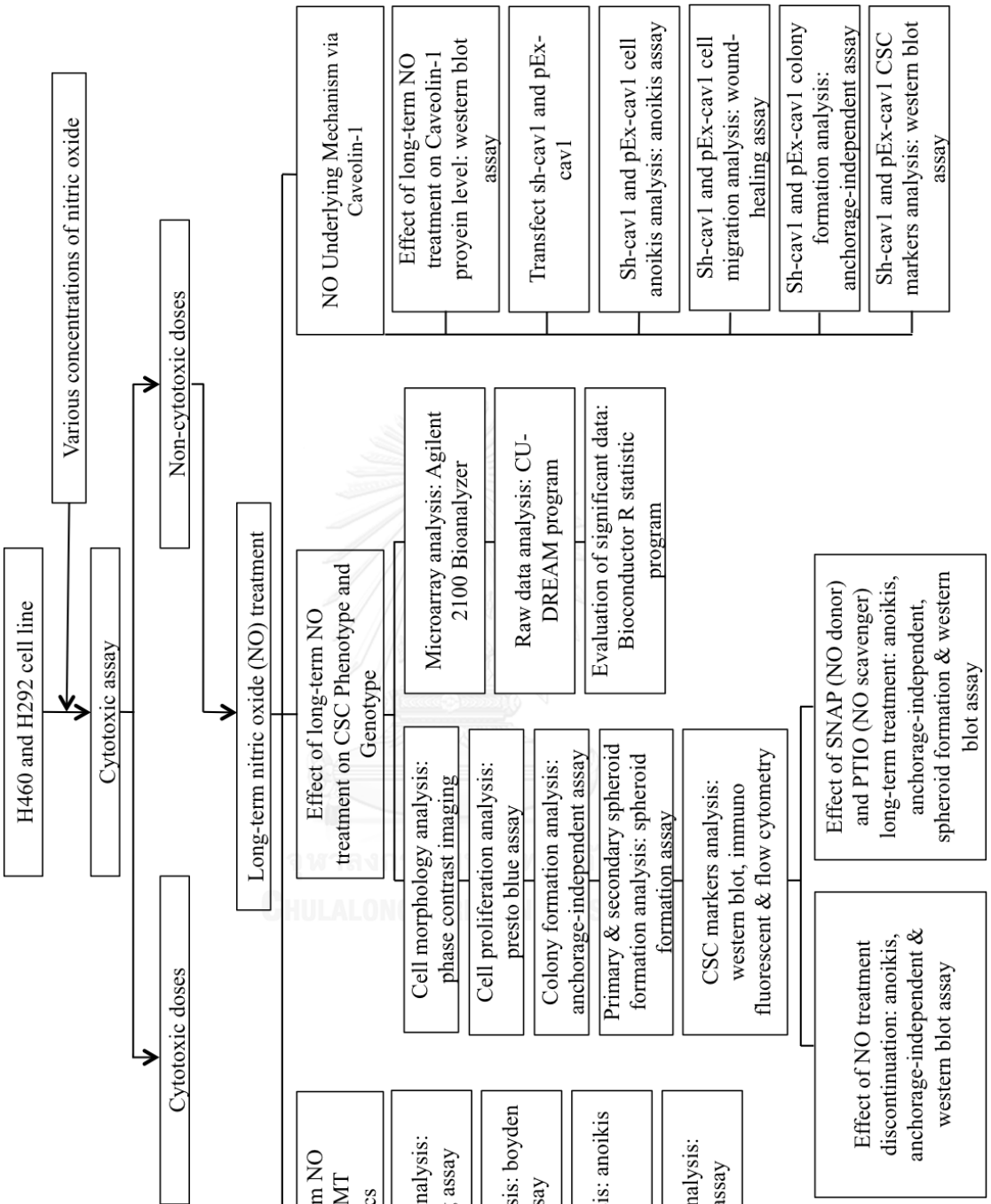

CHAPTER IV

RESULTS

Effect of DPTA NONOate on human lung cancer cell viability

DPTA NONOate cytotoxicity in H292 and H460 cell lines

Elevated NO levels have been associated with cancer cell behaviors such as anoikis resistance, increased cell motility, and chemoresistance (Sanuphan, 2013, Wongvaranon, 2013, Chanvorachote, 2006). To test whether NO might affect stem-like properties of lung cancer cells, first, the appropriate non-cytotoxic concentrations of NO donor was determined. Human lung cancer H292 and H460 cells were treated with various concentrations of DPTA NONOate (0-50 μM) and cell viability was determined after 24 hours by MTT assay. Figure 7A and B shows that DPTA NONOate was relatively non-toxic at the doses below 30 μM in H292 cells and 15 μM in H460 cells. Therefore, the DPTA NONOate doses chosen for further study are 0 μM, 10 μM and 25 μM for H292 cells and 0 μM, 5 μM and 10 μM for H460 cells where the 0 μM would be established as the non-treated control cells.

Low dose DPTA NONOate does not induce apoptotic nor necrotic cell death

Apoptosis and necrosis assays by Hoechst 33342 and PI staining further showed the absence of apoptotic and necrotic cell death in the low-dose DPTA treatments as indicated by the lack of DNA condensation/fragmentation and nuclear PI fluorescence, respectively (Fig. 8A and B).

A

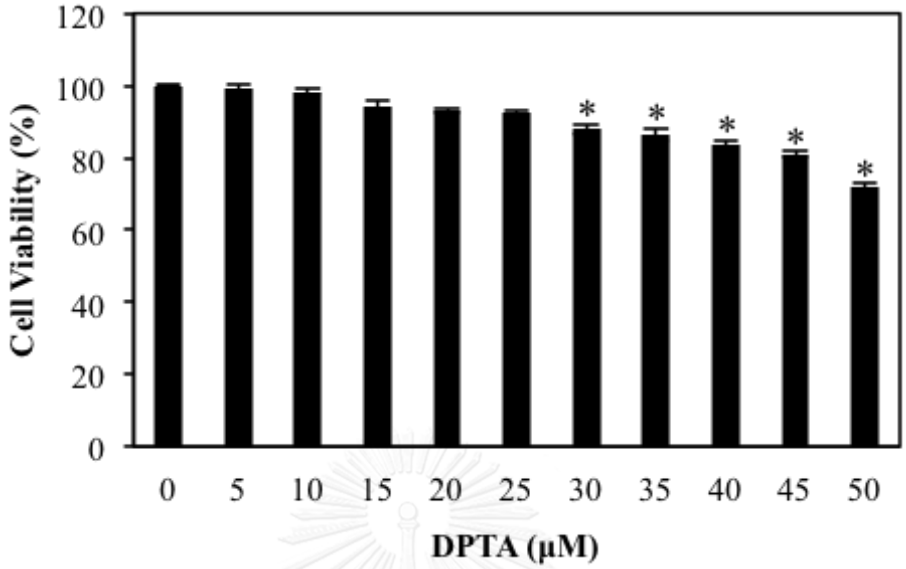

B

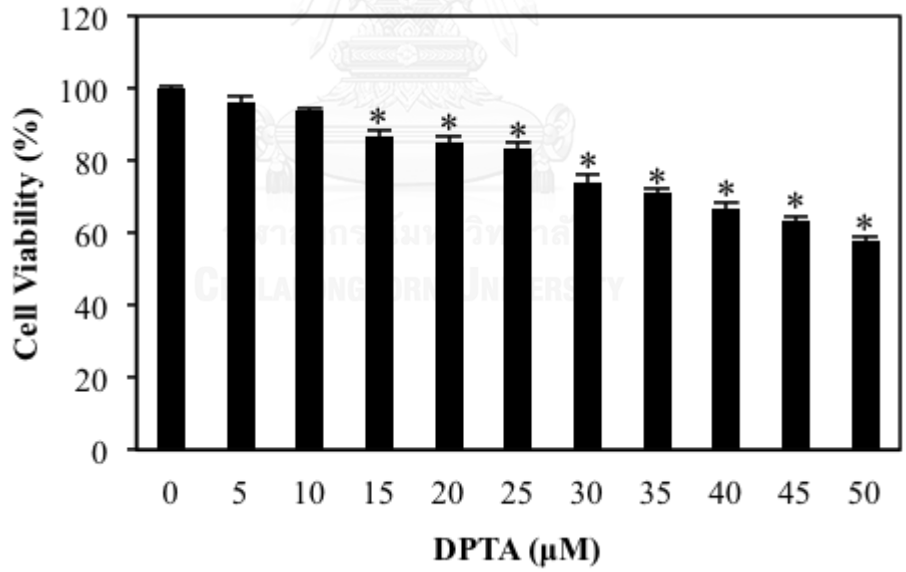

Figure 7 DPTA NONOate cytotoxicity in H292 and H460 cell lines. H292 (**A**) and H460 (**B**) cells were treated with various concentrations of DPTA NONOate (0-50 µM) for 24 h. Cell viability was determined by MTT assay. Plots are mean ± SD (n=4). *, $p < 0.05$ versus non-treated cells.

A

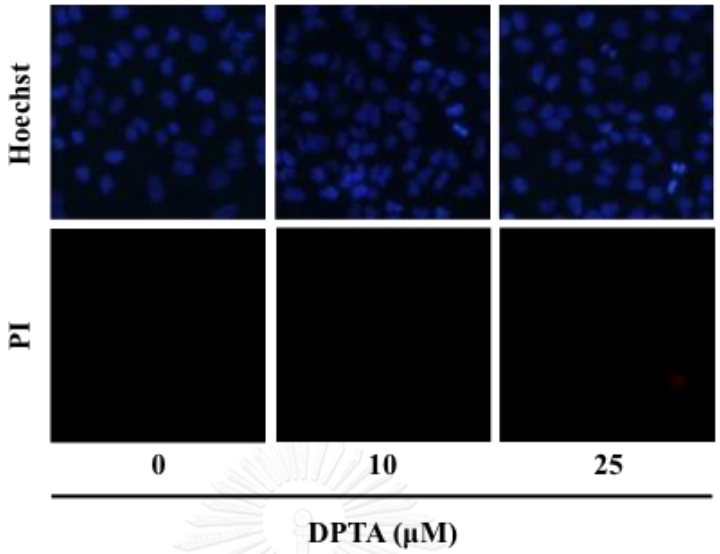

B

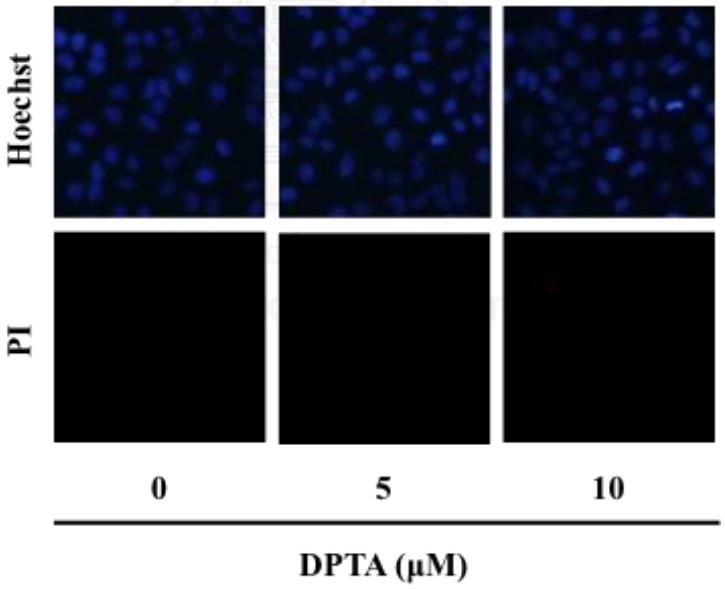

Figure 8 Effect of low-dose DPTA NONOate on H292 and H460 apoptotic and necrotic cell death. H292 (**A**) and H460 (**B**) cells were treated with two sub-cytotoxic concentration of DPTA NONOate, apoptosis and necrosis was determined by Hoechst 33342/propidium iodide staining assay.

Effect of long-term NO exposure on Human Lung Cancer Cell Epithelial-Mesenchymal Transition (EMT)

Long-term NO exposure increase cell motility

Having confirmed that the chosen DPTA sub-toxic doses does not induce H292 and H460 cells to undergoes apoptosis or necrosis cell death; cells were then cultured and treated for 7 and 14 days before being collected for further investigation. The effects of NO donor treatment on EMT characteristics such as cell migration, invasion and anoikis properties were examined. Cell migration and invasion were analyzed by wound healing and Boyden chamber invasion assays, respectively. Figure 9 and 10 shows that, in both cell lines, the motility rate of NO-treated cells were significantly increased relative to the non-treated controls. A 2.5-fold increase in the migration rate was observed in the H292 cells treated with 25μM of DPTA for 14 days (Fig. 9A), and a 2.3-fold increase was observed in the H460 cells treated with 10 μM of DPTA (Fig. 9B). Invasion assay similarly indicates the induction of cell invasivity in both cell lines by the NO donor in a dose- and time-dependent manner (Fig. 10A and B).

Not only EMT cells are well known for its metastatic ability, also previous studies have shown that CSCs possess increased cell motility for more efficient metastasis to secondary sites (Charafe-Jauffret, 2009, Croker, 2009, Hermann, 2007).

A

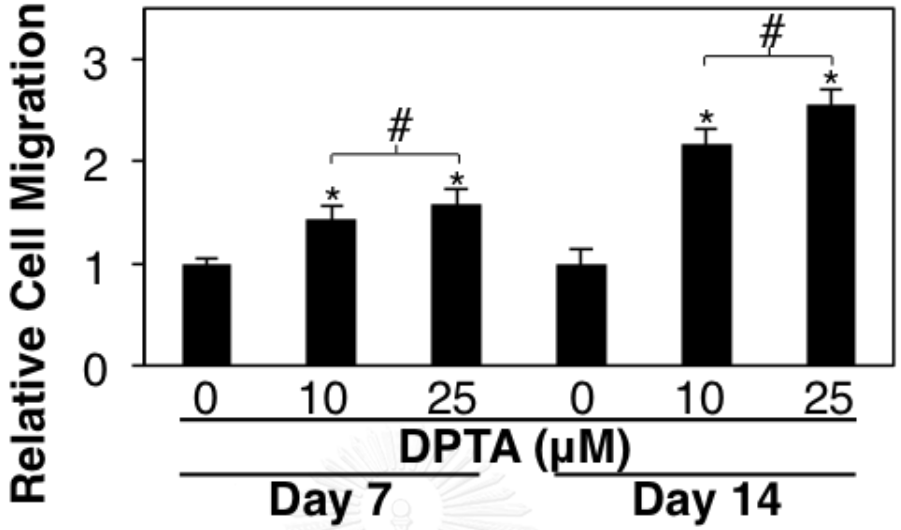

B

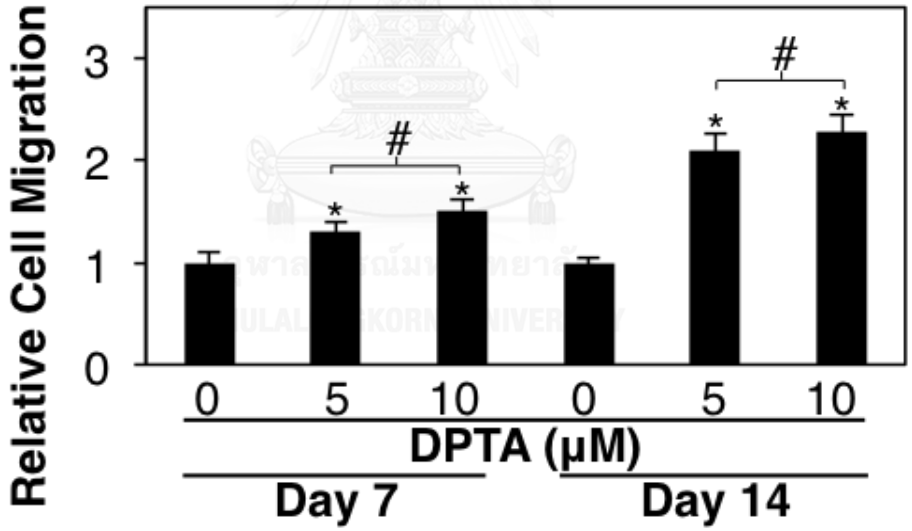

Figure 9 Effect of long-term NO exposure on H292 and H460 cell migration. Cell migration of H292 (**A**) and H460 (**B**) day 7 and day 14 cells was determined by wound-healing assay. The wound space from random fields were measured and represented as relative migration to the control cells. Plots are mean ± SD (n=4). *, $p < 0.05$ vs. non-treated cells. #, $p < 0.05$ vs. DPTA NONOate-treated cells.

A

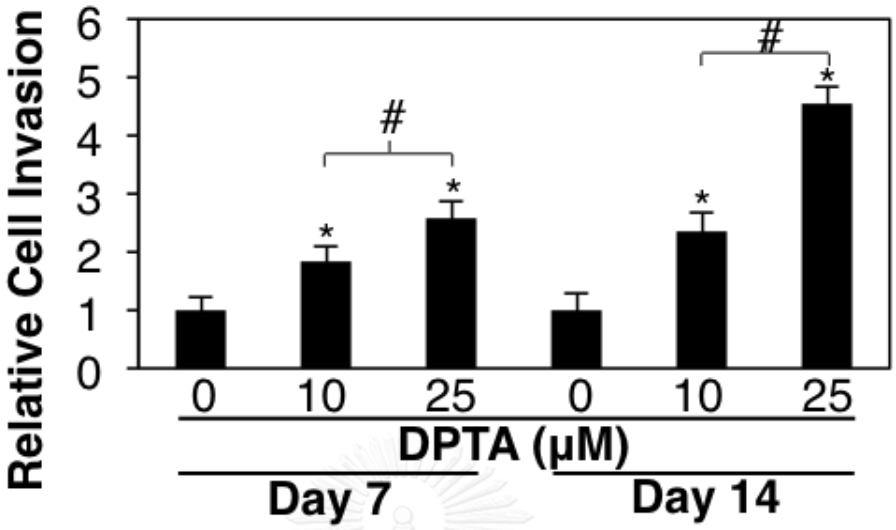

B

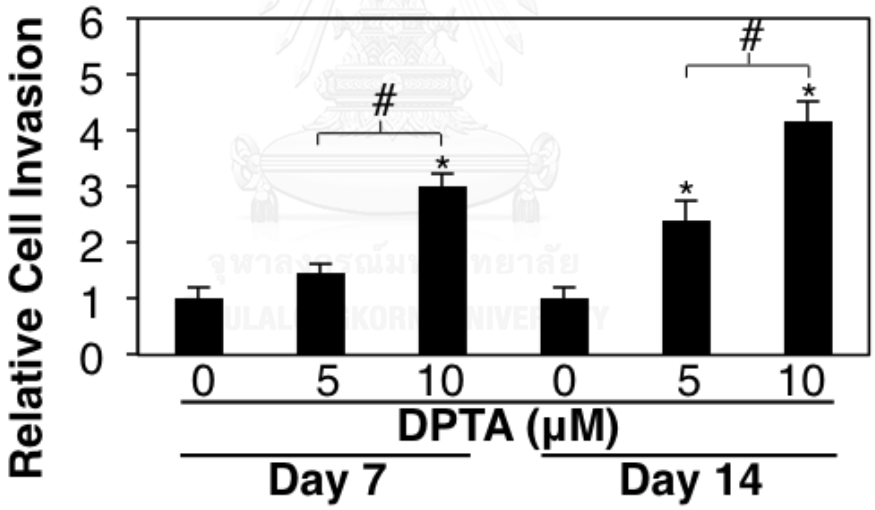

Figure 10 Effect of long-term NO exposure on H292 and H460 cell invasion. Invasive behavior of H292 (**A**) and H460 (**B**) day 7 and day 14 cells was evaluated by Boyden chamber assay. Invading cells attached to the lower side of the membrane filter were counted and represented as relative cell invasion to the control cells. Plots are mean ± SD (n=4). *, $p < 0.05$ vs. non-treated cells. #, $p < 0.05$ vs. DPTA NONOate-treated cells.

Long-term NO exposure induces anoikis resistance

Resistance to anoikis or detachment-induced apoptosis is a hallmark of aggressive cancer cells that have EMT or CSC properties. Figure 11A and B illustrates the viability of H292 and H460 cells in response to cell detachment. Cells were first treated with NO donor for 7 and 14 days, and analyzed for anoikis response at different time points. The results showed that the treated cells exhibited a significantly reduced anoikis response as compared to the non-treated controls, suggesting the ability of NO to induce EMT-like or CSC-like anoikis resistant phenotype.

Long-term NO exposure escalates EMT markers

H292 and H460 cells were treated with non-toxic dose of DPTA NONOate for 7 and 14 days before the cell lysate were collected for western blot analysis. The cells population lysate were probed for EMT markers, Vimentin and Snail by Western blotting. Figure 12A and B shows that the NO donor significantly induced Vimentin and Snail expression in a dose- and time-dependent manner. Approximately up to 4-fold increase in both Vimentin and Snail protein level were shown for H292 cells treated with 25 μM of DPTA for 14 days and approximately 3-fold for H460 cells treated with 10 μM of DPTA for 14 days.

A

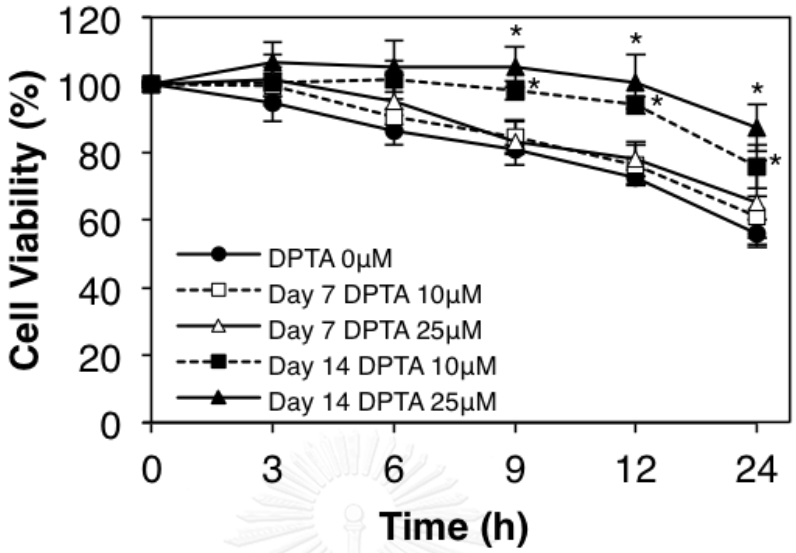

B

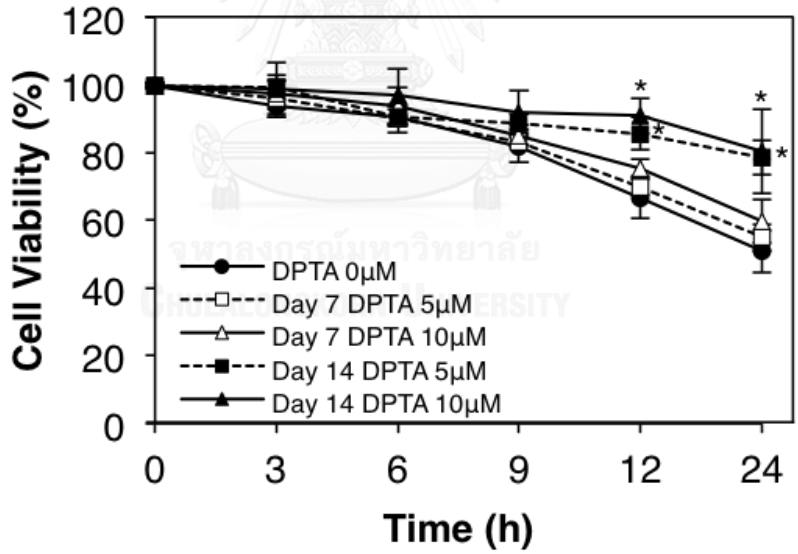

Figure 11 Effect of long-term NO exposure on H292 and H460 anoikis cell death. H292 (**A**) and H460 (**B**) cells were treated with DPTA NONOate for 7 and 14 days, and analyzed for anoikis by measuring the viability of detached cells at various time points by MTT assay.

A

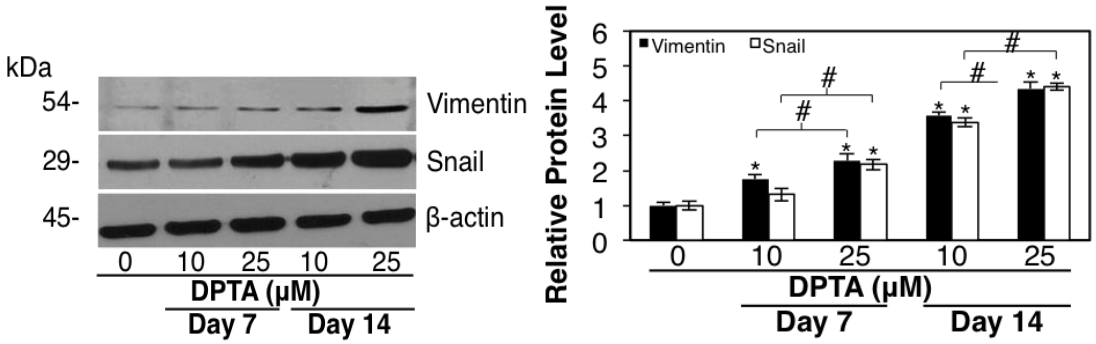

B

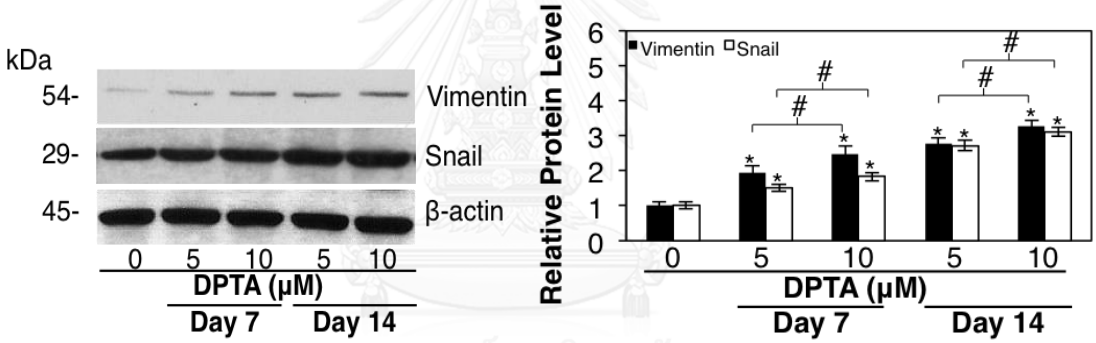

Figure 12 Effect of long-term NO exposure on EMT markers. H292 (**A**) and H460 (**B**) cells were treated with DPTA NONOate (0-25 μM) for 7 and 14 days, and analyzed for EMT markers, Vimentin and Snail, by Western blotting. The blots were reprobed with β-actin to confirm equal loading of the samples. Blots were quantified by densitometry, and mean data from independent experiments were normalized and presented. Plots are mean ± SD (n=4). *, $p < 0.05$ vs. non-treated cells. #, $p < 0.05$ vs. DPTA NONOate-treated cells.

Long-term NO exposure promotes CSC-like characteristics in human lung cancer cells

Effect of long-term NO exposure on cells morphology

To determine the effect of NO donor treatment on cell morphology, H292 and H460 cells were treated with the non-cytotoxic concentrations of DPTA NONOate and cell morphology was examined microscopically. Figure 13A and B shows phase contrast images of the treated cells on day 7 and 14 post-treatment. A gradual but clearly noticeable change in cell morphology towards the mesenchymal stem cell-like (spindle-like) phenotype was evident in both the H292 and H460-treated cells compared to non-treated controls.

Effect of long-term NO exposure on cells proliferation

Stem cells are known to be slow proliferators. Figure 14A and B shows that the DPTA treatment resulted in a significant reduction in the proliferation rate of both H292 and H460 cells. H292 treated with 25 μM of DPTA for 14 days grew 60% slower than non-treated controls. Similarly, H460 cells treated with 10 μM of DPTA for 14 days proliferate 54% slower than the control cells.

A

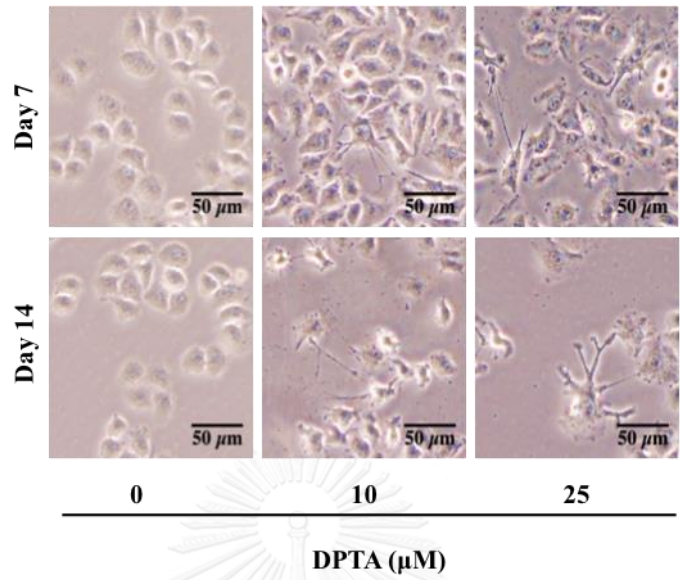

B

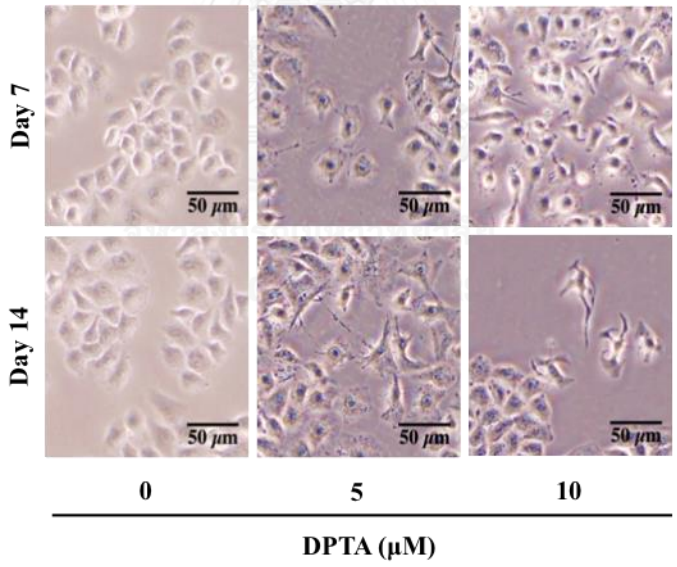

Figure 13 Effect of long-term NO exposure on H292 and H460 cell morphology. H292 (**A**) and H460 (**B**) cells were continuously treated with DPTA NONOate and cell morphology was examined by phase contrast microscopy after 7 and 14 days of treatment (10X). [Scale bar: 50 μm]

A

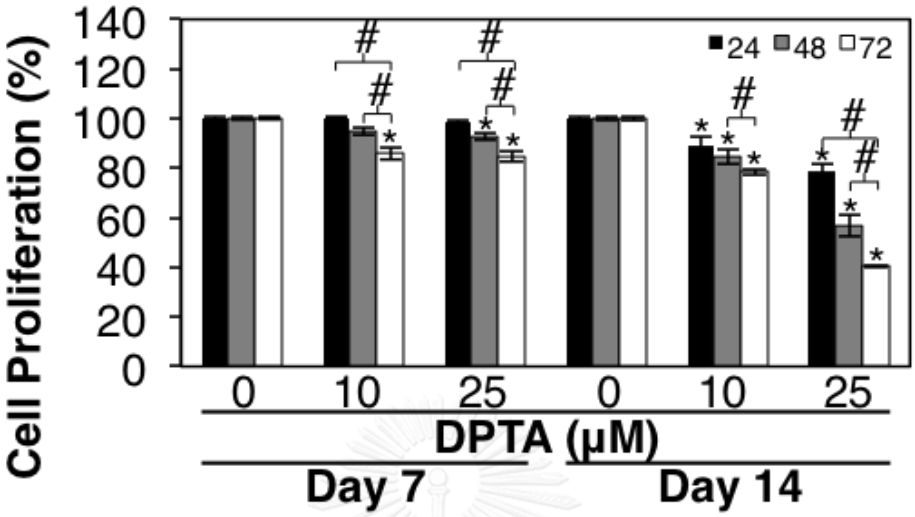

B

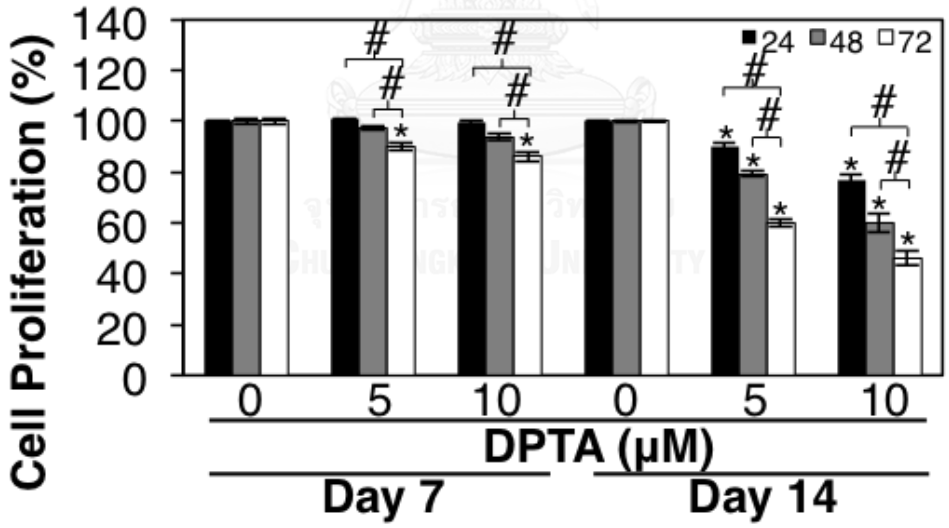

Figure 14 Effect of long-term NO exposure on H292 and H460 cell proliferation. H292 (**A**) and H460 (**B**) cells were treated with DPTA NONOate for 7 and 14 days, and analyzed for cell proliferation at 24, 48 and 72 hours by MTT assay. All plots are mean ± SD (n=4). *, $p < 0.05$ vs. non-treated cells. #, $p < 0.05$ vs. DPTA NONOate-treated cells.

Effect of long-term NO exposure on colony and spheroid formation

Finally, long-term NO exposed cells were tested for colony and spheroids formation, a distinguishing feature of CSCs.

Effect of long-term NO exposure on colony formation

H292 and H460 cells were similarly treated with the NO donor and analyzed for colony formation in anchorage-independent soft agar assay. Colony number and diameter were determined and expressed as relative values over non-treated control levels. Figure 15A displays the relative colony number and diameter of the treated and non-treated H292 cells. A significant (2.1-fold) increased in the number of colonies formed was recorded for the H292 cells treated with 10 μM of DPTA NONOate for 14 days, and a 2.5- and 3.4-fold increased was observed for the cells treated for 7 and 14 days with 25 μM of DPTA NONOate, respectively. For H460 cells, a significant increase in the colony number can only be seen for the high treatment dose of 10 μM at day 7 (2.7-fold) and day 14 (3.3-fold) (Fig. 16A). However, both treated cell lines showed no significant difference in the colony diameter when compared to controls. Representative images of the H292 and H460 colonies are shown in figure 15B and 16B with the circular photograph representing 1X image and the square representing 10X image of the colonies.

A

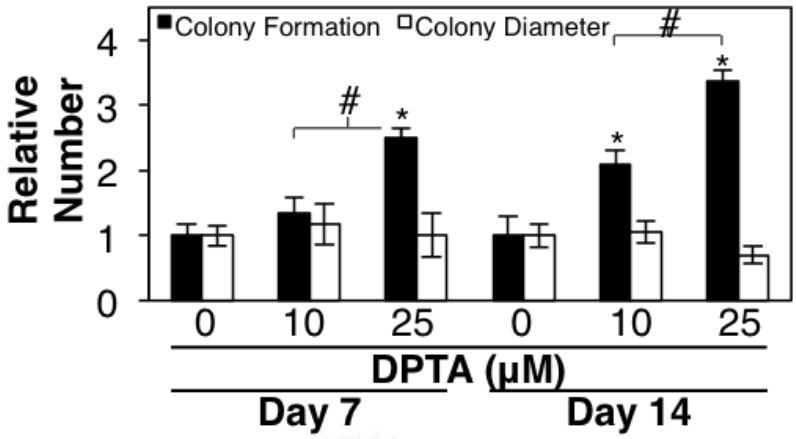

B

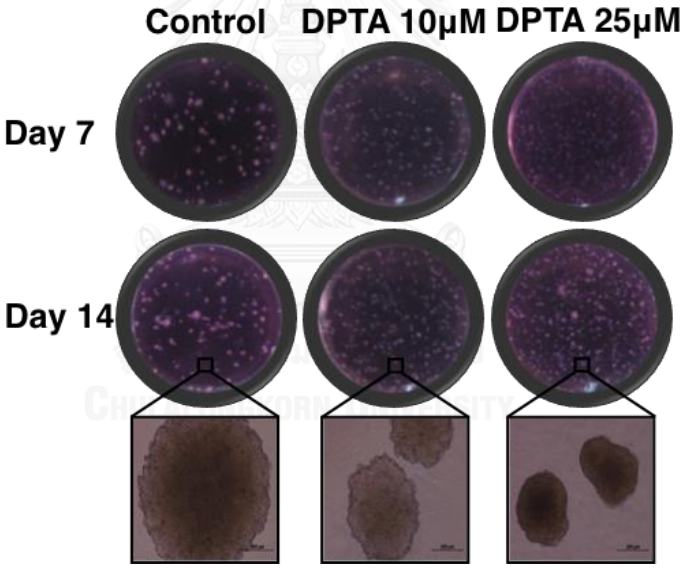

Figure 15 Effect of long-term NO exposure on H292 colony formation. After being treated with DPTA NONOate (0-25 μM) for 7 and 14 days, H292 cells were suspended and subjected to colony formation assay. Colony number and size were analyzed and calculated as relative number to the control cells (**A**). Colony 1X and 10X images were captured after two weeks of growth (**B**). All plots are mean ± SD (n=4). *, $p < 0.05$ vs. non-treated cells. #, $p < 0.05$ vs. DPTA NONOate-treated cells. [Scale bar: 200 μm]

A

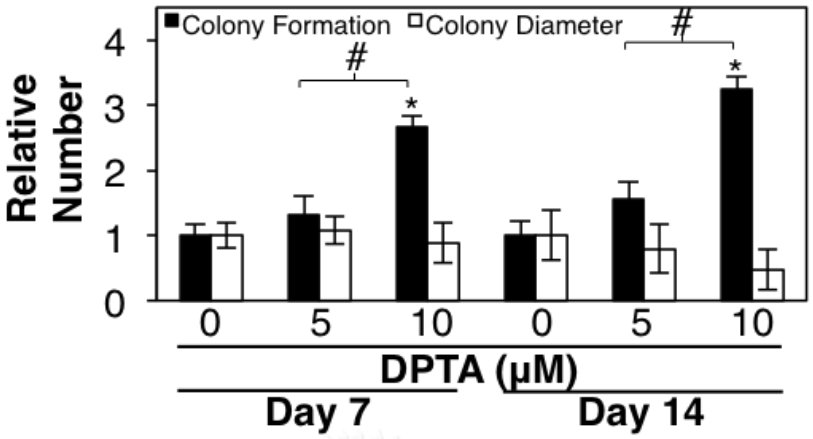

B

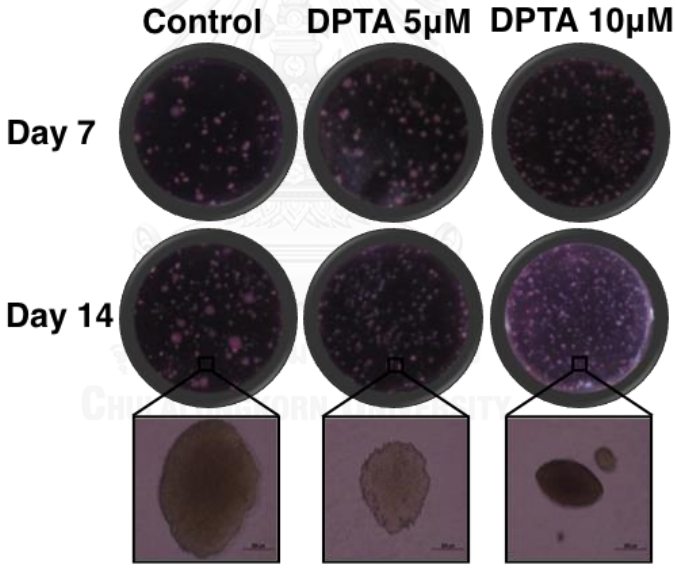

Figure 16 Effect of long-term NO exposure on H460 colony formation. After being treated with DPTA NONOate (0-10 μM) for 7 and 14 days, H460 cells were suspended and subjected to colony formation assay. Colony number and size were analyzed and calculated as relative number to the control cells (**A**). Colony 1X and 10X images were captured after two weeks of growth (**B**). All plots are mean ± SD (n=4). *, $p < 0.05$ vs. non-treated cells. #, $p < 0.05$ vs. DPTA NONOate-treated cells. [Scale bar: 200 μm]

Effect of long-term NO exposure on spheroid formation

Figure 17A and B displays 4X phase contrast image of day 7 H292 and H460 primary spheroids respectively. Cells were seeded at low density onto ultra-low attach plate and primary spheroids were allowed to formed for 7 days. Control non-treated cells tend to survive through E-cadherin mediated survival while DPTA NONOate treated cells can survive on their own as single cell and slowly proliferates to form dense spheroids. The primary spheroids were then re-suspended into single cells and secondary spheroids were allowed to grow for 30 days in RPMI serum free medium. By day 30, the control non-treated spheroids were deformed and had already undergone apoptosis, while DPTA NONOate treated spheroids still remains viable and intact [Fig. 18A and B].

A

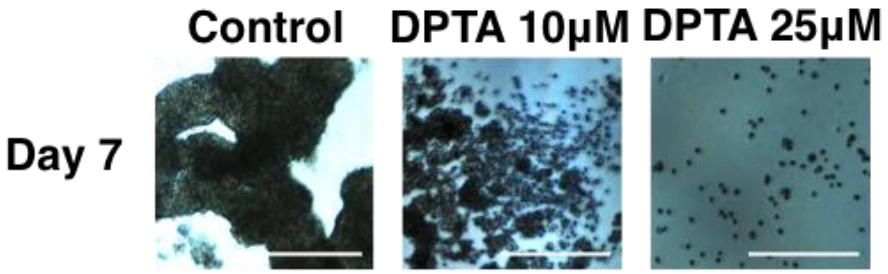

B

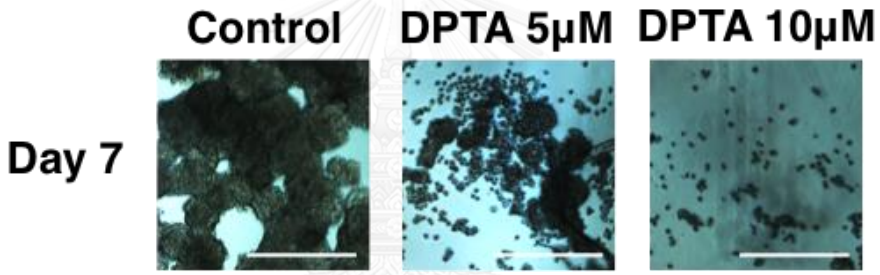

Figure 17 Effect of long-term NO exposure on H292 and H460 primary spheroid formation. 4X Phase contrast image of primary spheroids at day 7 were captured for H292 (**A**) and H460 (**B**) treated and non-treated cells. All plots are mean ± SD (n=4). *, $p < 0.05$ vs. non-treated cells. #, $p < 0.05$ vs. DPTA NONOate-treated cells. [Scale bar: 200 μm]

A

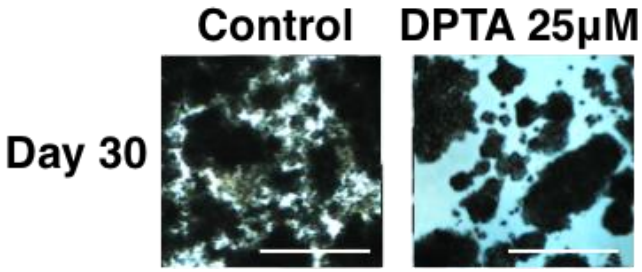

B

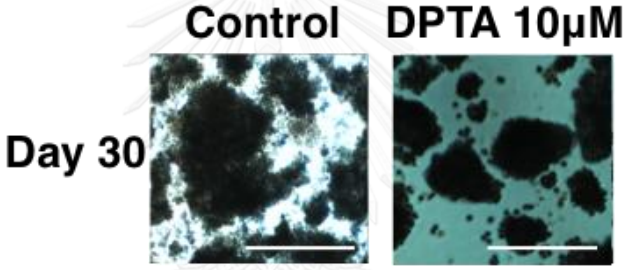

Figure 18 Effect of long-term NO exposure on H292 and H460 secondary spheroid formation. 4X Phase contrast image of secondary spheroids at day 30 were captured for H292 (**A**) and H460 (**B**) treated and non-treated cells. All plots are mean ± SD (n=4). *, $p < 0.05$ vs. non-treated cells. #, $p < 0.05$ vs. DPTA NONOate-treated cells. [Scale bar: 200 μm]

Long-term NO exposure induces CSC markers expression

Long-term NO exposures escalate CSC markers protein level

Two well-known CSC markers were used to verify the CSC-inducing effect of NO in H292 and H460 cells. The cells were cultivated in the presence or absence of DPTA NONOate for 7 and 14 days, the expression levels of CD133 and ALDH1A1 were determined by Western blotting. Figure 19A and B shows that the NO donor induced CD133 and ALDH1A1 expression in a dose- and time-dependent manner. A 7.1-fold increase in CD133 and 7.5-fold increase in ALDH1A1 expression were observed in the H292 cells treated with 25 μM of DPTA NONOate for 14 days (Fig. 19A). In H460 cells, a 4.8- and 5.8-fold increase in the two CSC markers expression was observed after treated with 10 μM of DPTA NONOate for 14 days (Fig. 19B).

Long-term NO exposures intensify CSC marker fluorescence

To confirm the results, immunofluorescence experiments were performed assessing the expression of CSC marker CD133 on the cells. H292 and H460 cells were treated with NO donor for 14 days and analyzed for CD133 expression by immunofluorescence staining (Fig. 20A and B). Consistent with the Western blot results, the immunofluorescence results indicate a dose-dependent increase in CD133 expression in both H292- and H460-treated cells.

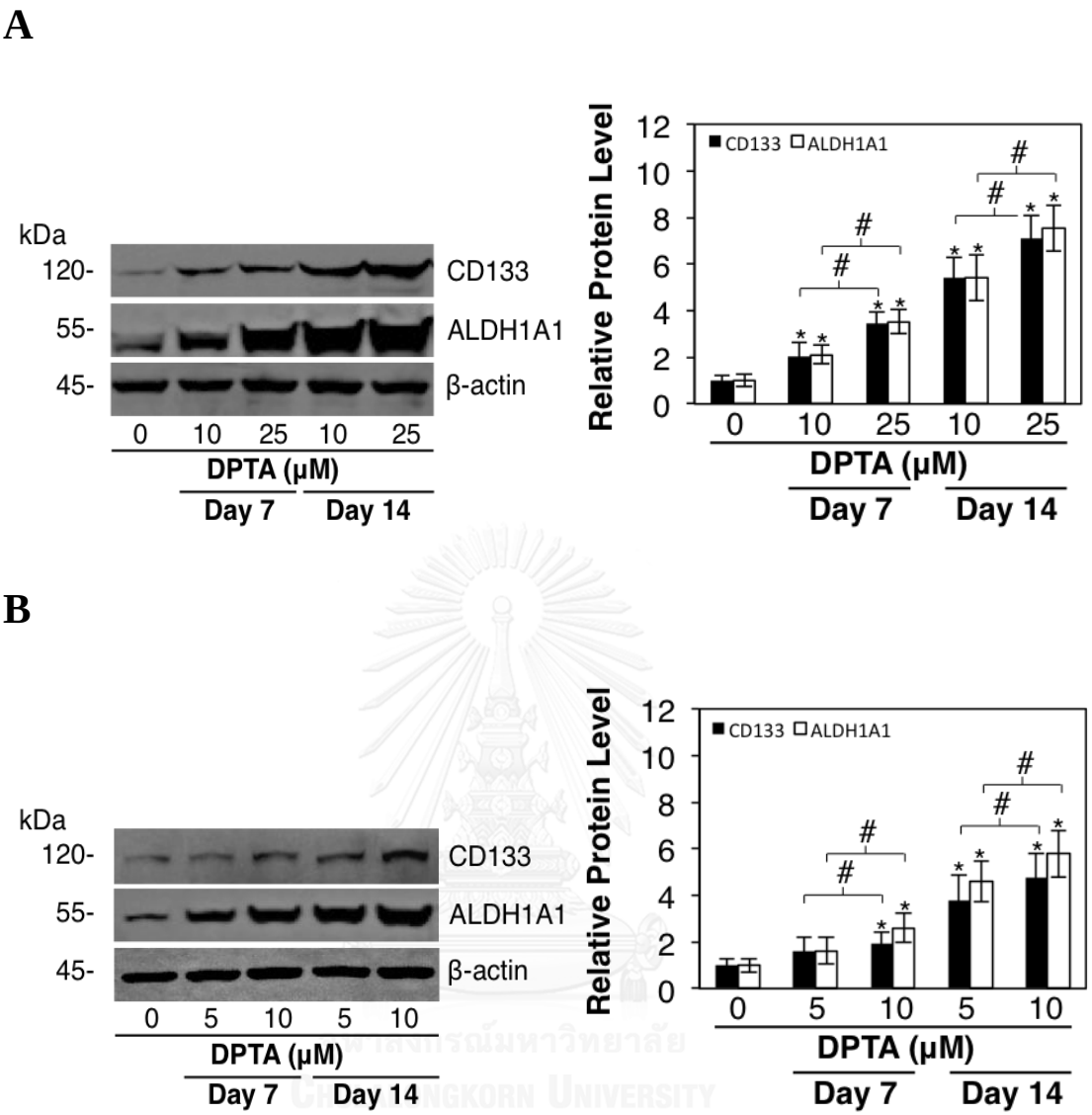

Figure 19 Long-term NO exposures escalate CSC markers protein level in H292 and H460 cell. H292 (**A**) and H460 (**B**) cells were treated with DPTA NONOate (0-25 μM) for 7 and 14 days, and analyzed for cancer stem cell markers, CD133 and ALDH1A1, by Western blotting. The blots were re-probed with β-actin to confirm equal loading of the samples. The immunoblot signals in H292 (**A**) and H460 (**B**) cells were quantified by densitometry, and mean data from independent experiments were normalized and presented. The bars are means ± SD (n=8). *, $p < 0.05$ vs. non-treated cells. #, $p < 0.05$ vs. DPTA NONOate-treated cells.

A

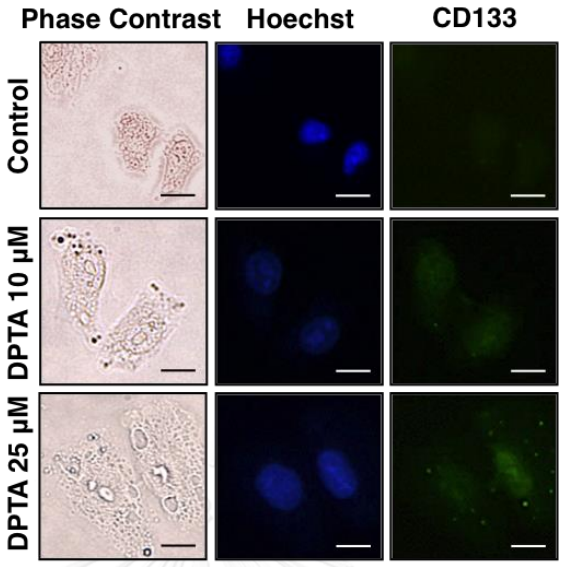

B

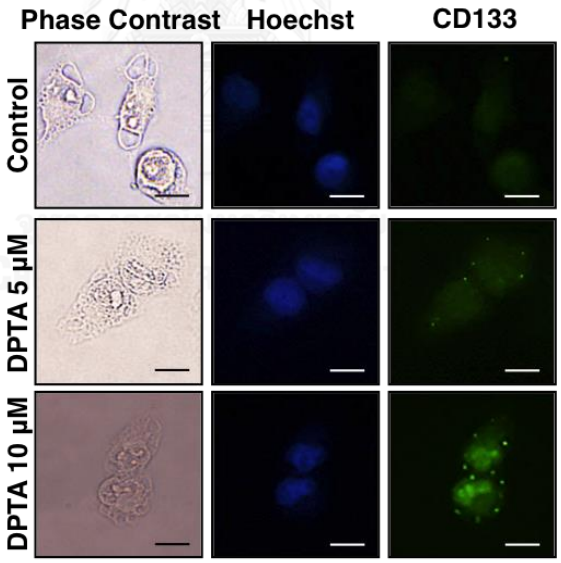

Figure 20 Long-term NO exposures intensify CSC marker fluorescence in H292 and H460 cell. The expression of CD133 in H292 (**A**) and H460 (**B**) cells were analyzed by fluorescence microscopy (40X). Cells were stained with Hoechst dye to aid visualization of the cell nucleus. [Scale bar: 10 μm]

Long-term NO exposure up-regulate CSC marker cell surface intensity

Furthermore, day 14 H292 and H460 treated and non-treated cells were analyzed for CD133 cell surface expression by flow cytometry, as shown in figure 21A and B respectively. CD133 on the cell surface intensify dose dependently for both cell type. The CD133 expression on each cell surface increases and the number of cells with high CD133 expression also increases. These results along with the findings of the NO effects on cell morphology and aggressive behaviors strongly support the role of NO in CSC-like properties of lung cancer cells.

Effect of long-term NO exposure on H460 genotype

H460 cells were treated with 10 μM of DPTA NONOate for 14 days before subjecting to microarray analysis. Raw data were analyzed by CU-DREAM program. Table 3 shows the analyzed data of the genes that encodes the focused EMT and CSCs marker proteins. *PROM1* gene encodes the CD133 protein; the gene expression increases but not significantly. Likewise the *ALDH1A1* gene that encode the ALDH1A1 protein, *CAV1* gene that encode the Cav-1 protein, *Vim* gene that encode the Vimentin protein and the *SNAI1* gene that encode the Snail protein all up regulated insignificantly. On the other hand, *CD24* and *THY1*, which are also established CSCs markers expression increased significantly (Table. 4). Also, the *NANOG* gene that was linked to CSCs pluripotency and *DDR1* gene that is a CSCs therapeutic target escalated significantly.

Gene probes with significant differences ($p < 0.01$, Fig. 22 or $p < 0.05$, Appendix B) were chosen for further evaluation using the Bioconductor R statistic program. A heat map was generated as an output of the Bioconductor R statistic program comparing the non-treated control H460 cells to the DPTA NONOate treated cells. The intensity of genes detected were represented by colors, ranging from white (high intensity), yellow, orange to red (low intensity). The cluster on the top indicates that the control and treated samples in n1 and n2 give similar result. The cluster on the left groups similar genes together, which suggest future pathways study.

A

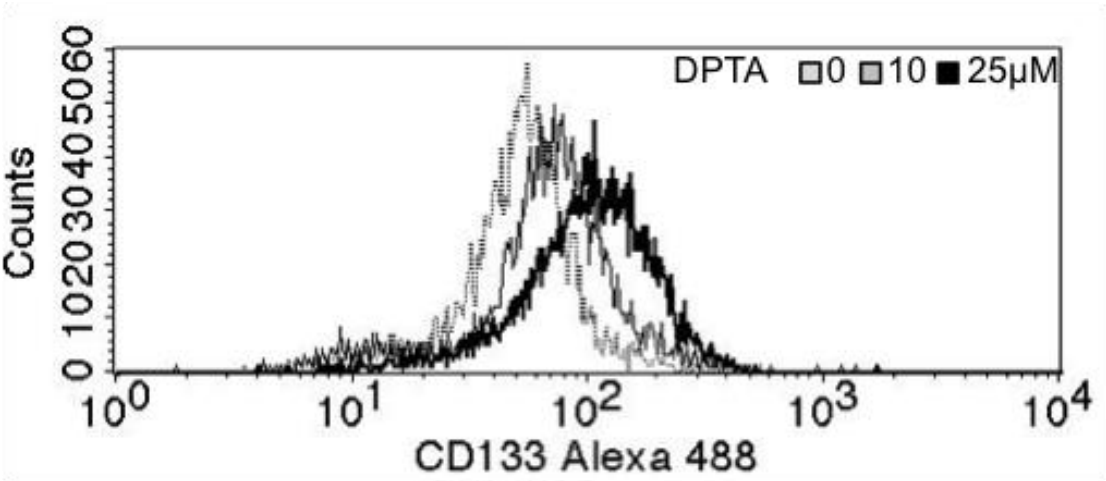

B

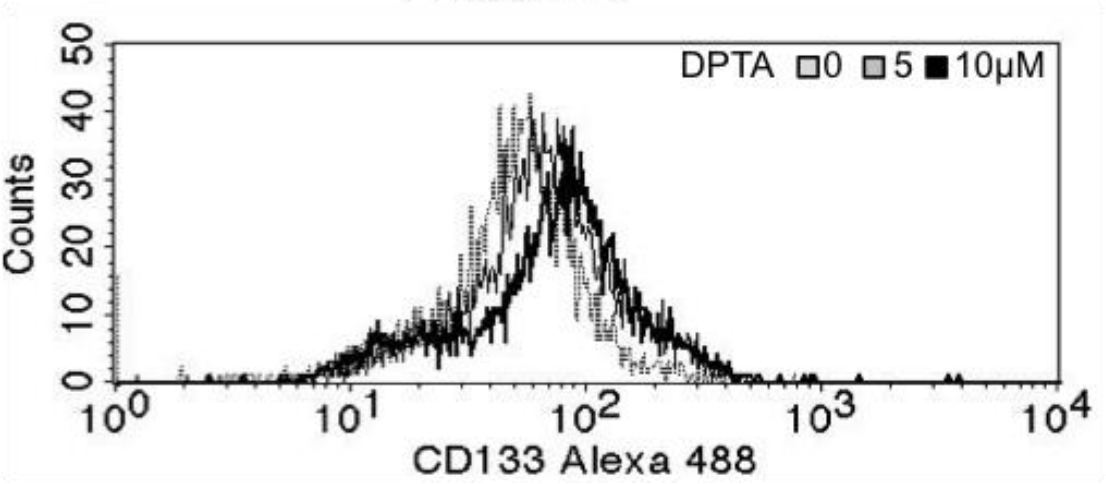

Figure 21 Long-term NO exposure up regulates CSC marker cells surface intensity in H292 and H460 cell. The level of CD133 cell surface expression was measured by flow cytometry for H292 (**A**) and H460 (**B**) treated and non-treated cells at day 14 of treatment.

Table 3 CU-DREAM analyzed data of genes that translate the focused EMT and CSCs proteins.

Probe ID	Gene Symbol	Gene Name	Control 1	Control 2	Treat1	Treat2	Treat mean – Control mean	*p*-value
8099476	NM_006017 /// NM_001145847 /// NM_001145848 /// NM_001145850 /// NM_001145849 /// NM_001145852 /// NM_001145851	*PROM1*	1.57	1.70	1.61	1.80	0.07	0.243
8161755	NM_000689	*ALDH1A1*	6.34	7.10	7.87	7.42	0.92	0.369
8135594	NM_001753 /// NM_001172895 /// NM_001172896 /// NM_001172897	*CAV1*	8.48	8.52	9.22	8.11	0.17	0.822
7926368	NM_003380	*VIM*	7.82	7.31	8.02	8.10	0.49	0.344
8063382	NM_005985	*SNAI1*	2.85	2.69	2.65	3.00	0.05	0.874

Table 4 CU-DREAM analyzed data of CSCs relate genes with $p < 0.05$.

Probe ID	Gene Symbol	Gene Name	Control 1	Control 2	Treat1	Treat2	Treat mean – Control mean	*p*-value
8177222	NM_013230	*CD24*	6.71	6.49	7.44	7.13	0.68	0.042
7952268	NM_006288	*THY1*	2.33	2.20	2.55	2.43	0.22	0.008
7953689	-	*NANOG P1 /// NANOG*	1.45	1.70	1.70	1.95	0.25	0.008
8117900	NM_001954 /// NM_013993 /// NM_013994	*DDR1*	3.48	3.38	3.88	3.78	0.41	0.001

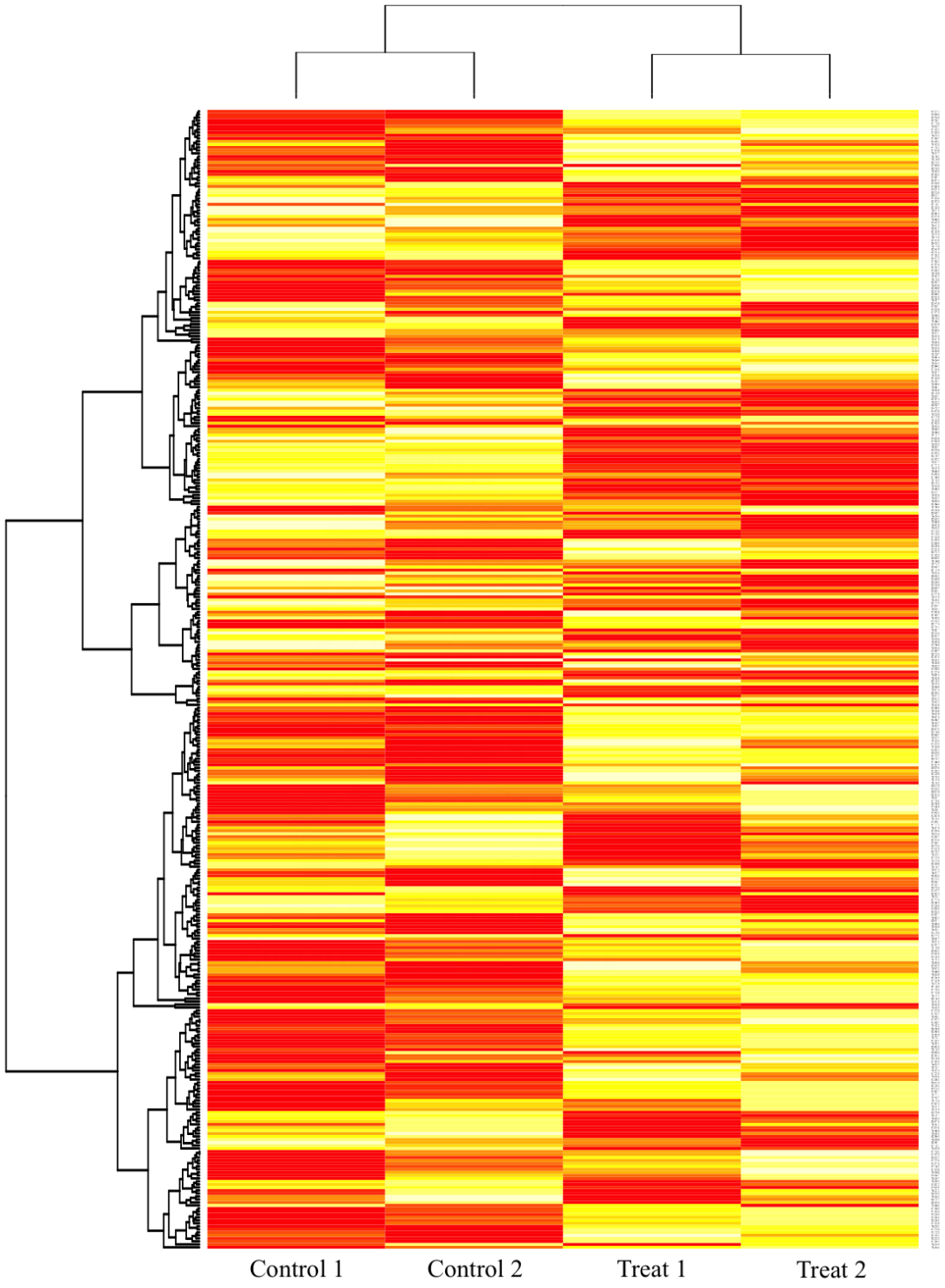

Figure 22 Heat map of genes with $p < 0.01$ generated by the Bioconductor R statistic program. H460 cells were treated with 10 μM of DPTA NONOate for 14 days then subjecting to microarray analysis.

Reversible effect of NO on CSC-like phenotypes

Having shown that NO drives the up-regulation of CSC markers and promotes CSC-like behaviors, the next step was to examine whether this effect of NO is reversible or not. The cells were first treated with 25 μM (H292) or 10 μM (H460) of DPTA NONOate for 14 days, after which they were further cultured in the absence of NO donor for an additional 7 days and analyzed for CSC markers and cellular behaviors.

Reversible effect of NO on H292 and H460 anoikis behavior

Figure 23A and B shows that the cells with discontinued NO treatment were less resistant to anoikis having their viability reverting to nearly the baseline level found in non-treated control cells.

Reversible Effect of NO on H292 and H460 colony formation

The discontinued treated cells also possessed weaker colony forming activity compared to the normal NO-treated cells (Fig. 24A and B). H292 cells treated with 25 μM of DPTA for 14 days originally form colonies of 3.4-fold relative to the non-treated control and in turns reduced to 2.3-fold after the NO treatment was ceased for 7 days (Fig. 24A). H460 cells treated with 10 μM of DPTA for 14 days form colonies of 3.3-fold relative to the control cells and the discontinued treatment cells colony formation is to 2.3-fold (Fig. 24B).

A

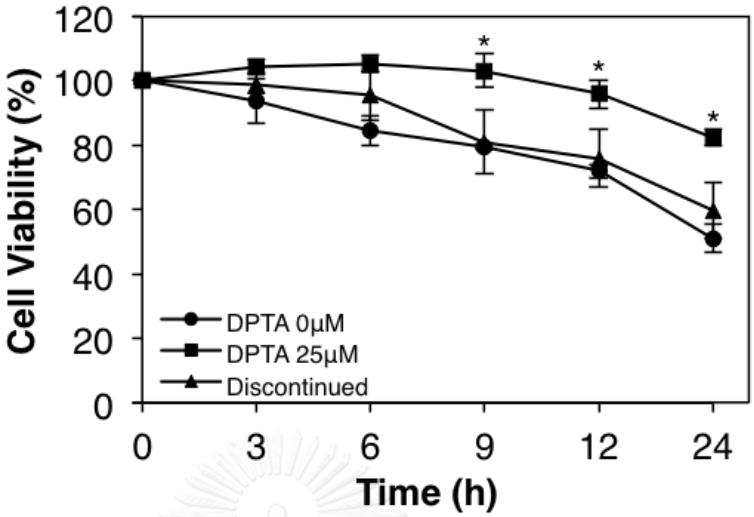

B

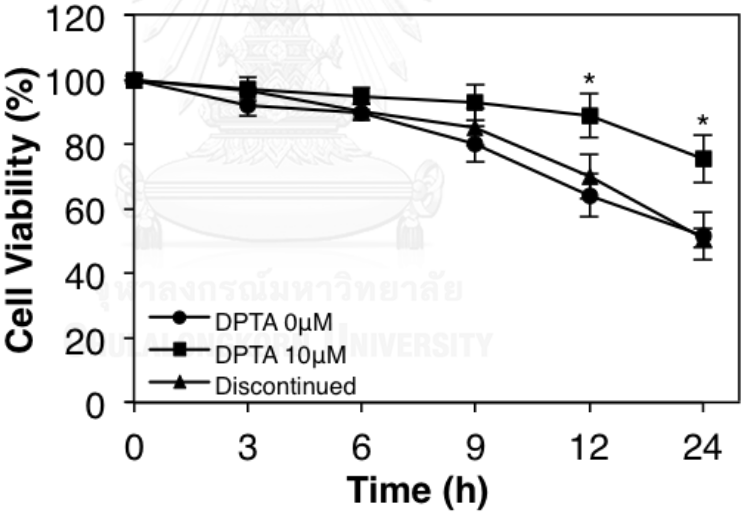

Figure 23 Reversible effect of NO on H292 and H460 anoikis behavior. After H292 and H460 cells were treated with 25 and 10 μM respectively of DPTA NONOate for 14 days, the cells were further cultured in the absence of NO donor for 7 days. H292 (**A**) and H460 (**B**) were detached for 0-24 hours. At indicated times, the detached cells' viability were measured using MTT assay. The bars are means ± SD (n=4). *, $p < 0.05$ vs. non-treated cells.

A

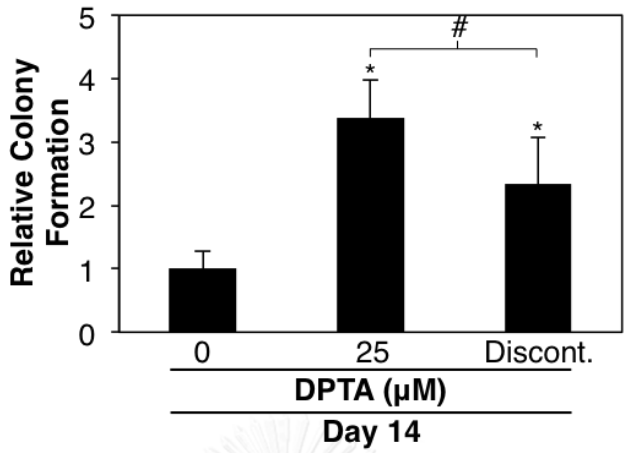

B

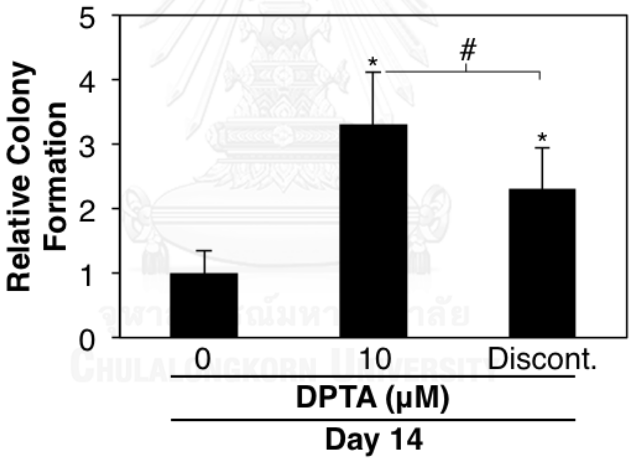

Figure 24 Reversible effect of NO on H292 and H460 colony formation. After H292 and H460 cells were treated with 25 and 10 μM respectively of DPTA NONOate for 14 days, the cells were further cultured in the absence of NO donor for 7 days. H292 (**A**) and H460 (**B**) cells were suspended and subjected to colony formation assay. After 14 days, colony number was analyzed and calculated as relative number to the control cells. The bars are means ± SD (n=4). *, $p < 0.05$ vs. non-treated cells. #, $p < 0.05$ vs. DPTA NONOate-treated cells.

Reversible effect of NO on H292 and H460 CSCs markers protein level

Moreover, the expression of CSC markers, CD133 and ALDH1A1, on these cells were significantly reduced after the discontinuation of the NO donor (Fig. 25A and B). As compared to the non-treated control cells, H292 cells treated with 25 μM of DPTA NONOate for 14 days exhibited a 6.6- and 6.9-fold increase respectively in the expression level of CD133 and ALDH1A1, respectively. After discontinuation of the NO donor, the CSC markers expression dropped to 4.2 and 3.3 folds over the control levels (Fig. 25A). A similar finding was observed in the H460 cells after the treatment and discontinuation of NO donor (Fig. 25B), supporting the generality of the effect of NO on CSC phenotypes.

A

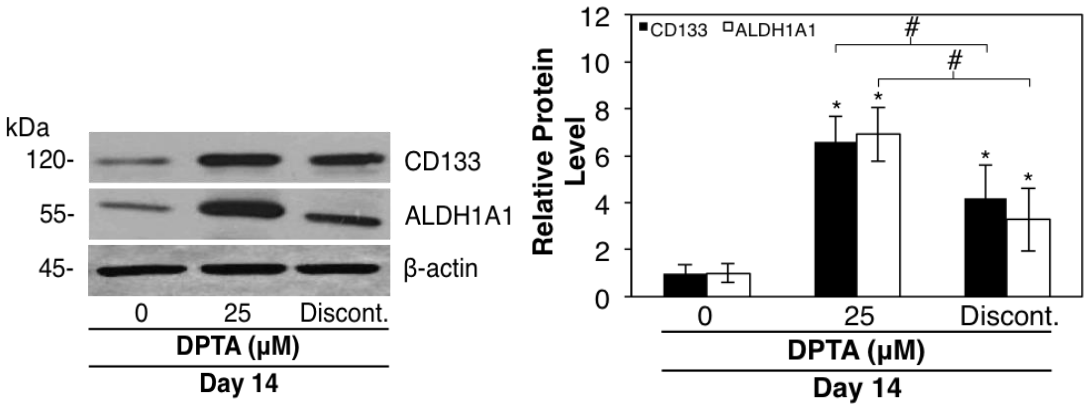

B

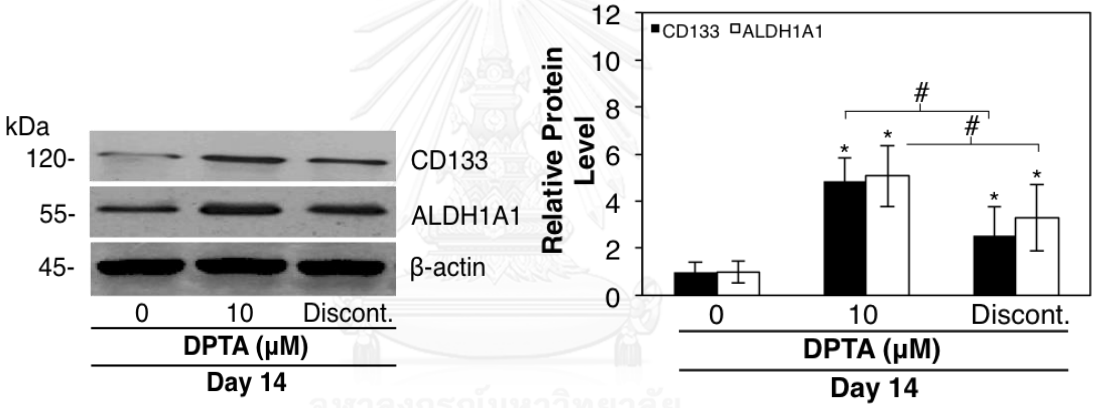

Figure 25 The effect of NO on cancer stem cell-like phenotypes is reversible. After H292 and H460 cells were treated with 25 and 10 μM respectively of DPTA NONOate for 14 days, the cells were further cultured in the absence of NO donor for 7 days. H292 (**A**) and H460 (**B**) cells were collected and cancer stem cell markers, CD133 and ALDH1A1, were analyzed by Western blotting. The blots were re-probed with β-actin to confirm equal loading. The immunoblot signals in H292 (**A**) and H460 (**B**) cells were quantified by densitometry, and mean data from independent experiments were normalized to the controls. The bars are means ± SD (n=8). *, $p < 0.05$ vs. non-treated cells. #, $p < 0.05$ vs. DPTA NONOate-treated cells.

Effects of NO donor (SNAP) and NO scavenger (PTIO) on CSC-like phenotypes

To confirm the effect of NO on CSC-like phenotypes, another NO donor *S*-nitroso-*N*-acetylpenicillamine (SNAP) and a NO scavenger PTIO were used. Cells were cultured in the presence or absence of NO modulators for 14 days and CSCs-like phenotypes were examined.

Effects of SNAP and PTIO on H292 and H460 anoikis behavior

Figure 26A shows that the SNAP-treated H292 cells displayed a dose-dependent increase in anoikis resistance as compared to the non-treated control. In contrast, treatment of the cells with NO scavenger had a reversal effect (Fig. 26A), supporting the role of NO in the resistance process. Consistent with this finding, a similar effect of NO donor and scavenger was observed in the H460 cells (Fig. 26B).

Effects of SNAP and PTIO on H292 and H460 colony formation

Colony formation studies also showed increased colony-forming activity of the SNAP-treated cells and decreased activity of the PTIO-treated cells, the effects that were observed in both H292 and H460 cells (Fig. 27A and B).

A

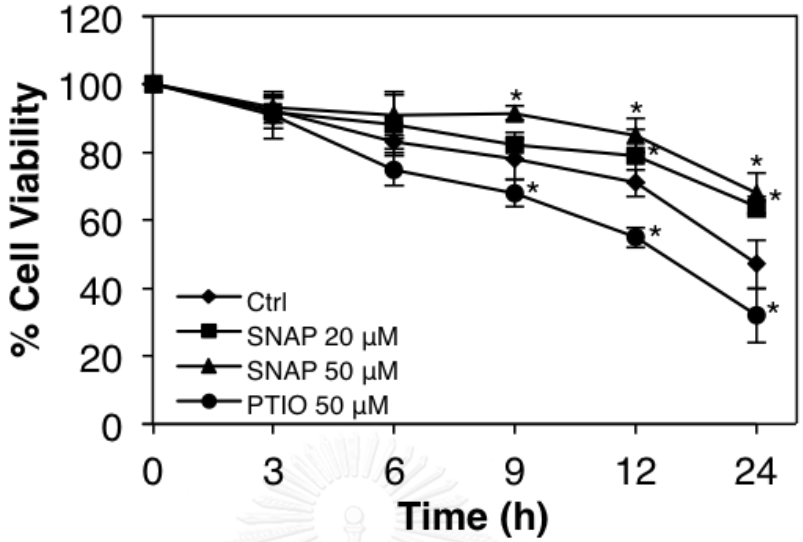

B

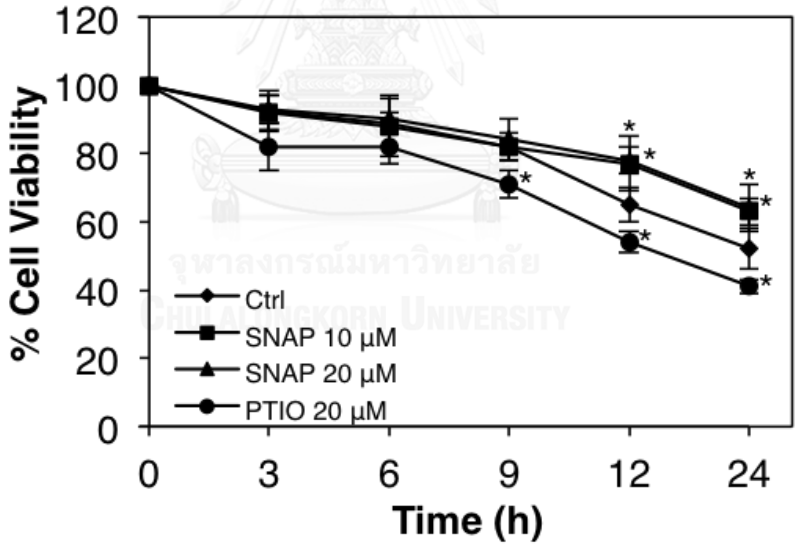

Figure 26 Effects of SNAP and PTIO on H292 and H460 anoikis behavior. H292 (**A**) and H460 (**B**) cells were either left untreated as control (Ctrl) or treated with SNAP (10-50 μM) or PTIO (20-50 μM) for 14 days, and analyzed for anoikis by measuring the viability of detached cells by MTT assay. The bars are means ± SD (n=4). *, $p < 0.05$ vs. non-treated control cells.

A

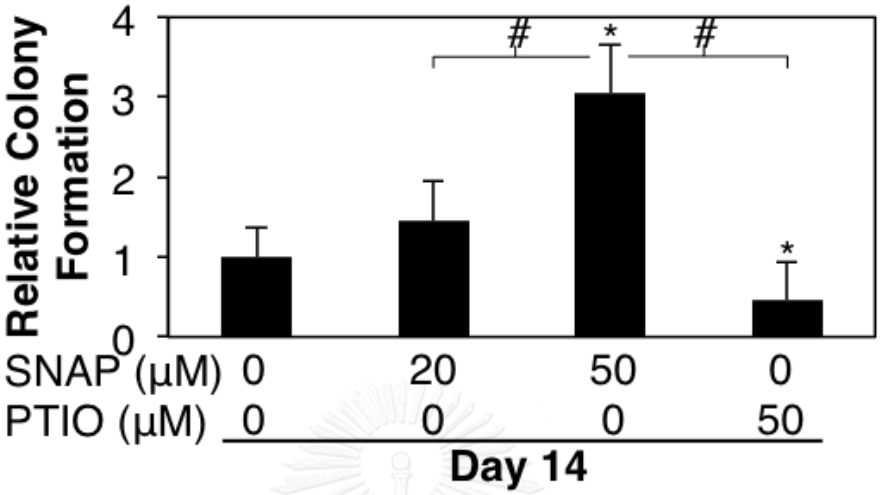

B

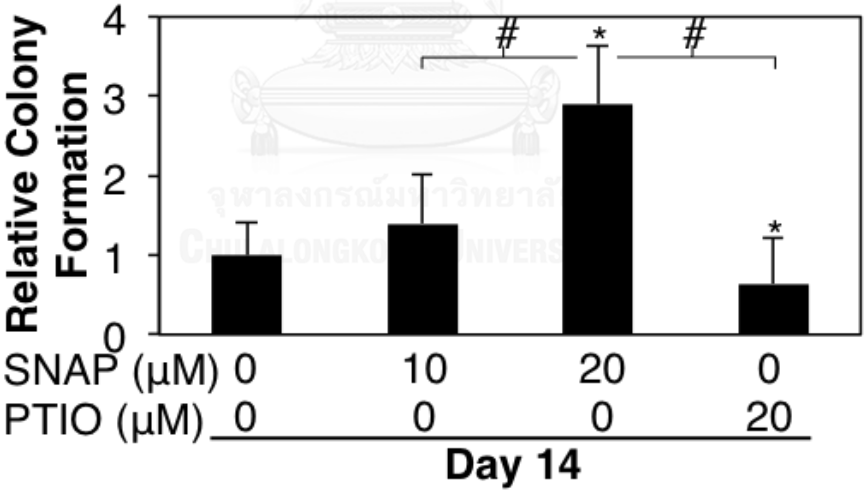

Figure 27 Effects of SNAP and PTIO on H292 and H460 colony formation. The SNAP and PTIO treated and control H292 (**A**) and H460 (**B**) cells were suspended and subjected to colony formation assay. The bars are means ± SD (n=4). *, $p < 0.05$ vs. non-treated control cells. #, $p < 0.05$ vs. treated cells.

Effects of SNAP and PTIO on H292 and H460 CSCs markers protein level

Moreover, the SNAP-treated cells displayed an increased expression of the CSC markers CD133 and ALDH1A1, while the PTIO-treated cells showed a reduced expression of the markers (Fig. 28A and B). H292 and H460 cells were cultivated in the presence or absence of SNAP or PTIO for 14 days; the expression levels of CD133 and ALDH1A1 were determined by Western blotting. A 3.5-fold increase in CD133 and 3.0-fold increase in ALDH1A1 expression were observed in the H292 cells treated with 50 μM of SNAP for 14 days, while a 0.48-fold of CD133 and 0.74-fold of ALDH1A1 were detected for H292 cells treated with 50 μM of PTIO for 14 days (Fig. 28A). In H460 cells, a 3.3- and 4.2-fold increase in the two CSC markers expression was observed after treated with 20 μM of SNAP for 14 days and 0.68- and 0.47-fold of the two CSC markers expression was detected for the 20 μM PTIO treated cells (Fig. 28B).

Effects of SNAP and PTIO on H292 and H460 spheroid formation

Figure 29A and B displays 4X phase contrast image of day 7 H292 and H460 spheroids formation respectively. Similar to DPTA NONOate treated cells, SNAP treated cells formed dense circular spheroids while control cells and PTIO treated cells clumps together to form a huge irregular shape spheroids surviving through E-cadherin mediated survival. Together, these results indicate the promoting role of NO in CSC-like properties of human lung cancer cells.

A

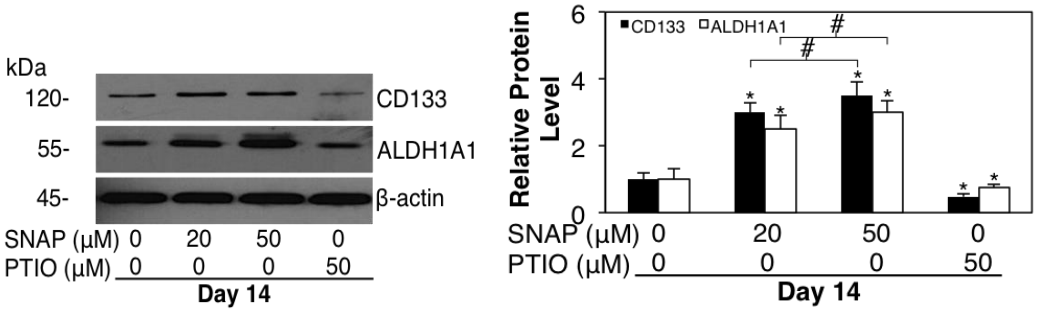

B

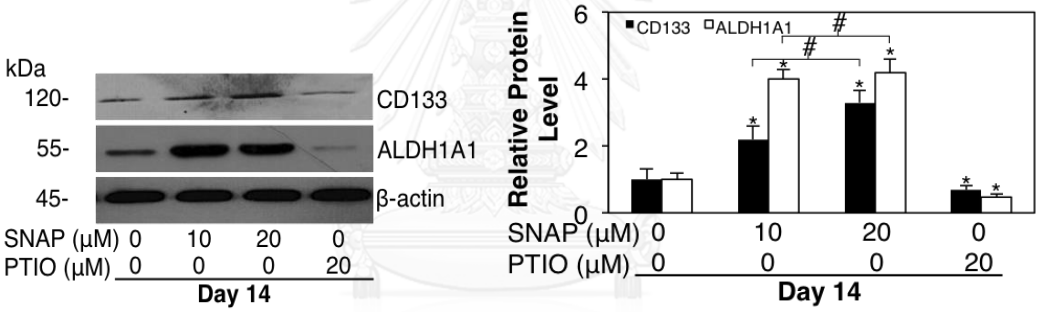

Figure 28 Effects of SNAP and PTIO on H292 and H460 CSC markers protein level. The SNAP and PTIO H292 (**A**) and H460 (**B**) treated cells were collected and cancer stem cell markers, CD133 and ALDH1A1, were analyzed by Western blotting. The blots were re-probed with β-actin to confirm equal loading. The immunoblot signals in H292 (**A**) and H460 (**B**) cells were quantified by densitometry, and mean data from independent experiments were normalized to the controls. The bars are means ± SD (n=4). *, $p < 0.05$ vs. non-treated control cells. #, $p < 0.05$ vs. treated cells.

A

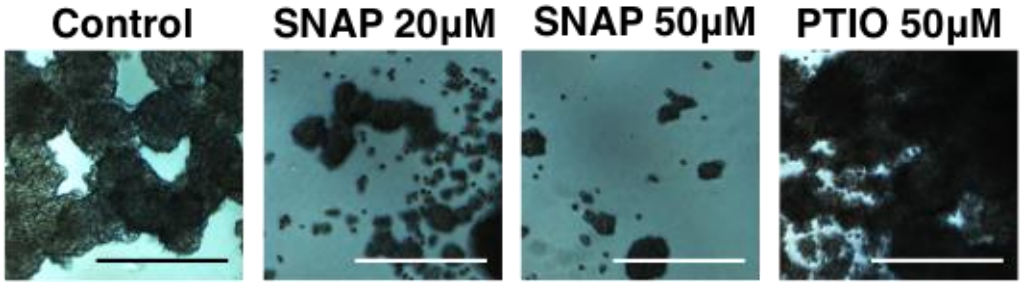

B

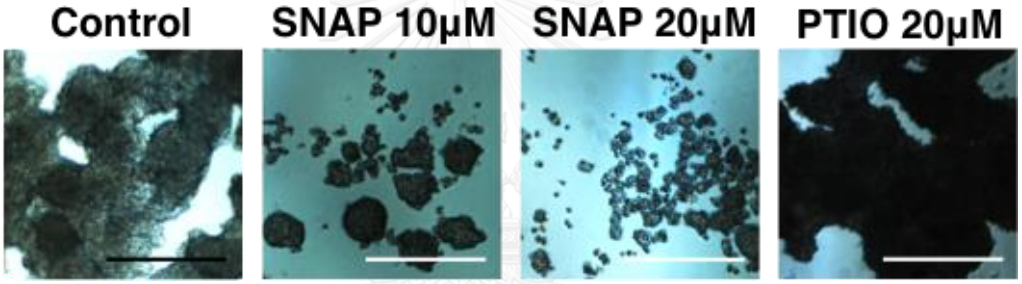

Figure 29 Effects of SNAP and PTIO on H292 and H460 primary spheroid formation. 4X Phase contrast image of primary spheroids at day 7 were captured for H292 (**A**) and H460 (**B**) SNAP treated, PTIO treated and non-treated cells. [Scale bar: 200 μm]

Caveolin-1 regulates aggressive behaviors of CSC-like cells but not CSC markers

Unveiling the key players underlying NO-mediated aggressive behaviors is of importance because of its potential applications in cancer therapy. Cav-1 is known to be involved in various cancer cell behaviors including migration, invasion and anoikis resistance (Chunhacha, 2012a, Grande-Garcia, 2007, Halim, 2012, Ho, 2002, Lin, 2005, Luanpitpong, 2010, Rungtabnapa, 2011) and is subjected to NO regulation (Chanvorachote, 2009, Halim, 2012). To explore the possible role of Cav-1 in NO-mediated CSC-like behaviors, Cav-1 expression was genetically modulated and its effect on cellular behaviors in NO-treated cells was examined.

Long-term DPTA NONOate treatment elevates caveolin-1 protein level

Figure 30A and B shows that Cav-1 level was strongly up regulated in the NO-treated cells in a dose- and time-dependent manner. The effect was found in both H292 and H460-treated cells where the H292 Cav-1 level increases up to 6.5-fold for the 25 μM DPTA day 14 treated cells and 3.9-fold for the H460 10 μM DPTA day 14 cells.

Stable transfection of knock down and over express caveolin-1 protein

To test whether Cav-1 is essential to the effect of NO on cellular behaviors, knock-downed of Cav-1 expression or enhanced by stable gene transfection, and their effects on NO-induced cellular behaviors were determined (Fig. 31A and B).

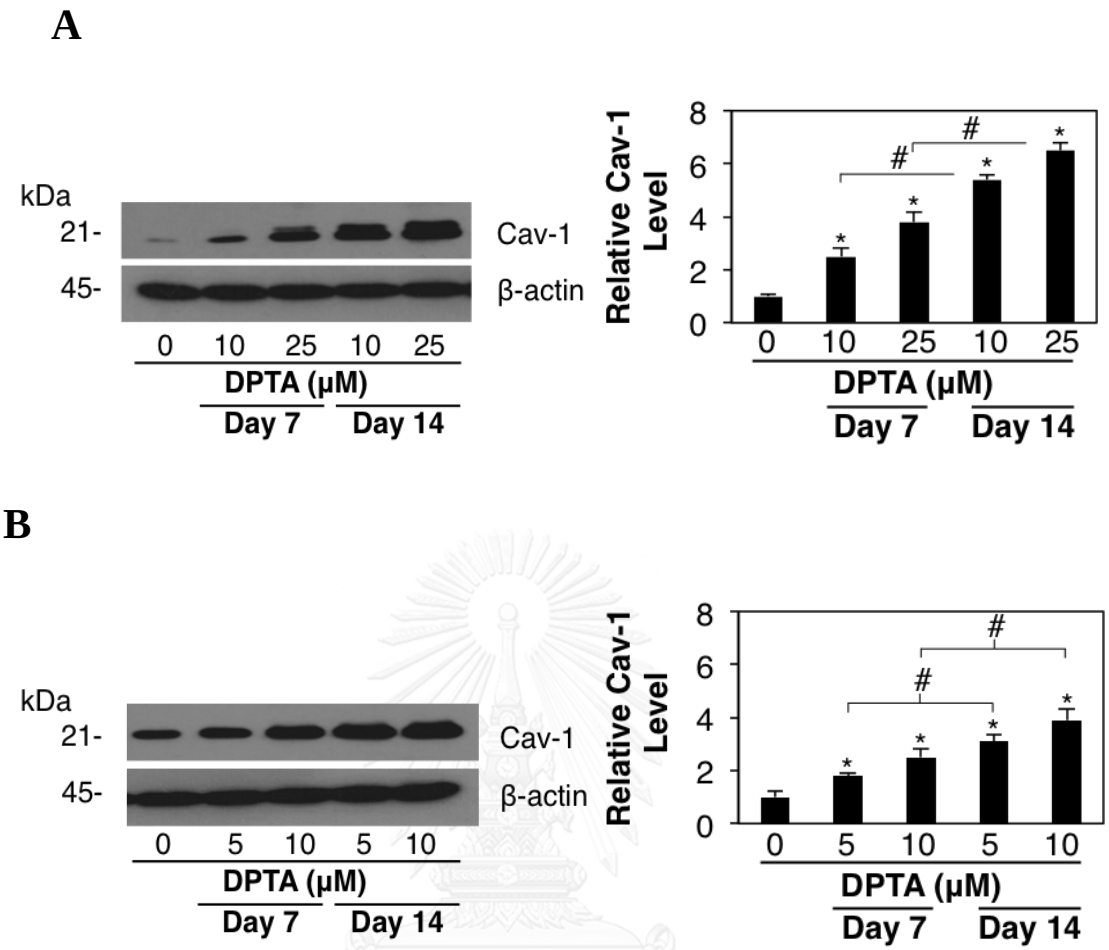

Figure 30 Effect of long-term NO exposure on caveolin-1 protein level. H292 (**A**) and H460 (**B**) cells were treated with 0-25 μM of DPTA NONOate for 7 and 14 days. Cells were collected and Cav-1 expression was determined by Western blotting. The blots were re-probed with β-actin to confirm equal loading. The immunoblot signals were quantified by densitometry, and mean data from independent experiments were normalized to the controls. The bars are means ± SD (n=4). *, $p < 0.05$ vs. non-treated control cells. #, $p < 0.05$ vs. treated cells at day 7.

A

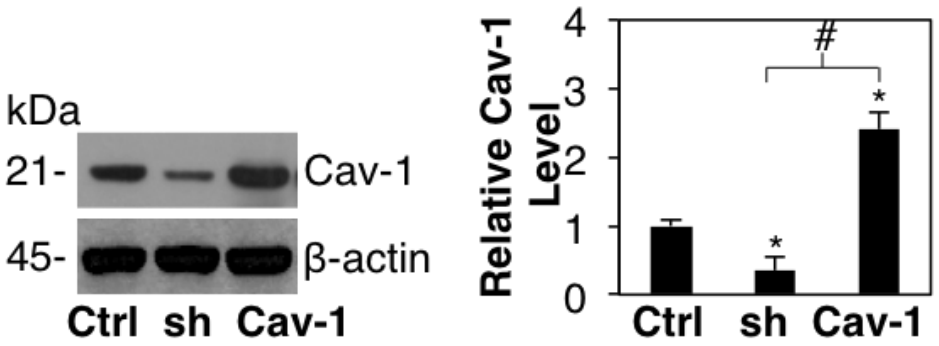

B

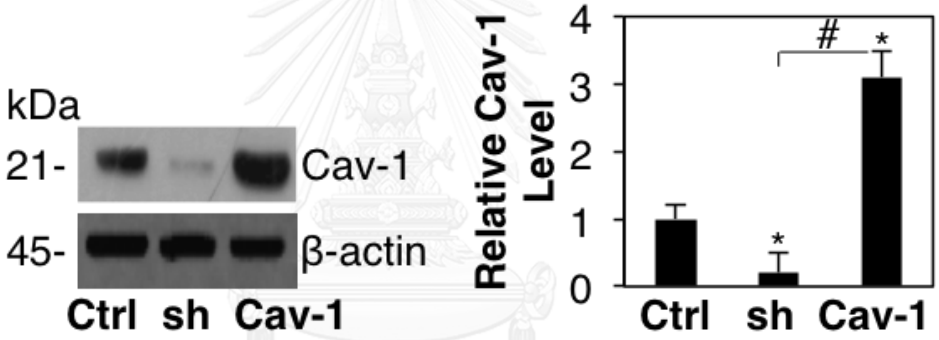

Figure 31 Stable transfection of knock down and over express caveolin-1 protein in H292 and H460 cells. H292 (**A**) and H460 (**B**) cells were stably transfected with Cav-1 overexpressing plasmid (Cav-1), short hairpin (sh) knockdown plasmid, or control (Ctrl) plasmid, and Cav-1 expression in these cells was determined by Western blotting. Blots were re-probed with β-actin as a loading control. The bars are means ± SD (n=4). *, $p < 0.05$ vs. control transfected cells. #, $p < 0.05$ vs. shCav-1 transfected cells.

Effect of caveolin-1 level on H292 and H460 anoikis behaviors

The genetically modified cells were treated with DPTA NONOate for 14 days (H292 25 μM, H460 10 μM) then examined for their anoikis behaviors. The results showed that Cav-1 knockdown cells were less resistant to anoikis than the control cells and the overexpressing cells were more resistant to anoikis then the control cells (Fig. 32A and B).

Effect of caveolin-1 level on H292 and H460 colony formation

The DPTA treated genetically modified cells were then investigated for their colony formation property. The result observed was that Cav-1 knockdown cells formed lesser amount of colony than the Cav-1 overexpressing cells (Fig. 33A and B).

Effect of caveolin-1 level on H292 and H460 migration

The NO exposed knocked down and over expressed caveolin-1 H292 and H460 cells were then subjected to wound healing assay in order to analyze their migration property. The results observed was Cav-1 knockdown cells migrate slower than the Cav-1 overexpressing cells (Fig. 34A and B). These results indicate that Cav-1 up regulated by long-term exposure of NO is required for the NO-mediated aggressive CSC-like behaviors.

A

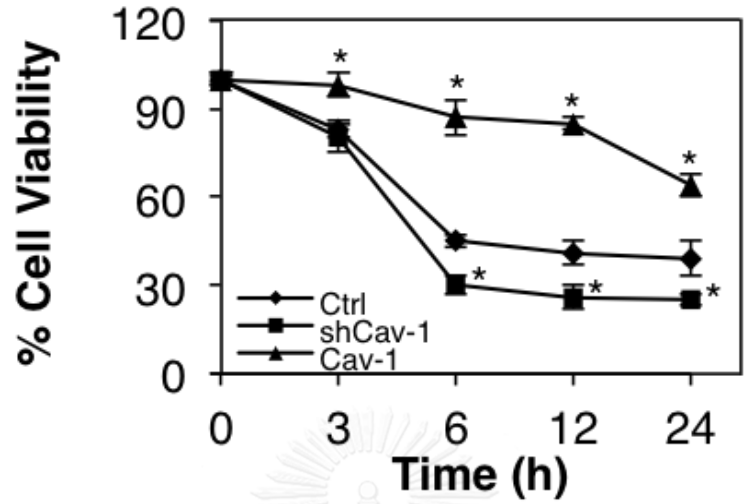

B

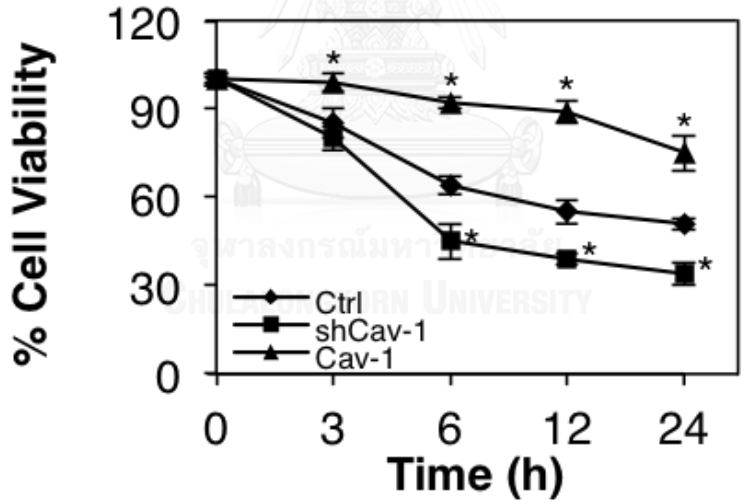

Figure 32 Effect of caveolin-1 level on H292 and H460 anoikis behaviors. Cav-1, sh and Ctrl H292 and H460 cells were treated with 25 μM and 10 μM of DPTA NONOate respectively for 14 days. H292 (**A**) and H460 (**B**) transfectants were detached and cell viability was analyzed for anoikis assay. The bars are means ± SD (n=4). *, $p < 0.05$ vs. control transfected cells.

A

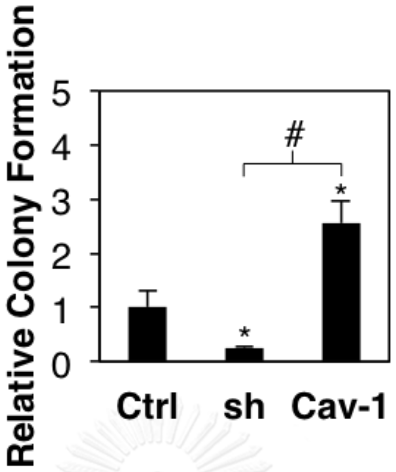

B

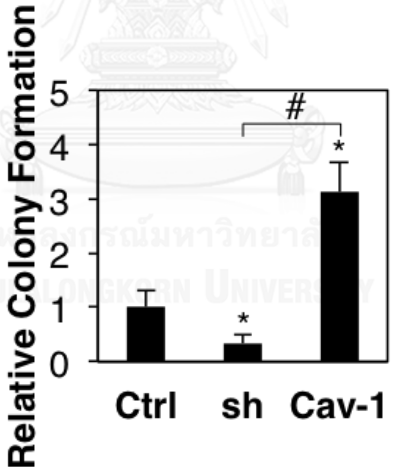

Figure 33 Effect of caveolin-1 level on H292 and H460 colony formation. H292 (**A**) and H460 (**B**) transfectants were subjected to colony formation assay. After 14 days, colony number was analyzed and calculated as relative number to the control cells. The bars are means ± SD (n=4). *, $p < 0.05$ vs. control transfected cells. #, $p < 0.05$ vs. shCav-1 transfected cells.

A

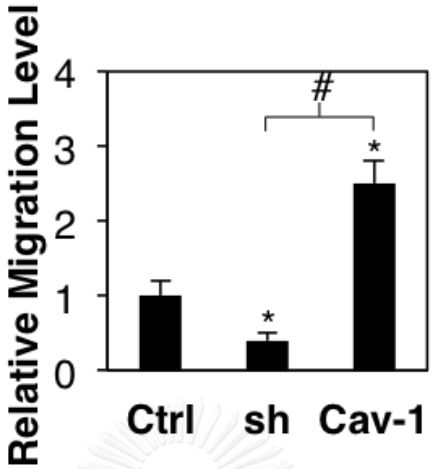

B

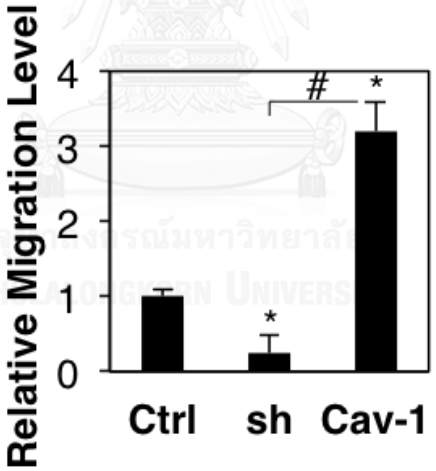

Figure 34 Effect of caveolin-1 level on H292 and H460 migration. The motility of H292 (**A**) and H460 (**B**) transfectants were determined by wound-healing assay. The wound space from random fields were measured and represented as relative migration to the control cells. The bars are means ± SD (n=4). *, $p < 0.05$ vs. control transfected cells. #, $p < 0.05$ vs. shCav-1 transfected cells.

Relative of caveolin-1 protein and CSCs markers

Furthermore, the effect of Cav-1 knockdown and overexpression on CSC markers was investigated. Cav-1 knockdown and overexpress H292 and H460 cells were treated with the NO donor for 14 days before collected for Western blot analysis. The expression levels of CD133 and ALDH1A1 were analyzed. The results showed that the level of these CSC markers did not correlate with the level of Cav-1 (Fig. 35A and B). Therefore, suggesting a non-Cav-1-dependent mechanism of CSC marker up regulation in the NO-treated cells.

A

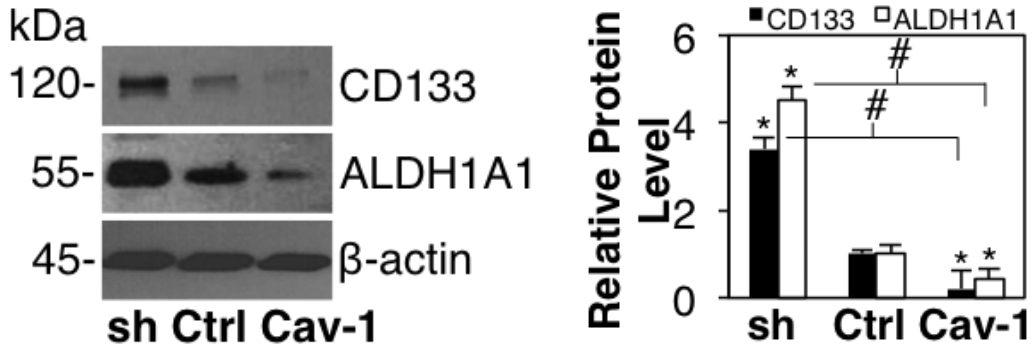

B

Figure 35 Effect of caveolin-1 level on CSC markers protein level. H292 (**A**) and H460 (**B**) transfectants were collected and CD133 and ALDH1A1 were analyzed by Western blotting. The blots were re probed with β-actin to confirm equal loading. The immunoblot signals were quantified by densitometry, and mean data from independent experiments were normalized to the controls. The bars are means ± SD (n=4). *, $p < 0.05$ vs. control transfected cells. #, $p < 0.05$ vs. shCav-1 transfected cells.

CHAPTER V

DISCUSSION AND CONCLUSION

The concept of cancer stem cells as a seed of malignant cells has garnered increasing attention and has been a subject of active research in recent years (Clevers, 2011, Dick, 2008, O'Connor, 2014). Although the detailed knowledge of this cell population remains obscure, the significant impact of this cell population in various forms of cancer have increasingly been reported. CSCs have been identified by their putative markers such as CD133 or ALDH1A1 (Croker, 2009, Kim, 2011, Silva, 2011) and by their cellular traits such as spindle-shaped morphology, colony/spheroid formation, and other aggressive behaviors (Fig.3) (Collins, 2005, Eramo, 2008, Li, 2007, Ma, 2007, Ponti, 2005, Ricci-Vitiani, 2007, Singh, 2003).

NO is a key molecule produced from crosstalk between cells and inflammation within the tumor microenvironment (Clancy, 1998, Cook, 2004, Decker, 2008). Several studies have reported an increased expression and activity of different forms of NOS in cancer cells (Thomsen, 1994, Thomsen, 1995, Ambs, 1998). Interestingly, both pro- and anti-tumorigenic roles of NO have been described, however it is generally accepted that the effect of NO on tumor progression is concentration dependent (Dhar, 2003, Jenkins, 1995, Muntané, 2010, Thomsen, 1998).

The concentration of NO in tumor microenvironment is hard to measure due to the fact that NO are free radicals that reacts instantly. Furthermore, different types of cancer have different NO concentration within the tumor microenvironment depending on the cancer type as well as activity of nitric oxide synthases found in the cancer cells.

The concentration of NO at the tumor site is higher than other non-cancerous site (Fukumura, 2006, Lala, 1998). NO concentration at tumor site can range from 1 nM to >300 nM in which different concentration induces different responses (Ridnour et al., 2008). DPTA NONOate is a NO donor that has a half-life of up to 5 hours. One mole of DPTA NONOate gives out two moles of NO. Treating the cells with 25 μM of DPTA NONOate = 25,000 nM of DPTA NONOate which would give off 50,000 nM of NO over a time period of 10 hours. Every second certain amount of NO are given off by NO-donors, some reacts and some are given off by the cells themselves creating a fluxion of NO concentration within the microenvironment. This sustained fluxion interestingly mimics the *in vivo* tumors microenvironment (Ridnour, 2008).

Previously studies have reported that NO promotes cell death resistance to Fas ligand (Chanvorachote, 2005) and cisplatin (Chanvorachote, 2006) in human lung cancer cells. In relevance to metastasis, researchers had found that NO mediates anoikis resistance of lung cancer cells (Chanvorachote, 2009). Together, these findings provide evidence supporting the role of NO in tumorigenesis and metastasis, consistent with the clinical observations showing a correlation between NO level and a high degree of tumor metastasis (Luanpitpong, 2010, Sanuphan, 2013). Several studies have demonstrated that CSCs possess an enhanced ability to migrate, invade, form tumor and resist to anoikis cell death (Collins, 2005, Eramo, 2008, Li, 2007, Ma, 2007, Ponti, 2005, Ricci-Vitiani, 2007, Singh, 2003). However, the linkage between NO and aggressive lung cancer phenotypes in the context of CSCs has not been investigated. This study demonstrated for the first time that NO regulate the stemness and aggressive behaviors of lung cancer cells. DPTA NONOate not only up regulates the expression of EMT markers, Vimentin and Snail, but also up regulates CD133 and ALDH1A1, the

well-known CSC markers. Furthermore, the NO donors stimulate H292 and H460 aggressive cellular behaviors. The migration, invasion, anoikis and colony/spheroid forming assay represent *in vivo* metastasis steps that cancer stem cells have to go through in order to mobile from the primary tumor site to the secondary site (Fig. 36).

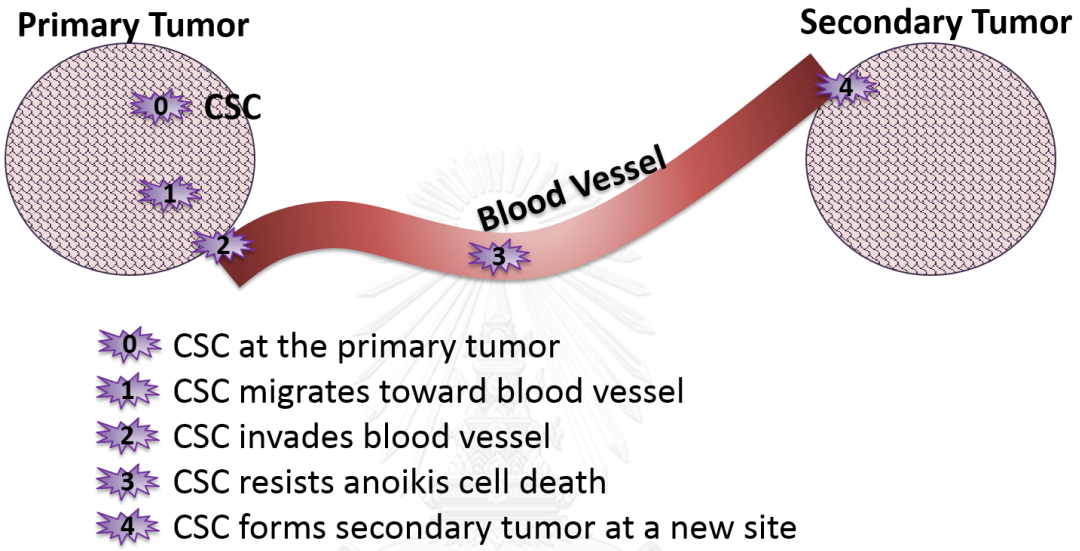

Figure 36 The cancer stem cell metastatic cascade.

The initial step of metastasis is that the cancer cells would migrate to the nearest vascular site; these cells typically emits EMT or CSCs property. Figure 9, shows that long-term NO exposed cells migrate faster than the non-treated controls. In order for the cells to invade blood or lymphatic vessels they would have to travel through extracellular matrix (EMC) by secreting enzymes that breaks down the EMC, then the cells would have to squeeze through the vessel's wall in order to get to the blood stream. The Boyden chambers are 8 μm pore inserts, which were pre-coated with Matrigel mimicking real life vessel's wall and EMC respectively. Figure 10 illustrates that NO

treated cells have higher ability to invade comparing to the control cells. After the cells were able to intravasate, they would have to survive during the detachment stage. Anoikis assay was used to analyze detachment induce apoptosis cell death, where cells with EMT or CSCs property would exhibit anoikis resistance. This step is a major step in distinguishing normal cancer cells from EMT and CSCs cells. The DPTA NONOate treated cells had a higher survival rate than the control cells, which significantly undergoes apoptosis within 9 hours (Fig. 11). Once the cells survive the detachment, they would start to proliferate and form colonies/spheroids. This step discriminate cells with CSCs property from the cells with EMT property. Figures 15-18 display that NO treated cells are more capable in forming colonies/spheroids than the non-treated control cells. Even though anoikis assay and spheroid formation assay were both constructed in ultra-low attach plates, but in anoikis assay the cells were triturated every 3 hours to prevent the cells from contacting while the spheroid assay were left stilled for a longer period of time. This allowed the control cells to come together to form spheroids and survived through E-cadherin mediation. As a result of E-cadherin mediated survival, the non-treated control cells survived and clumps together to form loose primary spheroids. In contrast, the NO treated spheroids were tightly packed and formed by original seeded cells propagating into circular shape spheroids. However, after the primary spheroids were dissociated and were left for 30 days to form secondary spheroids, the result observed was that NO-treated spheroids have more or less the same morphology as the primary spheroid but are bigger in size while the control spheroid had deformed and cells had already undergo apoptosis.

Reflecting perception on microarray results; the results may vary depending on the time point that the cells were collected. In mammalian, mRNAs have a half-life of

only 2-7 hours while protein half-life is approximately 48hrs, therefore, the correlation between the genes and their protein are said to be only 40% (Vogel, 2012). Furthermore, on average 2 mRNAs are transcribed per hour while dozens of proteins are translated per one mRNA per hour. This may be the reasoning behind the differences in CD133, ALDH1A1 and Cav-1 protein level detected by Western blotting and their genes expression. However, the significant up regulation of the *CD24* and *THY1 (CD90)* genes which are CSCs markers in combination with the increased in the *NANOG* gene expression which is the pluripotency marker helps confirmed the NO in CSCs theory. In addition, Jeter and his team had found out that increase in *NANOG* gene expression induces CD133 and ALDH1A1 protein level (Jeter et al., 2011). Moreover, the *DDR1* gene expression also increased drastically suggesting a therapeutic target, which open an interesting opportunity and should be investigated in the future.

The effect of NO on aggressive CSC-like behaviors was found to be reversible, which may explain the discrepancy of the NO effect on tumorigenesis. This reveals that stemness is not a black or white matter but considered to have many shades of grey, meaning that a cell cannot be accurately distinguish as a stem cell or not a stem cell because it can express varies stemness level. Discontinuation of NO exposure after a 2 week-treatment resulted in a reversal of the CSC-like effects of NO on cells, exhibiting lesser aggressiveness and loss of stemness was confirmed via western blotting. The western blot analysis was repeated 8 times to ensure the accuracy of the obtained results as cell lysate represents the mixed cell population which each passage may vary due to random sub-culturation. It is worth noting that level of NO in the tumor microenvironment differs depending on the expression of NOS and the activity of local and infiltrating immune cells. Therefore, the effect of NO on CSC-like behaviors may

vary depending on the availability of NO and pathological conditions. In turns this suggested that stemness is an inducible property. Recent studies have also exposed the possibility of cancer cells being induced by their surrounding microenvironment and gain CSCs properties. For instance, cancer cells exhibit cancer stem cell phenotypes after cancer chemotherapy (Yang, 2009).

The SNAP results were somewhat similar to the DPTA NONOate results, giving off the same trends in every experiment but exhibits a weaker potential. This may be because of the donor's property itself as SNAP is light sensitive and may obliterate easily. On the other hand, the NO scavenger PTIO suppresses the CSCs markers and decreases the aggressive behaviors (Fig. 26-29). These results suggest that NO may mediate its effects by regulating the stemness of cancer cells.

Caveolin-1 is a scaffold protein, an essential constituent of caveolae, a flask-shaped invagination that occupies up to 20% of cell membrane (Li, 1996). Several lines of evidence have pointed out that Cav-1 may contribute to the aggressiveness and chemoresistance of human cancer cells, including lung carcinoma, ovarian carcinoma, colon adenocarcinoma and breast adenocarcinoma cells (Ho, 2008, Lavie, 1998, Lavie, 2001). Cav-1 expression has been linked to increased cell motility and anoikis resistance (Chunhacha, 2012a, Grande-Garcia, 2007, Halim, 2012, Ho, 2002, Lin, 2005, Luanpitpong, 2010, Rungtabnapa, 2011, Chunhacha, 2012b), two important features of metastatic cancer cells. This study provide new evidence that NO increases the motility and resistance to anoikis of human lung cancer cells through Cav-1-dependent mechanism. Cav-1 is up regulated in the NO-treated cells in a dose- and time-dependent manner (Fig. 30). Such up regulation is positively associated with the ability of the cells to migrate, invade, form colony and resist anoikis. Gene knockdown

and overexpression studies confirm the positive regulatory role of Cav-1 in NO-mediated aggressive behaviors of lung cancer cells. This finding is however contradictory to the generally regarded role of Cav-1 as a tumor suppressor protein in other type of cancer (Lloyd, 2011). It is likely that Cav-1 may have multiple functions and may exert both positive and negative roles on cancer cell behaviors depending on the cancer stage, i.e. metastatic or non-metastatic, tissue of origin, and tumor microenvironment, i.e. presence of nitrosative and oxidative stress. In the environment with high NO level, Cav-1 is up regulated and pro-metastatic. Previous studies have also shown that NO stabilizes Cav-1 through a process of *S*-nitrosylation which inhibits ubiquitin-proteasomal degradation of the protein and in turns western blot detect the accumulated Cav-1 protein level (Chanvorachote, 2009). Furthermore, Cav-1 can interact with Mcl-1 and improve its stability leading to anoikis resistance of lung cancer cells (Chunhacha, 2012b).

In conclusion, these data provide evidence that NO plays an important role in the regulation of CSC-like phenotypes of human lung cancer cells. NO induces an up regulation of CSC markers CD133 and ALDH1A1 along with the increase in anoikis resistance, migration, invasion, and colony/spheroid formation activities. Such induction of the aggressive CSC-like behaviors is dependent on Cav-1 expression; however, the expression of CSC markers is independent or inversely dependent of the Cav-1 expression this may be due to the fact that the Cav-1 protein is believed to have two-sides of the coin (Lloyd, 2011). The transfected overexpressed Cav-1 cells already consist of high Cav-1 protein level so when NO treatment further increases the Cav-1 level, in turn it might suppress the CSCs marker. Because increased NO production has been associated with several human cancers, NO may be one of the key regulators of

CSCs and metastasis. This novel finding on the role of NO and Cav-1 in CSC regulation may have important implications in cancer chemotherapy and prevention.

REFERENCES

AKUNURU, S., JAMES ZHAI, Q., ZHENG, Y. 2012. Non-small cell lung cancer stem/progenitor cells are enriched in multiple distinct phenotypic subpopulations and exhibit plasticity. *Cell Death and Disease,* 3.

AL-HAJJ, M., WICHA, M.S., BENITO-HERNANDEZ, A., MORRISON, S.J., CLARKE, M.F. 2003. Prospective identification of tumorigenic breast cancer cells. *Proceedings of the National Academy of Sciences of the United State of America,* 100**,** 6.

ALAMGEER, M., GANJU, V., SZCZEPNY, A., RUSSELL, P.A., PRODANOVIC, Z., KUMAR, B., WAINER, Z., BROWN, T., SCHNEIDER-KOISKY, M., CONRON, M., WRIGHT, G., WATKINS, D.N. 2013. The prognostic significance of aldehyde dehydrogenase 1A1 (ALDH1A1) and CD133 expression in early stage non-small cell lung cancer. *Thorax,* 0**,** 10.

AMBS, S., MERRIAM, W.G., BENNETT, W.P., FELLEY-BOSCO, E., OGUNFUSIKA, M.O., OSER, S.M., KLEIN, S., SHIELDS, P.G., BILLIAR, T.R., HARRIS, C.C. 1998. Frequent nitric oxide synthase-2 expression in human colon adenomas: implication for tumor angiogenesis and colon cancer progression. *Cancer Research* 58**,** 8.

APORNTEWAN, C., MUTIRANGURA, A. 2011. Connection up- and down-regulation expression analysis of microarrays (CU-DREAM): a physiogenomic discovery tool. *Asian Biomedicine,* 5**,** 6.

ARIAS-DÍAZ, J., VARA, E., TORRES-MELERO, J., GARCÍA, C., BAKI, W., RAMÍREZ-ARMENGOL, J.A., BALIBREA, J.L. 1994. Nitrite/nitrate and cytokine levels in bronchoalveolar lavage fluid of lung cancer patients *Cancer,* 74**,** 6.

BAO, S., WU, Q., MCLENDON, R. E., HAO, Y., SHI, Q., HJELMELAND, A. B., DEWHIRST, M. W., ET AL. 2006. Glioma stem cells promote radioresistance by preferential activation of the DNA damage response *Nature,* 444**,** 5.

BERTOLINI, G., ROZ, L., PEREGO, P., TORTORETO, M., FONTANELLA, E., GATTI, L., PRATESI, G., FABBRI, A., ANDRIANI, F., TINELLI, S., ROZ, E., CASERINI, R., LO VULLO, S., CAMERINI, T., MARIANI, L., DELIA, D., CALABRO, E., PASTORINO, U., SOZZI, G. 2009. Highly tumorigenic lung cancer CD133+ cells display stem-like features and are spared by cisplatin treatment *Proceedings of the National Academy of Science* 106**,** 6.

BONNET, D., & DICK, J. E. 1997. Human acute myeloid leukemia is organized as a hierarchy that originates from a primitive hematopoietic cell. *Nature medicine,* 3**,** 8.

BORING, C. C., SQUIRES, T.S., TONG, T., MONTGOMERY, S. 1994. Cancer Statistics, 1994. *CA: A Cancer Journal for Clinicians,* 44**,** 20.

CHANVORACHOTE, P., & CHUNHACHA, P. 2013. Caveolin-1 regulates endothelial adhesion of lung cancer cells via reactive oxygen species-dependent mechanism *PLoS. One,* 8.

CHANVORACHOTE, P., NIMMANNIT, U., LU, Y., TALBOTT, S., JIANG, B.H., ROJANASAKUL, Y. 2009. Nitric oxide regulates lung carcinoma cell anoikis through inhibition of ubiquitin-proteasomal degradation of caveolin-1 *Journal of Biological Chemistry* 284**,** 9.

CHANVORACHOTE, P., NIMMANNIT, U., STEHLIK, C., WANG, L., JIANG, B.H., ONGPIPATANAKUL, B., ROJANASAKUL, Y. 2006. Nitric oxide regulates cell sensitivity to cisplatin-induced apoptosis through S-nitrosylation and inhibition of Bcl-2 ubiquitination *Cancer research* 66**,** 8.

CHANVORACHOTE, P., NIMMANNIT, U., WANG, L., STEHLIK, C., LU, B., AZAD, N., ROJANASAKUL, Y. 2005. Nitric oxide negatively regulates Fas CD95-induced apoptosis through inhibition of ubiquitin-proteasome-mediated degradation of FLICE inhibitory protein *Journal of Biological Chemistry* 280**,** 7.

CHARAFE-JAUFFRET, E., GINESTIER, C., LOVINO, F., WICINSKI, J., CERVERA, N., FINETTI, P., HUR, M.H., DIEBEL, M.E., MONVILLE, F., DUTCHER, J., BROWN, M., VIENS, P., XERRI, L., BERTUCCI, F., STASSI, G., DONTU, G., BIRNBAUM, D., WICHA, M.S. 2009. Breast cancer cell lines contain functional cancer stem cells with metastatic capacity and a distinct molecular signature *Cancer research* 69**,** 12.

CHUNHACHA, P., & CHANVORACHOTE, P. 2012a. Roles of caveolin-1 on anoikis resistance in non small cell lung cancer *International Journal of Physiol, Pathophysiol and Pharmacol* 4**,** 7.

CHUNHACHA, P., PONGRAKHANANON, V., ROJANASAKUL, Y., CHANVORACHOTE, P. 2012b. Caveolin-1 regulates Mcl-1 stability and anoikis in lung carcinoma cells *American Journal of Physiology - Cell Physiology* 302**,** 9.

CLANCY, R. M., & ABRAMSON, S.B. 1995. Nitric oxide: a novel mediator of inflammation. *Proceedings of the Society for Experimental Biology and Medicine,* 210**,** 9.

CLANCY, R. M., AMIN, A.R., ABRAMSON, S.B. 1998. The role of nitric oxide in inflammation and immunity. *Arthritis & Rheumatism,* 41**,** 11.

CLEVERS, H. 2011. The cancer stem cell: premises, promises and challenges *Nature Medicine,* 17**,** 7.

COLAKOGULLARI, M., ULUKAYA, E., YILMAZTEPE, A., OCAKOGLU, G., YILMAZ, M., KARADAG, M., TOKULLUGIL, A. 2006. Higher serum nitrate levels are associated with poor survival in lung cancer patients. *Clinical Biochemistry,* 39**,** 6.

COLLINS, A. T., BERRY, P.A., HYDE, C., STOWER, M.J., MAITLAND, N.J. 2005. Prospective Identification of Tumorigenic Prostate Cancer Stem Cells. *Cancer Research,* 65**,** 6.

COOK, J. A., GIUS, D., WINK, D.A., KRISHNA, M.C., RUSSO, A., MITCHELL, J.B. 2004. Oxidative stress, redox, and the tumor microenvironment. *Seminars in Radiation Oncology,* 14**,** 8.

CREIGHTON, C. J., LI, X., LANDIS, M., DIXON, J.M., NEUMEISTER, V.M., SJOLUND, A., RIMM, D.L., WONG, H., RODRIGUEZ, A., HERSCHKOWITZ, J.I., FAN, C., ZHANG, X., HE, X., PAVLICK, A., GUTIERREZ, M.C., RENSHAW, L., LARIONOV, A.A., FARATIAN, D., HILSENBECK, S.G., PEROU, C.M., LEWIS, M.T., ROSEN, J.M., CHANG, J.C. 2009. Residual breast cancers after conventional therapy display mesenchymal as well as tumor-initiating features *Proceedings of the National Academy of Science* 106**,** 6.

CROKER, A. K., GOODALE, D., CHU, J., POSTENKA, C., HEDLEY, B.D., HESS, D.A., ALLAN, A.L. 2009. High aldehyde dehydrogenase and expression of cancer stem cell markers selects for breast cancer cells with enhanced malignant and metastatic ability. *Journal of Cellular and Molecular Medicine,* 13**,** 17.

DECKER, N. K., ABDELMONEIM, S.S., YAQOOB, U., HENDRICKSON, H., HORMES, J., BENTLEY, M., PITOT, H., URRUTIA, R., GORES, G.J., SHAH, V.H. 2008. Nitric Oxide Regulates Tumor Cell Cross-Talk with Stromal Cells in the Tumor Microenvironment of the Liver *The American Journal of Pathology,* 173**,** 11.

DHAR, A., BRINDLEY, J.M., STARK, C., CITRO, M.L., KEEFER, L.K., COLBURN, N.H. 2003. Nitric oxide does not mediate but inhibits transformation and tumor phenotype *Molecular Cancer Therapeutics,* 2**,** 9.

DICK, J. E. 2008. Stem cell concepts renew Cancer research. *Blood,* 112**,** 15.

DOMEN, J., CHESHIER, S.H., WEISSMAN, I.L. 2000. The role of apoptosis in the regulation of hematopoietic stem cells: overexpression of Bcl-2 increases both their number and repopulation potential. *Journal of Experimental Medicine,* 191**,** 12.

DOMEN, J., GANDY, K.L., WEISSMAN, I.L. 1998. Systemic overexpression of BCL-2 in the hematopoiectic system protects transgenic mice from the consequences of lethal irradiation *Blood,* 91**,** 11.

ERAMO, A., LOTTI, F., SETTE, G., PILOZZI, E., BIFFONI, M., DI VIRGILIO, A., CONTICELLO, C., RUCO L., PESCHLE, C., DE MARIA, R. 2008. Identification and expansion of the tumorigenic lung cancer stem cell population. *Cell Death and Differentiation,* 15**,** 11.

ESME, H., CEMEK, M., SEZER, M., SAGLAM, H., DEMIR, A., MELEK, H., UNLU, M. 2008. High levels of oxidative stress in patients with advanced lung cancer. *Respirology,* 13**,** 5.

FUJIMOTO, H., ANDO, Y., YAMASHITA, T., TERAZAKI, H., TANAKA, Y., SASAKI, J., MATSUMOTO, M., SUGA, M., ANDO, M. 1997. Nitric oxide synthase activity in human lung cancer. *Japanese journal of cancer research,* 88**,** 9.

FUKUMURA, D., KASHIWAGI, S., JAIN, R.K. 2006. The role of nitric oxide in tumour progression. *Nature Reviews Cancer* 6**,** 14.

FULDA, S., & PERVAIZ, S. 2010. Apoptosis signaling in cancer stem cells. *The International Journal of Biochemistry & Cell Biology,* 42**,** 8.

GOODELL, M. A., BROSE, K., PARADIS, G., CONNER, A.S., MULLIGAN, R.C. 1996. Isolation and functional properties of murine hematopoietic stem cells that are replicating in vivo. *The Journal of Experimental Medicine,* 183**,** 10.

GRANDE-GARCIA, A., ECHARRI, A., DE ROOIJ, J., ALDERSON, N.B., WATERMAN-STORER, C.M., VALDIVIELSO, J.M., DEL POZO, M.A. 2007. Caveolin-1 regulates cell polarization and directional migration through Src kinase and Rho GTPases *Journal of Cell Biology,* 177**,** 12.

HALIM, H., LUANPITPONG, S., CHANVORACHOTE, P. 2012. Acquisition of anoikis resistance up-regulates caveolin-1 expression in human non-small cell lung cancer cells *Anticancer research* 32**,** 10.

HAN, F., GU, D., CHEN, Q., ZHU, H. 2009. Caveolin-1 acts as tumor suppressor by down-regulation epidermal growth factor receptor-mitogen-activated protein kinase signaling pathway in pancreatic carcinoma cell lines. *Pancreas,* 38**,** 9.

HERMANN, P. C., HUBER, S.L., HERRLER, T., AICHER, A., ELLWART, J.W., GUBA, M., BRUNS, C.J., ET AL. 2007. Distinct Populations of Cancer Stem Cells Determine Tumor Growth and Metastatic Activity in Human Pancreatic Cancer *Cell Stem Cell,* 1**,** 11.

HINO, M., DOIHARA, H., KOBAYASHI, K., AOE, M., SHIMIZU, N. 2003. Caveolin-1 as tumor suppressor gene in breast cancer. *Surgery Today,* 33**,** 5.

HO, C. C., HUANG, P.H., HUANG, H.Y., CHEN, Y.H., YANG, P.C., HSU, S.M. 2002. Up-regulated caveolin-1 accentuates the metastasis capability of lung adenocarcinoma by inducing filopodia formation *American Journal of Pathology* 161**,** 10.

HO, C. C., KUO, S.H., HUANG, P.H., HUANG, H.Y., YANG, C.H., YANG, P.C. 2008. Caveolin-1 expression is significantly associated with drug resistance and poor prognosis in advanced non-small cell lung cancer patients treated with gemcitabine-based chemotherapy. *Lung Cancer* 59**,** 6.

JEMAL, A., SIEGEL, R., WARD, E., HAO, Y., XU, J., THUN, M.J. 2009. Cancer Statistics, 2009. *CA: A Cancer Journal for Clinicians,* 59**,** 25.

JEMAL, A., TIWARI, R.C., MURRAY, T., GHAFOOR, A., SAMUELS, A., WARD, E., FEUER, E.J., THUN, M.J. 2004. Cancer Statistics, 2004. *CA: A Cancer Journal for Clinicians,* 54**,** 22.

JENKINS, D. C., CHARLES, I.G., THOMSEN, L.L.E., MOSS, D.W., HOLMES, L.S., BAYLIS, S.A., RHODES, P., WESTMORE, K., EMSON, P.C., MONCADA, S. 1995. Roles of nitric oxide in tumor growth *Proceedings of the National Academy of Sciences,* 92**,** 5.

JETER, C. R., LIU, B., LIU, X., CHEN, X., LIU, C., CALHOUN-DAVIS, T., REPASS, J., ZAEHRES, H., SHEN, J. J. & TANG, D. G. 2011. NANOG promotes cancer stem cell characteristics and prostate cancer resistance to androgen deprivation. *Oncogene,* 30**,** 3833-3845.

KANTARA, C., O'CONNELL, M., SARKAR, S. 2014. Curcumin promotes autophagic survival of a subset of colon cancer stem cells, which are ablated by DCLK1-siRNA *Cancer research,* 74**,** 12.

KIM, M. P., FLEMING, J.B., WANG, H., ABBRUZZESE, J.L., CHOI, W., KOPETZ, S., MCCONKEY, D.J., EVANS D.B., GALLICK, G.E. 2011. ALDH Activity Selectively Defines an Enhanced Tumor-Initiating Cell Population Relative to CD133 Expression in Human Pancreatic Adenocarcinoma. *PLoS ONE,* 6.

KISLEY, L. R., BARRETT, B.S., BAUER, A.K., DWYER-NIELD, L.D., BARTHEL, B., MEYER, A.M., THOMPSON, D.C., MALKINSON, A.M. 2002. Genetic ablation of inducible nitric oxide synthase decreases mouse lung tumorigenesis. *Cancer Research,* 62**,** 7.

KITAMURA, H., OKUDELA, K., YAZAWA, T., SATO, H., SHIMOYAMADA, H. 2009. Cancer stem cell: Implications in cancer biology and therapy with special reference to lung cancer. *Lung Cancer,* 66**,** 7.

LALA, P. K., & ORUCEVIC, A. 1998. Role of nitric oxide in tumor progression: lessons from experimental tumors. *Cancer and Metastasis Reviews,* 17**,** 16.

LANDIS, S. H., MURRAY, T., BOLDEN, S., WINGO, P.A. 1999. Cancer Statistics, 1999. *CA: A Cancer Journal for Clinicians,* 49**,** 24.

LAVIE, Y., FIUCCI, G., LISCOVITCH, M. 1998. Up-regulation of caveolae and caveolar constituents in multidrug-resistant cancer cells. *Journal of Biological Chemistry* 273**,** 4.

LAVIE, Y., FIUCCI, G., LISCOVITCH, M. 2001. Upregulation of caveolin in multidrug resistant cancer cells: functional implications *Advanced Drug Delivery Reviews* 49**,** 7.

LEVINA, V., MARRANGONI, A.M., DEMARCO, R., GORELIK, E., LOKSHIN, A.E. 2008. Drug-selected human lung cancer stem cells: cytokine network, tumorigenic and metastatic properties. *PLoS One* 3.

LI, C., HEIDT, D.G., DALERBA, P., BURANT, C.F., ZHANG, L., ADSAY, V., WICHA, M., CLARKE, M.F., SIMEONE, D.M. 2007. Identification of Pancreatic Cancer Stem Cells. *Cancer Research,* 67**,** 8.

LI, S., COUET, J., LISANTI, M.P. 1996. Src tyrosine kinases, Galpha subunits, and H-Ras share a common membrane-anchored scaffolding protein, caveolin: Caveolin binding negatively regulates the auto-activation of Src tyrosine kinases *Journal of Biological Chemistry* 271**,** 9.

LIN, M., DIVITO, M.M., MERAJVER, S.D., BOYANAPALLI, M., VAN GOLEN, K.L. 2005. Regulation of pancreatic cancer cell migration and invasion by RhoC GTPase and Caveolin-1. *Molecular Cancer* 4**,** 1.

LIU, C. Y., WANG, C.H., CHEN, T.C., LIN, H.C., YU, C.T., KUO, H. P. 1998. Increased level of exhaled nitric oxide and up-regulation of inducible nitric oxide synthase in patients with primary lung cancer *British Journal of Cancer,* 78**,** 8.

LLOYD, P. G., & HARDIN, C.D. 2011. Caveolae in cancer: two sides of the same coin? Focus on "Hydrogen peroxide inhibits non-small cell lung cancer cell anoikis through the inhibition of caveolin-1 degradation". *American Journal of Physiology - Cell Physiology,* 300**,** 3.

LOBO, N. A., SHIMONO, Y., QIAN, D., CLARKE, M.F. 2007. The biology of cancer stam cells. *The Annual Review of Cell and Developmental,* 23**,** 25.

LUANPITPONG, S., TALBOTT, S.J., ROJANASAKUL, Y., NIMMANNIT, U., PONGRAKHANANON, V., WANG, L., CHANVORACHOTE, P. 2010. Regulation of lung cancer cell migration and invasion by reactive oxygen species and caveolin-1 *Journal of Biological Chemistry* 285**,** 9.

MA, S., CHAN, K.W., HU, L., LEE, T.K.W., WO, J.Y.H., NG, I.O.L., ZHENG, B.J., GUAN, X.Y. 2007. Identification and Characterization of Tumorigenic Liver Cancer Stem/Progenitor Cells *Gastroenterology,* 132**,** 15.

MARIE-EGYPTIENNE, D. T., LOHSE, I., HILL, R.P. 2012. Cancer stem cells, the epithelial to mesenchymal transition (EMT) and radioresistance: Potential role of hypoxia *Cancer Letter,* 341**,** 10.

MARLETTA, M. A. 1993. Nitric oxide synthase structure and mechanism. *Journal of Biological Chemistry,* 268**,** 4.

MASRI, F. A., COMHAIR, S.A.A., KOECK, T., XU, W., JANOCHA, A., GHOSH, S., DWEIK, R.A., GOLISH, J., KINTER, M., STUEHR, D.J., ERZURUM, S.C., AULAK, K.S. 2005. Abnormalities in nitric oxide and its derivatives in

lung cancer *American Journal of Respiratory and Critical Care Medicine* 172**,** 9.

MATHER, J. P. 2012. Concise Review: Cancer Stem Cells: In Vitro Models. *Stem Cells,* 30**,** 5.

MERLOS-SUÁREZ, A., BARRIGA, F.M., JUNG, P., IGLESIAS, M., CÉSPEDES, M.V., ROSSELL, D., SEVILLANO, M., HERNANDO-MOMBLONA, X., SILVA-DIZ, V., MUÑOZ, P., CLEVERS, H., SANCHO, E., MANGUES, R., BATLLEET, E. 2011. The intestinal stem cell signature identifies colorectal cancer stem cells and predicts disease relapse. *Cell Stem Cell* 8**,** 14.

MIHATSCH, J., TOULANY, M., BAREISS, P.M., GRIMM, S., LENGERKE, C., KEHLBACH, R., RODEMANN, H.P. 2011. Selection of radioresistant tumor cells and presence of ALDH1 activity in vitro. *Radiotherapy and Oncology* 99**,** 7.

MIRAGLIA, S., GODFREY, W., YIN, A.H., ATKINS, K., WARNKE, R., HOLDEN, J.T., BRAY, R.A., EDMUND, K.W., BUCK, D.W. 1997. A novel five-transmembrane hematopoietic stem cell antigen: isolation, characteriazation, and molecular cloning. *Blood,* 90**,** 9.

MONCADA, S., PALMER, J.R.M., HIGGS, A.E. 1989. Biosynthesis of nitric oxoide from L-arginine: a pathway for the regulation of cell function and communication *Biochemical Pharmacology,* 38**,** 7.

MONCADA, S., PALMER, R., HIGGS, E.A. 1991. Nitric oxide: physiology, pathophysiology, and pharmacology. *Pharmacological reviews,* 43**,** 34.

MUNTANÉ, J., & DE LA MATA, M. 2010. Nitric oxide and cancer *World Journal of Hepatology,* 2**,** 8.

O'BRIEN, C. A., POLLETT, A., GALLINGER, S., DICK, J.E. 2007. A human colon cancer cell capable of initiating tumour growth in immunodeficient mice *Nature,* 445**,** 5.

O'CONNOR, M. L., XIANG, D., SHIGDAR, S., MACDONALD, J., LI, Y., WANG, T., PU, C., WANG, Z., QIAO, L., DUAN, W. 2014. Cancer stem cells: A contentious hypothesis now moving forward. *Cancer Letter* 344**,** 8.

PERONA, R., LÓPEZ-AYLLÓN, B.D., CASTRO CARPEÑO, J., BELDA-INIESTA, C. 2011. A role for cancer stem cells in drug resistance and metastasis in non-small-cell lung cancer *Clinical and Translational Oncology* 13**,** 5.

PIROZZI, G., TIRINO, V., CAMERLINGO, R., FRANCO, R., LA ROCCA, A., LIGUORI, E., MARTUCCI, N., PAINO, F., NORMANNO, N., ROCCO, G. 2011. Epithellial to mesenchymal transition by TGFβ-1 induction increases stemness characteristics in primary non small cell lung cancer cell line. *PLoS ONE,* 6**,** e21548.

PONTI, D., COSTA, A., ZAFFARONI, N., PRATESI, G., PETRANGOLINI, G., CORADINI, D., PILOTTI, S., PIEROTTI, M.A., DAIDONE, M.G. 2005. Isolation and in vitro propagation of tumorigenic breast cancer cells with stem/progenitor cell properties *Cancer research* 65**,** 6.

PUHAKKA, A., KINNULA, V., NÄPÄNKANGAS, U., SÄILY, M., KOISTINEN, P., PÄÄKKÖ, P., SOINI, Y. 2003. High expression of nitric oxide synthases is a favorable prognostic sign in non-small cell lung carcinoma *Acta Pathologica, Microbiologica et Immunologica Scandinavica.* , 111**,** 10.

RICCI-VITIANI, L., LOMBARDI, D.G., PILOZZI, E., BIFFONI, M., TODARO, M., PESCHLE, C., DE MARIA, R. 2007. Identification and expansion of human colon-cancer-initiating cells. *Nature,* 445**,** 5.

RIDNOUR, L. A., THOMAS, D. D., SWITZER, C., FLORES-SANTANA, W., ISENBERG, J. S., AMBS, S., ROBERTS, D. D. & WINK, D. A. 2008. Molecular mechanisms for discrete nitric oxide levels in cancer. *Nitric Oxide,* 19**,** 73-6.

ROSSI, D. J., JAMIESON, C.H., WEISSMAN, I.L. 2008. Stems cells and the pathways to aging and cancer. *Cell,* 132**,** 16.

RUNGTABNAPA, P., NIMMANNIT, U., HALIM, H., ROJANASAKUL, Y., CHANVORACHOTE, P. 2011. Hydrogen peroxide inhibits non-small cell lung cancer cell anoikis through the inhibition of caveolin-1 degradation *American Journal of Physiology - Cell Physiology,* 300**,** 11.

SANUPHAN, A., CHUNHACHA, P., PONGRAKHANANON, V., CHANVORACHOTE, P. 2013. Long-term nitric oxide exposure enhances lung cancer cell migration. *BioMed Research International,* 2013**,** 1.

SIEGEL, R., MA, J., ZOU, Z., JEMAL, A. 2014. Cancer Statistics, 2014. *CA: A Cancer Journal for Clinicians,* 64**,** 21.

SILVA, I. A., BAI, S., MCLEAN, K., YANG, K., GRIFFITH, K., THOMAS, D., GINESTIER, C., JOHNSTON C., KUECK A., REYNOLDS R.K., WICHA M.S., BUCKANOVICH R.J. 2011. Aldehyde Dehydrogenase in Combination with CD133 Defines Angiogenic Ovarian Cancer Stem Cells That Portend Poor Patient Survival. *Cancer Research,* 71**,** 11.

SINGH, S. K., CLARKE, I.D., TERASAKI, M., BONN, V.E., HAWKINS, C., SQUIRE, J., DIRKS, P.B. 2003. Identification of a cancer stem cell in human brain tumors *Cancer Research,* 63**,** 8.

SORELLE, R. 1998. Nobel prize awarded to scientists for nitric oxide discoveries. *Circulation,* 98**,** 2.

SPANGRUDE, G. J., HEIMFELD, S., WEISSMAN, I.L. 1988. Purification and characterization of mouse hematopoietic stem cells. *Science,* 241**,** 5.

THOMSEN, L. L., & MILES, D.W. 1998. Role of nitric oxide in tumour progression: lessons from human tumours *Cancer and Metastasis Reviews,* 17**,** 12.

THOMSEN, L. L., LAWTON, F.G., KNOWLES, R.G., BEESLEY, J.E., RIVEROS-MORENO, V., MONCADA, S. 1994. Nitric oxide synthase activity in human gynecological cancer *Cancer research* 54**,** 3.

THOMSEN, L. L., MILES, D.W., HAPPERFIELD, L., BOBROW, L.G., KNOWLES, R.G., MONCADA, S. 1995. Nitric oxide synthase activity in human breast cancer *British Journal of Cancer* 72**,** 4.

VERMEULEN, L., TODARO, M., DE SOUSA, M.F., SPRICK, M.R., KEMPER, K., PEREZ, A.M., ET AL. 2008. Single-cell cloning of colon cancer stem cells reveals a multi-lineage differentiation capacity. *Proceedings of the National Academy of Science of the United Statees of America,* 105**,** 6.

VOGEL, C., & MARCOTTE, E.M. 2012. Insights into the regulation of protein abundance from proteomic and transcriptomic analyses. *Nat Rev Genet,* 13**,** 227-232.

WEIMING, X., LI ZHI, L., MARILENA LOIZIDOU, M.A., IAN, G.C. 2002. The role of nitric oxide in cancer *Cell research,* 12**,** 10.

WIECHEN, K., SERS, C., AGOULNIK, A., ARLT, K., DIETEL, M., SCHLAG, P.M., SCHNEIDER, U. 2001. Down-regulation of caveolin-1, a candidate tumor suppressor gene, in sarcomas. *American Journal of Pathology,* 158**,** 7.

WINK, D. A., VODOVOTZ, Y., LAVAL, J., LAVAL, F., DEWHIRST, M.W., MITCHELL, J.B. 1998. The multifaceted roles of nitric oxide in cancer. *Carcinogenesis,* 19**,** 10.

WONGVARANON, P., PONGRAKHANANON, V., CHUNHACHA, P., CHANVORACHOTE, P. 2013. Acquired resistance to chemotherapy in lung cancer cells mediated by prolonged nitric oxide exposure *Anticancer research* 33**,** 12.

YANG, G., LU, X., FU, H., JIN, L., YAO, L., LU, Z. 2009. Chemotherapy not only enriches but also induces cancer stem cells *Bioscience Hypotheses,* 2**,** 3.

ZHANG, Y., WANG, Z., YU, J., SHI, J.Z., WANG, C., FU, W.H., CHEN, Z.W., YANG, J. 2012. Cancer stem-like cells contribute to cisplatin resistance and progression in bladder cancer *Cancer Letters,* 322**,** 8.

APPENDIX

APPENDIX A
TABLE OF EXPERIMENTAL RESULTS

Table 5. DPTA NONOate (0-50 μM) cytotoxicity in H292 at 24 hours

DPTA (μM)	%Cell viability
0	100.00±0.51
5	98.99±1.23
10	98.33±0.67
15	94.48±1.30
20	93.12±0.54
25	92.38±0.95
30	87.91±1.28*
35	86.46±1.69*
40	83.74±1.39*
45	81.04±0.91*
50	71.90±0.89*

Each value represents mean ± SD (n=4). *, $p < 0.05$ versus non-treated control cells.

Table 6. DPTA NONOate (0-50 μM) cytotoxicity in H460 at 24 hours

DPTA (μM)	%Cell viability
0	100.00±0.72
5	96.38±1.62
10	93.90±0.88
15	86.98±1.21*
20	85.26±1.40*
25	83.39±1.46*
30	74.16±2.18*
35	70.99±1.21*
40	66.87±1.76*
45	63.37±1.43*
50	57.99±1.04*

Each value represents mean ± SD (n=4). *, $p < 0.05$ versus non-treated control cells.

Table 7. The effect of long-term NO exposure on H292 cell migration

Day	DPTA (μM)	Relative cell migration
Day 7	Control	1.00±0.21
	10 μM	1.43±0.13*
	25 μM	1.59±0.24*#
Day 14	Control	1.00±0.15
	10 μM	2.17±0.19*
	25 μM	2.56±0.32*#

Each value represents mean ± SD (n=4). *, $p < 0.05$ vs. non-treated cells. #, $p < 0.05$ vs. 10 μM DPTA NONOate-treated cells.

Table 8. The effect of long-term NO exposure on H460 cell migration

Day	DPTA (μM)	Relative cell migration
Day 7	Control	1.00±0.11
	5 μM	1.31±0.09*
	10 μM	1.50±0.21*#
Day 14	Control	1.00±0.10
	5 μM	2.09±0.18*
	10 μM	2.28±0.23*#

Each value represents mean ± SD (n=4). *, $p < 0.05$ vs. non-treated cells. #, $p < 0.05$ vs. 5 μM DPTA NONOate-treated cells.

Table 9. The effect of long-term NO exposure on H292 cell invasion

Day	DPTA (μM)	Relative cell invasion
Day 7	Control	1.00±0.12
	10 μM	1.83±0.14*
	25 μM	2.59±0.16*#
Day 14	Control	1.00±0.15
	10 μM	2.37±0.21*
	25 μM	4.56±0.25*#

Each value represents mean ± SD (n=4). *, $p < 0.05$ vs. non-treated cells. #, $p < 0.05$ vs. 10 μM DPTA NONOate-treated cells.

Table 10. The effect of long-term NO exposure on H460 cell invasion

Day	DPTA (μM)	Relative cell invasion
Day 7	Control	1.00±0.11
	5 μM	1.45±0.09
	10 μM	3.00±0.12*#
Day 14	Control	1.00±0.10
	5 μM	2.39±0.18*
	10 μM	4.18±0.17*#

Each value represents mean ± SD (n=4). *, $p < 0.05$ vs. non-treated cells. #, $p < 0.05$ vs. 5 μM DPTA NONOate-treated cells.

Table 11. The effect of long-term NO exposure on H292 anoikis cell death

Day	DPTA (μM)	%Cell viability at 0 hr	%Cell viability at 3 hrs	%Cell viability at 6 hrs	%Cell viability at 9 hrs	%Cell viability at 12 hrs	%Cell viability at 24 hrs
Day 7	Control	100.00±0.79	94.54±5.33	86.51±4.27	80.95±1.26	72.77±2.28	55.93±3.97
	10 μM	100.00±0.91	99.89±3.31	90.40±2.18	84.30±4.87	76.30±6.07	60.92±6.19
	25 μM	100.00±0.81	101.39±7.48	94.92±8.19	82.98±6.68	78.03±5.11	65.20±12.46
Day 14	10 μM	100.00±0.62	100.73±4.46	101.49±5.71	98.33±2.89*	93.98±2.64*	75.78±6.38*
	25 μM	100.00±0.49	106.57±6.18	105.42±7.63	105.18±5.88*	100.84±7.93*	87.34±7.07*

Each value represents mean ± SD (n=4). *, $p < 0.05$ vs. non-treated cells.

Table 12. The effect of long-term NO exposure on H460 anoikis cell death

Day	DPTA (μM)	%Cell viability at 0 hr	%Cell viability at 3 hrs	%Cell viability at 6 hrs	%Cell viability at 9 hrs	%Cell viability at 12 hrs	%Cell viability at 24 hrs
	Control	100.00±0.91	93.75±3.39	90.56±1.81	81.93±4.70	66.67±6.09	50.85±6.22
Day 7	5 μM	100.00±0.80	95.97±5.32	90.08±4.62	83.38±1.27	69.69±2.28	54.97±3.57
	10 μM	100.00±0.70	97.35±4.59	93.79±5.59	85.18±2.89	75.63±2.64	59.82±6.38
Day 14	5 μM	100.00±0.92	99.53±3.69	90.77±3.04	88.63±2.77	85.76±4.80*	78.51±5.13*
	10 μM	100.00±0.83	98.99±7.49	96.84±8.37	91.83±6.71	90.84±5.13*	80.48±12.51*

Each value represents mean ± SD (n=4). *, $p < 0.05$ vs. non-treated cells.

Table 13. The effect of NO on EMT markers in H292 cell

Day	DPTA (μM)	Vimentin	Snail
Day 7	Control	1.00±0.15	1.00±0.19
	10 μM	1.75±0.19*	1.31±0.25
	25 μM	2.28±0.24*#	2.17±0.21*#
Day 14	10 μM	3.58±0.12*	3.39±0.18*
	25 μM	4.35±0.23*#	4.41±0.16*#

Each value represents mean ± SD (n=4). *, $p < 0.05$ vs. non-treated cells. #, $p < 0.05$ vs. 10 μM DPTA NONOate-treated cells.

Table 14. The effect of NO on EMT markers in H460 cell

Day	DPTA (μM)	Vimentin	Snail
Day 7	Control	1.00±0.17	1.00±0.10
	5 μM	1.94±0.26*	1.51±0.15*
	10 μM	2.48±0.29*#	1.83±0.18*#
Day 14	5 μM	2.77±0.25*	2.72±0.20*
	10 μM	3.26±0.24*#	3.11±0.17*#

Each value represents mean ± SD (n=4). *, $p < 0.05$ vs. non-treated cells. #, $p < 0.05$ vs. 5 μM DPTA NONOate-treated cells.

Table 15. The effect of long-term NO exposure on H292 cells proliferation

Day	DPTA (μM)	%Cell proliferation at 24 hrs	%Cell proliferation at 48 hrs	%Cell proliferation at 72 hrs
Day 7	Control	100.00±0.50	100.00±0.49	100.00±0.39
	10 μM	100.34±0.47#	94.82±1.60#	85.92±2.45*
	25 μM	98.65±0.58#	92.87±1.48*#	84.62±1.99*
Day 14	Control	100.00±0.52	100.00±0.66	100.00±0.87
	10 μM	89.25±3.43*	84.66±2.98*#	78.41±1.08*
	25 μM	78.68±3.19*#	56.84±4.35*#	40.45±0.40*

Each value represents mean ± SD (n=4). *, $p < 0.05$ vs. non-treated cells. #, $p < 0.05$ vs. 72hrs DPTA NONOate-treated cells.

Table 16. The effect of long-term NO exposure on H460 cells proliferation

Day	DPTA (μM)	%Cell proliferation at 24 hrs	%Cell proliferation at 48 hrs	%Cell proliferation at 72 hrs
Day 7	Control	100.00±0.27	100.00±1.00	100.00±1.21
	5 μM	100.80±0.57#	97.20±0.69#	89.93±1.32*
	10 μM	99.32±0.71#	94.07±1.47#	86.06±1.93*
Day 14	Control	100.00±0.69	100.00±0.43	100.00±0.23
	5 μM	89.79±1.60*#	79.40±1.10*#	59.98±1.70*
	10 μM	76.58±2.43*#	60.05±3.78*#	46.10±2.73*

Each value represents mean ± SD (n=4). *, $p < 0.05$ vs. non-treated cells. #, $p < 0.05$ vs. 72hrs DPTA NONOate-treated cells.

Table 17. The effect of long-term NO exposure on H292 colony formation

Day	DPTA (μM)	Relative colony No.	Diameter
Day 7	Control	1.00±0.12	1.00±0.13
	10 μM	1.34±0.22	1.17±0.23
	25 μM	2.51±0.09*#	1.01±0.31
Day 14	Control	1.00±0.24	1.00±0.15
	10 μM	2.10±0.17*	1.05±0.13
	25 μM	3.37±0.14*#	0.70±0.08

Each value represents mean ± SD (n=4). *, $p < 0.05$ vs. non-treated cells. #, $p < 0.05$ vs. 10 μM DPTA NONOate-treated cells.

Table 18. The effect of long-term NO exposure on H460 colony formation

Day	DPTA (μM)	Relative colony No.	Diameter
Day 7	Control	1.00±0.13	1.00±0.15
	5 μM	1.32±0.24	1.08±0.20
	10 μM	2.67±0.12*#	0.89±0.26
Day 14	Control	1.00±0.19	1.00±0.35
	5 μM	1.57±0.22	0.79±0.33
	10 μM	3.26±0.14*#	0.48±0.30

Each value represents mean ± SD (n=4). *, $p < 0.05$ vs. non-treated cells. #, $p < 0.05$ vs. 5 μM DPTA NONOate-treated cells.

Table 19. The effect of NO on cancer stem cell markers in H292 cell

Day	DPTA (μM)	CD133	ALDH1A1
Day 7	Control	1.00±0.23	1.00±0.25
	10 μM	2.05±0.56*	2.12±0.39*
	25 μM	3.43±0.49*#	3.53±0.53*#
Day 14	10 μM	5.44±0.87*	5.39±0.98*
	25 μM	7.10±1.01*#	7.54±0.99*#

Each value represents mean ± SD (n=8). *, $p < 0.05$ vs. non-treated cells. #, $p < 0.05$ vs. 10 μM DPTA NONOate-treated cells.

Table 20. The effect of NO on cancer stem cell markers in H460 cell

Day	DPTA (μM)	CD133	ALDH1A1
Day 7	Control	1.00±0.29	1.00±0.30
	5 μM	1.58±0.61	1.63±0.59
	10 μM	1.93±0.50*#	2.61±0.65*#
Day 14	5 μM	3.80±1.09*	4.59±0.88*
	10 μM	4.77±1.00*#	5.78±1.01*#

Each value represents mean ± SD (n=8). *, $p < 0.05$ vs. non-treated cells. #, $p < 0.05$ vs. 5 μM DPTA NONOate-treated cells.

Table 21. The reversible effect of NO exposure on H292 anoikis cell death

DPTA (μM)	%Cell viability at 0 hr	%Cell viability at 3 hrs	%Cell viability at 6 hrs	%Cell viability at 9 hrs	%Cell viability at 12 hrs	%Cell viability at 24 hrs
Control	100.00±0.75	93.65±7.03	84.51±4.71	79.59±0.67	71.97±2.21	50.95±4.37
25 μM	100.00±1.01	104.57±2.81	105.11±7.64	103.18±9.81*	95.84±8.96*	82.34±8.72*
Discontinued	100.00±0.50	99.01±2.20	95.38±2.70	80.98±5.13	75.83±4.54	59.75±2.45

Each value represents mean ± SD (n=4). *, $p < 0.05$ vs. non-treated cells.

Table 22. The reversible effect of NO exposure on H460 anoikis cell death

DPTA (μM)	%Cell viability at 0 hr	%Cell viability at 3 hrs	%Cell viability at 6 hrs	%Cell viability at 9 hrs	%Cell viability at 12 hrs	%Cell viability at 24 hrs
Control	100.00±0.99	92.17±3.56	89.84±2.52	79.97±5.47	64.12±6.75	51.67±7.51
10 μM	100.00±1.00	96.99±0.90	94.84±0.34	92.83±5.72	88.84±6.90*	75.48±2.82*
Discontinued	100.00±0.52	96.39±1.76	90.19±1.46	85.20±2.71	70.09±1.08	50.91±0.63

Each value represents mean ± SD (n=4). *, $p < 0.05$ vs. non-treated cells.

Table 23. The reversible effect of NO on H292 colony formation

DPTA (μM)	Relative colony No.
Control	1.00±0.36
25 μM	3.39 ±0.51*#
Discontinued	2.33±0.72*

Each value represents mean ± SD (n=4). *, $p < 0.05$ vs. non-treated cells. #, $p < 0.05$ vs. discontinued treatment cells.

Table 24. The reversible effect of NO on H460 colony formation

DPTA (μM)	Relative colony No.
Control	1.00±0.40
10 μM	3.31 ±0.78*#
Discontinued	2.29±0.65*

Each value represents mean ± SD (n=4). *, $p < 0.05$ vs. non-treated cells. #, $p < 0.05$ vs. discontinued treatment cells.

Table 25. The reversible effect of NO on cancer stem cell markers in H292 cell

DPTA (μM)	CD133	ALDH1A1
Control	1.00±0.40	1.00±0.42
25 μM	6.58 ±1.26*#	6.91±1.13*#
Discontinued	4.18±1.44*	3.28±1.46*

Each value represents mean ± SD (n=8). *, $p < 0.05$ vs. non-treated cells. #, $p < 0.05$ vs. discontinued cells.

Table 26. The reversible effect of NO on cancer stem cell markers in H460 cell

DPTA (μM)	CD133	ALDH1A1
Control	1.00±0.40	1.00±0.45
10 μM	4.85±1.32*#	5.07±1.55*#
Discontinued	2.52±1.43*	3.30±1.58*

Each value represents mean ± SD (n=8). *, $p < 0.05$ vs. non-treated cells. #, $p < 0.05$ vs. discontinued cells.

Table 27. The effect of SNAP/PTIO exposure on H292 anoikis cell death

Treatment (μM)	%Cell viability at 0 hr	%Cell viability at 3 hrs	%Cell viability at 6 hrs	%Cell viability at 9 hrs	%Cell viability at 12 hrs	%Cell viability at 24 hrs
Control	100.00±0.14	92.50±7.21	83.28±5.51	78.43±4.16	71.23±3.90	47.52±8.21
SNAP 20 μM	100.00±0.21	92.16±4.06	88.24±2.33	82.41±6.13	79.09±4.73*	64.36±7.22*
SNAP 50 μM	100.00±0.11	93.49±5.11	91.21±9.09	91.52±4.70*	85.09±8.17*	68.03±3.29*
PTIO 50 μM	100.00±0.16	91.27±3.32	75.14±7.50	68.76±2.81*	55.39±5.10*	32.52±6.18*

Each value represents mean ± SD (n=4). *, $p < 0.05$ vs. non-treated cells.

Table 28. The effect of SNAP/PTIO exposure on H460 anoikis cell death

Treatment (μM)	%Cell viability at 0 hr	%Cell viability at 3 hrs	%Cell viability at 6 hrs	%Cell viability at 9 hrs	%Cell viability at 12 hrs	%Cell viability at 24 hrs
Control	100.00±0.20	92.48±7.08	89.02±5.15	82.17±3.99	65.29±3.78	52.05±2.21
SNAP 10 μM	100.00±0.23	92.16±4.15	87.93±1.78	82.97±7.01	77.21±3.93*	63.00±7.79*
SNAP 20 μM	100.00±0.19	93.47±3.98	90.11±10.02	84.28±3.87	78.23±7.90*	64.28±4.34*
PTIO 20 μM	100.00±0.12	82.37±5.77	82.03±6.83	71.92±1.99*	54.10±4.87*	41.49±6.00*

Each value represents mean ± SD (n=4). *, $p < 0.05$ vs. non-treated cells.

Table 29. The effect of SNAP/PTIO exposure on H292 colony formation

Treatment (μM)	Relative colony No.
Control	1.00±0.38
SNAP 20 μM	1.45±0.57#
SNAP 50 μM	3.05±0.76*
PTIO 50 μM	0.46±0.55*#

Each value represents mean ± SD (n=4). *, $p < 0.05$ vs. non-treated cells. #, $p < 0.05$ vs. SNAP 50 μM treated cells

Table 30. The effect of SNAP/PTIO exposure on H460 colony formation

Treatment (μM)	Relative colony No.
Control	1.00±0.41
SNAP 10 μM	1.43±0.48#
SNAP 20 μM	2.91±0.88*
PTIO 20 μM	0.64±0.52*#

Each value represents mean ± SD (n=4). *, $p < 0.05$ vs. non-treated cells. #, $p < 0.05$ vs. SNAP 20 μM treated cells

Table 31. The effect of SNAP/PTIO exposure on cancer stem cell markers in H292 cell

Treatment (μM)	CD133	ALDH1A1
Control	1.00±0.20	1.00±0.40
SNAP 20 μM	3.02±0.44*#	2.49±0.58*#
SNAP 50 μM	3.56±0.60*	3.05±0.46*
PTIO 50 μM	0.48±0.04*	0.74±0.02*

Each value represents mean ± SD (n=4). *, $p < 0.05$ vs. non-treated cells. #, $p < 0.05$ vs. SNAP 50 μM treated cells

Table 32. The effect of SNAP/PTIO exposure on cancer stem cell markers in H460 cell

Treatment (μM)	CD133	ALDH1A1
Control	1.00±0.43	1.00±0.20
SNAP 10 μM	2.25±0.48*#	4.04±0.33*#
SNAP 20 μM	3.37±0.45*	4.20±0.46*
PTIO 20 μM	0.68±0.09*	0.47±0.02*

Each value represents mean ± SD (n=4). *, $p < 0.05$ vs. non-treated cells. #, $p < 0.05$ vs. SNAP 20 μM treated cells

Table 33. The effect of long-term NO exposure on caveolin-1 protein level in H292 cell

Day	DPTA (μM)	Caveolin-1
	Control	1.00±0.09
Day 7	10 μM	2.51±0.43*
	25 μM	3.83±0.51*
Day 14	10 μM	5.42±0.24*#
	25 μM	6.56±0.48*#

Each value represents mean ± SD (n=4). *, $p < 0.05$ vs. non-treated cells. #, $p < 0.05$ vs. day 7 treated cells

Table 34. The effect of long-term NO exposure on caveolin-1 protein level in H460 cell

Day	DPTA (μM)	Caveolin-1
	Control	1.00±0.22
Day 7	10 μM	1.83±0.16*
	25 μM	2.56±0.32*
Day 14	10 μM	3.17±0.25*#
	25 μM	3.94±0.40*#

Each value represents mean ± SD (n=4). *, $p < 0.05$ vs. non-treated cells. #, $p < 0.05$ vs. day 7 treated cells

Table 35. Level of caveolin-1 in H292 transfected cell

Cell Type	Caveolin-1
Control	1.00±0.12
Sh	0.35±0.23*
Cav-1	2.42±0.25*#

Each value represents mean ± SD (n=4). *, $p < 0.05$ vs. non-treated cells. #, $p < 0.05$ vs. sh-transfected cells

Table 36. Level of caveolin-1 in H460 transfected cell

Cell Type	Caveolin-1
Control	1.00±0.20
Sh	0.24±0.35*
Cav-1	3.17±0.47*#

Each value represents mean ± SD (n=4). *, $p < 0.05$ vs. non-treated cells. #, $p < 0.05$ vs. sh-transfected cells

Table 37. The effect of caveolin-1 level on H292 anoikis cell death

Cell Type	%Cell viability at 0 hr	%Cell viability at 3 hrs	%Cell viability at 6 hrs	%Cell viability at 12 hrs	%Cell viability at 24 hrs
Control	100.00±1.02	83.13±3.79	45.63±2.03	41.70±4.48	39.23±6.13
Sh cav-1	100.00±1.14	80.27±5.10	30.91±3.49*	26.65±4.59*	25.05±2.09*
Cav-1	100.00±2.32	98.30±4.30*	87.25±6.00*	85.44±2.61*	64.29±4.71*

Each value represents mean ± SD (n=4). *, $p < 0.05$ vs. non-treated cells.

Table 38. The effect of caveolin-1 level on H460 anoikis cell death

Cell Type	%Cell viability at 0 hr	%Cell viability at 3 hrs	%Cell viability at 6 hrs	%Cell viability at 12 hrs	%Cell viability at 24 hrs
Control	100.00±2.00	85.49±2.98	64.57±2.01	55.82±4.90	51.73±6.21
Sh cav-1	100.00±1.42	80.92±4.92	45.42±2.57*	39.50±3.99*	34.10±2.13*
Cav-1	100.00±2.50	99.11±4.10*	92.93±6.55*	89.81±2.46*	75.26±4.04*

Each value represents mean ± SD (n=4). *, $p < 0.05$ vs. non-treated cells.

Table 39. The effect of caveolin-1 level on H292 colony formation

Cell Type	Relative colony No.
Control	1.00±0.34
Sh	0.24±0.05*
Cav-1	2.56±0.49*#

Each value represents mean ± SD (n=4). *, $p < 0.05$ vs. non-treated cells. #, $p < 0.05$ vs. sh-transfected cells

Table 40. The effect of caveolin-1 level on H460 colony formation

Cell Type	Relative colony No.
Control	1.00±0.11
Sh	0.24±0.25*
Cav-1	3.20±0.44*#

Each value represents mean ± SD (n=4). *, $p < 0.05$ vs. non-treated cells. #, $p < 0.05$ vs. sh-transfected cells

Table 41. The effect of caveolin-1 level H292 cell migration

Cell Type	Relative cell migration
Control	1.00±0.27
Sh	0.43±0.15*
Cav-1	2.51±0.43*#

Each value represents mean ± SD (n=4). *, $p < 0.05$ vs. non-treated cells. #, $p < 0.05$ vs. sh-transfected cells

Table 42. The effect of caveolin-1 level on H460 cell migration

Cell Type	Relative cell migration
Control	1.00±0.11
Sh	0.24±0.25*
Cav-1	3.20±0.44*#

Each value represents mean ± SD (n=4). *, $p < 0.05$ vs. non-treated cells. #, $p < 0.05$ vs. sh-transfected cells

Table 43. The effect of caveolin-1 level on cancer stem cell markers in H292 cell

Cell Type	CD133	ALDH1A1
Control	1.00±0.34	1.00±0.25
Sh	3.41±0.20*#	4.58±0.17*#
Cav-1	0.21±0.24*	0.43±0.48*

Each value represents mean ± SD (n=4). *, $p < 0.05$ vs. non-treated cells. #, $p < 0.05$ vs. sh-transfected cells

Table 44. The effect of caveolin-1 level on cancer stem cell markers in H460 cell

Cell Type	CD133	ALDH1A1
Control	1.00±0.41	1.00±0.30
Sh	2.98±0.28*#	3.25±0.12*#
Cav-1	0.17±0.26*	0.74±0.45*

Each value represents mean ± SD (n=4). *, $p < 0.05$ vs. non-treated cells. #, $p < 0.05$ vs. sh-transfected cells

APPENDIX B
SUPPLEMENTARY MICROARRAY RESULTS

Table 45. Microarray results (First 100 genes of $p < 0.01$)

	Probe ID	Gene Symbol	Mean of Treat - Mean of Control	P-value
1	8013360		0.24	3.45E-09
2	8088864		-0.01	3.10E-08
3	8159249	NM_016034	-0.23	1.40E-05
4	7893492		-0.34	1.85E-05
5	7894571		0.76	2.10E-05
6	7895304		-0.14	2.27E-05
7	7915204		0.11	2.91E-05
8	8178754	NM_030651	0.1	3.08E-05
9	8179950	NM_030651	0.1	3.08E-05
10	7957602		0.1	3.22E-05
11	8141363	NM_033017	0.09	3.73E-05
12	7895666		0.87	4.02E-05
13	8179967	NM_001136	0.08	4.12E-05
14	7893226		-1.64	4.65E-05
15	8172193		0.24	7.86E-05
16	8155550		-0.38	1.01E-04
17	7901592		0.03	1.03E-04
18	8071981	NM_001145206	-0.02	1.39E-04
19	8078284		-0.02	1.64E-04
20	8173308		0.42	1.65E-04
21	8019910		0.02	2.09E-04
22	8176789	NM_005058	0.11	2.12E-04
23	8172154	NM_002952	-0.09	2.47E-04
24	8052204	NM_020532	-0.11	2.53E-04
25	8109201	NM_014983	-0.25	2.58E-04
26	8176753	NM_001006121	0.13	2.69E-04
27	8177290	NM_001006121	0.13	2.69E-04
28	8037614	NM_005282	-0.5	3.23E-04
29	8100310		0.47	3.83E-04
30	8169385		-0.14	3.88E-04
31	8174448	NM_001522	0.13	3.94E-04
32	8136795	NM_002769	-0.23	3.94E-04
33	7921840	NM_001077482	0.18	4.40E-04
34	8011018	NM_016823	0.31	4.40E-04
35	7893772		0.25	4.40E-04

	Probe ID	Gene Symbol	Mean of Treat - Mean of Control	P-value
36	8055348		0.5	4.68E-04
37	7981724		-0.62	5.00E-04
38	7895935		-1.84	5.62E-04
39	8058415	NM_017759	-0.4	5.75E-04
40	8026496		0.28	5.91E-04
41	8160084		0.36	5.95E-04
42	8147307		-0.33	6.02E-04
43	8149857	NM_017634	-0.12	6.12E-04
44	8073194	NM_004810	-0.18	6.30E-04
45	8136811	NM_004445	0.22	6.51E-04
46	8052305		0.26	6.82E-04
47	8033813	NM_017703	0	7.45E-04
48	7944527		0.4	8.06E-04
49	8009727	NM_001545	-0.16	8.32E-04
50	8091867	NM_000055	-0.33	8.45E-04
51	8117900	NM_001954	0.41	9.00E-04
52	8154363	NM_001029	0.44	9.09E-04
53	7956423	NM_005538	0.29	1.04E-03
54	8095435	NM_002159	0.46	1.05E-03
55	8048116		-0.39	1.09E-03
56	7945944	NM_001665	0.11	1.12E-03
57	7904429		-0.19	1.13E-03
58	7945377	NM_001135053	0.28	1.15E-03
59	8097282	NM_005841	0.09	1.16E-03
60	7908988	NM_003094	0.21	1.17E-03
61	8045497		0.31	1.18E-03
62	8052742	NM_001024680	0.47	1.22E-03
63	8117583	NM_003509	0.58	1.23E-03
64	7923438	NM_001030	-0.46	1.32E-03
65	7894672		0.53	1.32E-03
66	8175683		0.38	1.35E-03
67	8168817	NM_001939	0.44	1.36E-03
68	7948906		-0.84	1.38E-03
69	8171170		-0.06	1.39E-03
70	7968798		0.43	1.45E-03

	Probe ID	Gene Symbol	Mean of Treat - Mean of Control	P-value
71	8165684		0.63	1.49E-03
72	8116096	NM_016222	-0.19	1.55E-03
73	7894178		1.78	1.62E-03
74	7957221	NM_013381	0.16	1.63E-03
75	7895865		-0.3	1.67E-03
76	8176532	NM_001077697	0.08	1.69E-03
77	8084607	NM_021627	-0.33	1.71E-03
78	8144584		-0.33	1.74E-03
79	8121729	NM_002667	0.25	1.76E-03
80	8105517	NM_173667	0.32	1.78E-03
81	7967969	NM_138284	0.48	1.78E-03
82	8070891		0.41	1.84E-03
83	7894328		-1.74	1.84E-03
84	7955797	NM_020547	0.32	1.89E-03
85	8175662		0.39	1.92E-03
86	7892507		-0.24	1.98E-03
87	7894236		-0.27	2.00E-03
88	8114653	NM_005642	0.4	2.10E-03
89	8122452	NM_001013623	0.22	2.22E-03
90	7931930	NM_006257	-0.12	2.30E-03
91	7904967		0.09	2.46E-03
92	8100971	NM_002704	0.16	2.46E-03
93	8169006	NM_001031834	0.66	2.50E-03
94	8034454	NM_001930	-0.37	2.53E-03
95	8024660	NM_006339	0.25	2.55E-03
96	8159566	NM_016219	-0.02	2.56E-03
97	7960553	NM_016497	0.6	2.56E-03
98	8144947		0.2	2.58E-03
99	7895170		-0.31	2.60E-03
100	8030982	NM_001040185	-0.5	2.70E-03

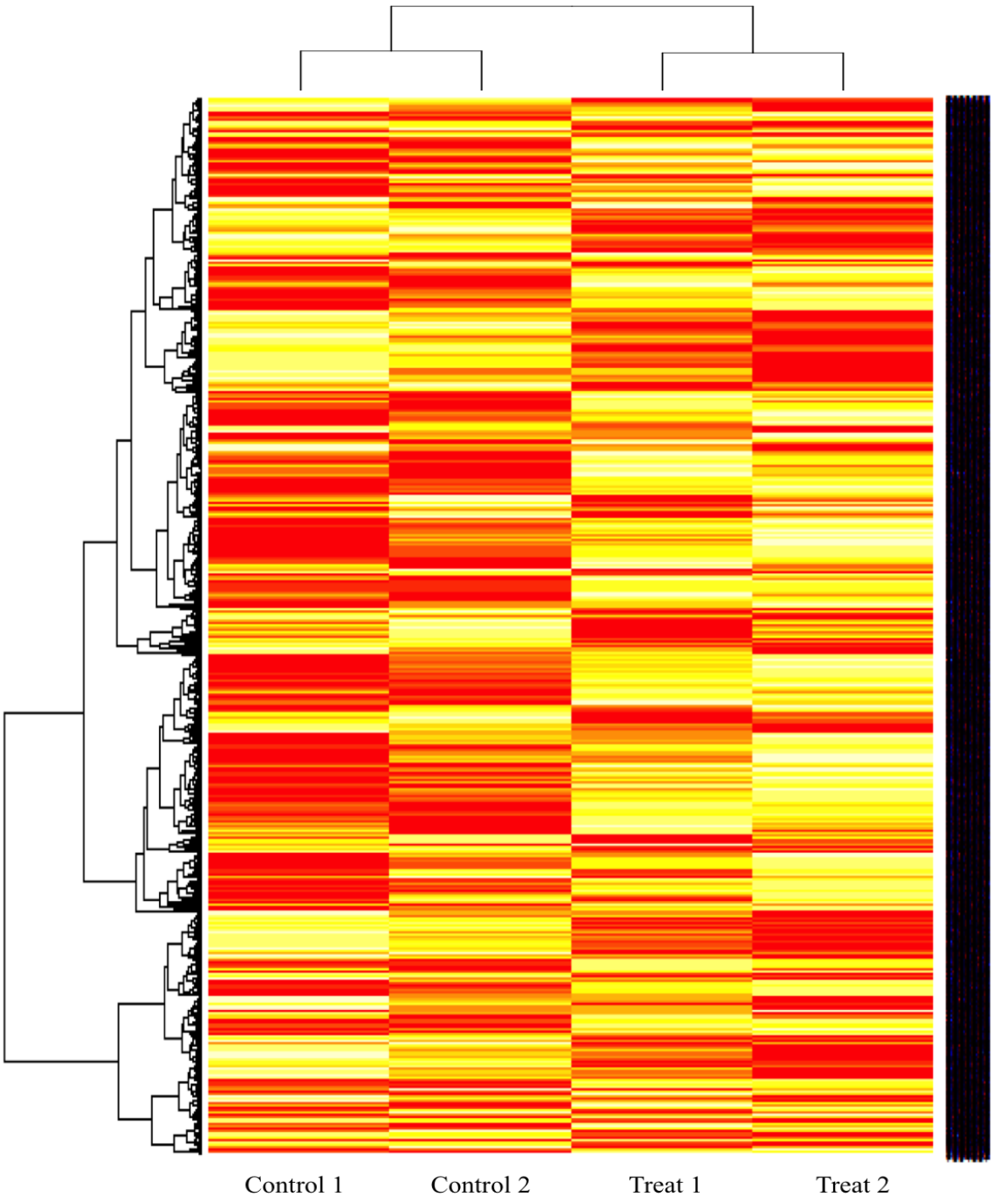

Figure 37 Heat map of genes with $p < 0.05$ generated by the Bioconductor R statistic program. H460 cells were treated with 10 μM of DPTA NONOate for 14 days then subjecting to microarray analysis.

VITA

Nuttida Yongsanguanchai was born in Bangkok, Thailand. She studied in the elementary school program and high school program in Bangkok Patana International School (BPS). At the age of 15 she entered the Faculty of Science, Chulalongkorn University to studied Bachelor of Science in Applied Chemistry (BSAC). In November of the year 2008 she and her team entered the 'Global Innovation Tournament', an annual worldwide tournament set by Stanford University and won the 'viral marketing award'. After four years of bachelor degree she enrolled in the International Graduate Program in Pharmaceutical Technology, Faculty of Pharmaceutical Science, Chulalongkorn University to study the Degree of Doctor of Philosophy in the year 2010. She received THE 90TH ANNIVERSARY OF CHULALONGKORN UNIVERSITY FUND (Ratchadaphiseksomphot Endowment Fund) grant during her doctoral study. She has always been an eager learner and loves to gain new knowledge. She likes to teach and is interested in running a business. She hopes to improve Thailand education and help improve humans and animals well being.